Clueless is a novel mitochondria-associated ribonucleoprotein particle

by

Kelsey Maria Sheard

Dissertation submitted to the Faculty of the
Molecular and Cell Biology Graduate Program
Uniformed Services University of the Health Sciences
In partial fulfillment of the requirements for the degree of
Doctor of Philosophy 2022

Distribution Statement

Distribution A: Public Release.

The views presented here are those of the author and are not to be construed as official or reflecting the views of the Uniformed Services University of the Health Sciences, the Department of Defense or the U.S. Government.

UNIFORMED SERVICES UNIVERSITY OF THE HEALTH SCIENCES
SCHOOL OF MEDICINE GRADUATE PROGRAMS
Graduate Education Office (A 1045), 4301 Jones Bridge Road, Bethesda, MD 20814

FINAL EXAMINATION/PRIVATE DEFENSE FOR THE DEGREE OF DOCTOR OF PHILOSOPHY IN THE MOLECULAR AND CELL BIOLOGY GRADUATE PROGRAM

Name of Student: Kelsey M. Sheard

Date of Examination: January 25, 2022
Time: 10:00 AM

DECISION OF EXAMINATION COMMITTEE MEMBERS:

	PASS	FAIL
SMYTH.JEREMY.T.1180138249 Digitally signed by SMYTH.JEREMY.T.1180138249 Date: 2022.01.25 13:35:43 -05'00'	_X__	____
Dr. Jeremy Smyth DEPARTMENT OF ANATOMY, PHYSIOLOGY & GENETICS Committee Chair		
Rachel Cox Digitally signed by Rachel Cox Date: 2022.01.25 14:01:44 -05'00'	_X_	____
Dr. Rachel Cox DEPARTMENT OF BIOCHEMISTRY & MOLECULAR BIOLOGY Dissertation Advisor		
FENG.YUANYI.1541550271 Digitally signed by FENG.YUANYI.1541550271 Date: 2022.01.26 10:37:13 -05'00'	_X_	____
Dr. Yuanyi Feng DEPARTMENT OF BIOCHEMISTRY & MOLECULAR BIOLOGY Committee Member		
[redacted] Digitally signed by FLAGG.THOMAS.P.1376882930 Date: 2022.01.25 15:13:57 -05'00'	__X_	____
Dr. Thomas Flagg DEPARTMENT OF ANATOMY, PHYSIOLOGY & GENETICS Committee Member		
Lilly, Mary (NIH/NICHD) [E] Digitally signed by Lilly, Mary (NIH/NICHD) [E] Date: 2022.02.01 13:28:43 -05'00'	_X__	____
Dr. Mary Lilly NICHD, NIH Committee Member		

UNIFORMED SERVICES UNIVERSITY OF THE HEALTH SCIENCES
SCHOOL OF MEDICINE GRADUATE PROGRAMS
Graduate Education Office (A 1045), 4301 Jones Bridge Road, Bethesda, MD 20814

APPROVAL OF THE DOCTORAL DISSERTATION IN THE MOLECULAR AND CELL BIOLOGY GRADUATE PROGRAM

Title of Dissertation: "Clueless is a novel mitochondria-associated ribonucleoprotein particle"

Name of Candidate: Kelsey M. Sheard
Doctor of Philosophy Degree

DISSERTATION AND ABSTRACT APPROVED:

DATE:

SMYTH.JEREMY.T.1180138249 Digitally signed by SMYTH.JEREMY.T.1180138249 Date: 2022.01.25 13:36:11 -05'00'

Dr. Jeremy Smyth
DEPARTMENT OF ANATOMY, PHYSIOLOGY & GENETICS
Committee Chair

Rachel Cox Digitally signed by Rachel Cox Date: 2022.01.25 14:02:04 -05'00'

Dr. Rachel Cox
DEPARTMENT OF BIOCHEMISTRY & MOLECULAR BIOLOGY
Dissertation Advisor

FENG.YUANYI.1541550271 Digitally signed by FENG.YUANYI.1541550271 Date: 2022.01.26 11:20:29 -05'00'

Dr. Yuanyi Feng
DEPARTMENT OF BIOCHEMISTRY & MOLECULAR BIOLOGY
Committee Member

[redacted] Digitally signed by FLAGG.THOMAS.P.1376882930 Date: 2022.01.25 15:14:31 -05'00'

Dr. Thomas Flagg
DEPARTMENT OF ANATOMY, PHYSIOLOGY & GENETICS
Committee Member

Lilly, Mary (NIH/NICHD) [E] Digitally signed by Lilly, Mary (NIH/NICHD) [E] Date: 2022.02.01 13:28:14 -05'00'

Dr. Mary Lilly
NICHD, NIH
Committee Member

ACKNOWLEDGMENTS

I would first like to extend a huge thank you to my advisor and mentor, Dr. Rachel Cox. Your mentorship and guidance has been exceptional over the years. You have greatly increased my confidence as a student and my development as a scientist. Thank you for your patience, support, and tirelessly advocating for me as well as all the other graduate students.

Next, I would like to acknowledge my committee members, Dr. Smyth, Dr. Feng, Dr. Flagg, and Dr. Lilly. Your insightfulness, curiosity, and feedback were invaluable to this work as well as my graduate school career. Thank you for your time, mentorship, and willingness to share as much knowledge as possible.

To the Cox and Smyth lab members, it was a joy to have you as colleagues. Thank you all for never hesitating to lend the helping hand and motivation that allowed me to make it through this journey.

To my family and friends, thank you for your abundant love and encouragement and for always having my back.

Finally, I would like to give a very special thank you to Mychelle and Gyliann. Mychelle, your dedication and presence has allowed me so much growth these past few years. Thank you for being a safe space, giving me the tools to thrive, and always helping me hold on another day. Gyliann, there are not enough words of gratitude to express how thankful I am to have you as a friend and second family. You will do amazing things in your PhD journey, and I can only hope to be as much of a support system for you as you have been for me. Thank you both for always being unapologetically you, and for giving me the courage to do the same.

DEDICATION

This work is dedicated to my family,

My mom and siblings, Tasia, Jordan, Justin, and Jeremy,

Everything that I am is because of you. I love you, and you mean the world to me.

COPYRIGHT STATEMENT

The author hereby certifies that the use of any copyrighted material in the dissertation manuscript entitled: “Clueless is a novel mitochondria-associated ribonucleoprotein particle” is appropriately acknowledged and, beyond brief excerpts, is with the permission of the copyright owner.

[Signature] 

Kelsey Sheard

May 21, 2022

Publication Clearance Process: Dissertations

All publications, including theses and dissertations, must be cleared by the Office of External Affairs before submission or release. Standard USU disclaimers below must be included with every dissertation, and are now automatically included in the GEO dissertation template. If any of the additional disclaimers apply to you, please include those in manuscripts/talks and on the "Disclaimers" page of the dissertation template.

Disclaimers required for EVERY publication/presentation/thesis clearance:

"The opinions and assertions expressed herein are those of the author(s) and do not reflect the official policy or position of the Uniformed Services University of the Health Sciences or the Department of Defense."

"References to non-Federal entities or products do not constitute or imply a Department of Defense or Uniformed Services University of the Health Sciences endorsement."

NOTE: Contractors must follow their employer's guidance on adding additional disclaimers, but under no circumstance should a contractor disclaimer be melded into a USU disclaimer. If you are a HJF contractor, please include the following text on the "Disclaimers" page, separated by 2 line breaks from the USU disclaimers:

"The opinions and assertions expressed herein are those of the author(s) and do not reflect the official policy or position of the Henry M. Jackson Foundation for the Advancement of Military Medicine, Inc."

Additional disclaimers required if applicable to any publication/presentation by a military or civilian Federal employee, and may be warranted by a contractor:

For Conflicts of Interest - use the disclaimer below OR list relevant COIs here.

"Neither I nor my family members have a financial interest in any commercial product, service, or organization providing financial support for this research."

If you performed research involving animals or human subjects (requiring IACUC or IRB approval:

"This research protocol was reviewed and approved by the ***[insert entity name] [insert either institutional review board (IRB) or institutional animal care and use committee (IACUC)]*** *in accordance with all applicable Federal regulations governing the protection of animals in research."*

Note: if any of your research involved foreign collaborators or sites, please check with your PI to ensure Form 1325B (Proposal for USU International Research Collaboration or Education Program) was completed.

Kelsey Sheard [redacted]

Printed Name and Signature

ABSTRACT

Clueless is a novel mitochondria-associated ribonucleoprotein particle

Kelsey Sheard, PhD, 2022

Thesis directed by: Rachel Cox, PhD, Associate Professor, Biochemistry and Molecular Biology

Mitochondria require products of mitochondrial DNA and nuclear DNA to function properly, and mutations and dysregulation of either product gives rise to mitochondrial disorders and neurodegeneration. The mechanisms which regulate import of nucleus-encoded mitochondrial proteins are not well-characterized. We have demonstrated that the protein Clueless (Clu) is required for mitochondrial function and regulation in *Drosophila*. *Drosophila clueless* mutants have systemic mitochondrial dysfunctions including reduced ATP levels, mitochondria with abnormal morphology and clustered localization, drastically shortened lifespans, flight muscle defects, and sterility. We have also shown that Clu is a ribonucleoprotein. Clu physically interacts with mRNAs through its tetratricopeptide repeat domain and others have shown these mRNAs predominantly encode proteins destined for mitochondria. Using co-immunoprecipitation and mass spectrometry analysis, we have shown that Clu physically interacts with many ribosomal subunit proteins present in the small and large ribosomal subunits, multiple translation initiation and translation elongation factors, and the mitochondrial transporters

TOM20 and Porin in the outer mitochondrial membrane. Mitochondrial protein levels are also reduced in *Drosophila clu* mutants. Clu exists in cytoplasmic, mitochondria-associated aggregates ("particles") that are absent in cells mutant for various genes involved in mitochondrial function, but without any obvious decrease in Clu protein levels suggesting Clu particle formation and dissolution is a dynamic process independent of protein levels. Given that Clu associated with mRNA, Clu particles are reminiscent of ribonucleoprotein (RNP) granules: cytoplasmic, non-membranous aggregates which function in temporal and spatial post-transcriptional regulation of their mRNA cargos. An immediate mechanism to regulate gene expression under cell stress is localization of mRNA to ribonucleoprotein (RNP) granules for post-transcriptional regulation. Upregulation of RNP granules such as stress granules and P-bodies is well-characterized in cellular stress responses, where they affect transport, translation, and stability of mature mRNAs. However, we did not understand how cell stress affects Clu particle dynamics, or how these dynamics might be controlled.

Based on these findings, our current model is that Clu particle formation ties nutritional cues to mitochondrial function and that particles may be RNP granules which regulate mRNAs encoding proteins destined for mitochondrial protein import. This work aims to characterize Clu particles as a new ribonucleoprotein granule which affects mitochondrial function by (1) determining Clu particle dynamics and behavior in stressed and unstressed conditions in order to determine what conditions control Clu particle formation, (2) identifying signaling pathways that control Clu particle formation, (3) standardize using the presence of Clu particles and normal mitochondrial localization in germ cells as a control for healthy cells during live-imaging, and (4) determining how

decreased translation affects Clu particle dynamics. This is a significant goal as mitochondrial dysfunction is a major contributor to mitochondrial diseases and neurodegeneration. Better understanding this mechanism of regulating mitochondrial function will contribute knowledge to the pathology of mitochondrial diseases and neurodegeneration resulting from mitochondrial dysfunction as well as improved means to treat these disorders.

TABLE OF CONTENTS

LIST OF TABLES

CHAPTER 2: MANUSCRIPT 1 – "Visualizing the effects of oxidative damage on *Drosophila* egg chambers using live imaging"

LIST OF FIGURES

CHAPTER 1: Introduction

CHAPTER 2: MANUSCRIPT 1 – "Visualizing the effects of oxidative damage on *Drosophila* egg chambers using live imaging"

CHAPTER 3: MANUSCRIPT 2 – "Clueless forms dynamic, insulin-responsive bliss particles sensitive to stress"

CHAPTER 4: Elucidating how translation affects Clu particle dynamics

CHAPTER 1: INTRODUCTION

MITOCHONDRIAL FUNCTION AND MITOCHONDRIAL DISEASES

Mitochondria are essential organelles which supply the cell with ATP via oxidative phosphorylation and have specialized functions in fatty acid beta oxidation, heme, steroid, and nucleotide biosynthesis, intracellular Ca^{2+} homeostasis, and apoptosis (10; 80). Mitochondria arose through an endosymbiotic relationship between an archaeon (which provided the nucleus) and a protobacterium (which provided the ATP source and evolved into the first mitochondrion). Consequently, mitochondria in eukaryotic cells contain their own DNA, mitochondrial DNA (mtDNA), which encodes for 13 proteins, all of which are required for oxidative phosphorylation, 22 tRNAs, and 2 rRNAs (Figure 1, (80)) (80). Pathogenic mutations of both the mitochondrial DNA and nuclear DNA (Figure 2, (36)) as well as defects in the protein import process give rise to mitochondrial diseases, a group of severe and heterogeneous disorders with a prevalence of about 1:4300 people. Mitochondrial diseases lead to mitochondrial dysfunction and inadequate production of energy through disruptions in oxidative phosphorylation (10; 18; 37; 80). Mitochondrial disorders have multi-systemic effects, with high-energy demand tissues including the brain, muscles, heart, liver, nerves, eyes, ears and kidneys being most commonly affected and corresponding clinical manifestations of myopathy, problems with vision and hearing, heart, liver, and kidney disease, and seizures, dementia, and other cognitive disorders (18). Notably, abnormal mitochondrial morphology and dysfunction has been linked to severe neurodegenerative disorders including Parkinson's Disease, Alzheimer's disease, amyotrophic lateral sclerosis, and Huntington's Disease

(51; 73). Due to the complex presentations and compounding genetic causes of mitochondrial diseases, they are often difficult to diagnose, and there are currently no cures and few effective treatments for mitochondrial diseases. Current therapeutics for mitochondrial diseases include supportive treatment focused on alleviating symptoms, including exercise, rest, and other somatic therapy, and the use of vitamins, antioxidants, and nutritional supplements (54; 88). As such, there is a great need to understand the causes and pathologies of mitochondrial dysfunction in order to develop more targeted molecular and cellular therapeutics to correct mitochondrial diseases (40; 87). The pathological mechanisms by which mutations in mtDNA and nuclear DNA genes contribute to mitochondrial diseases are well characterized. However, there is a need for better understanding the molecular and cellular mechanisms which regulate nuclear-encoded proteins to further assist in the treatment and therapy of mitochondrial diseases.

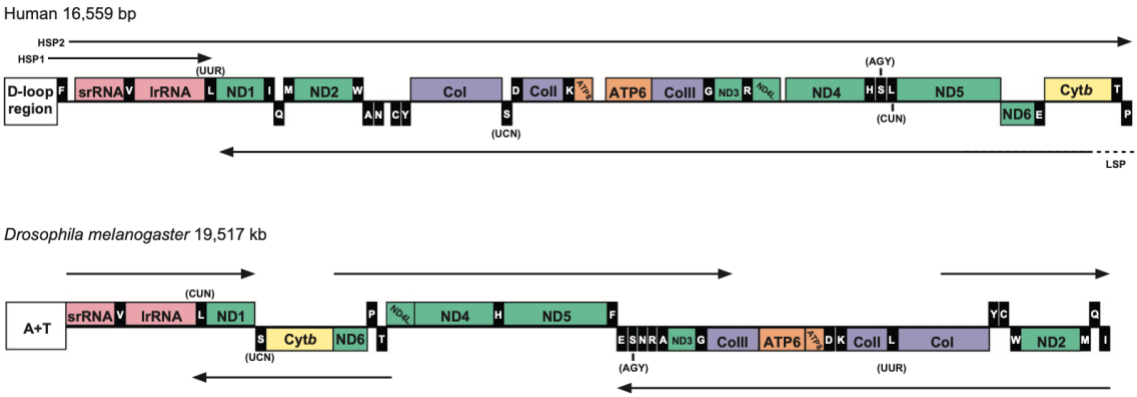

Figure 1. Comparison of human and *Drosophila* mitochondrial DNA.
Human (top) and *Drosophila* (bottom) mitochondrial DNA encode for the same products: 13 proteins necessary for oxidative phosphorylation (green), 22 tRNAs (black), and 2 rRNAs (pink) (80).

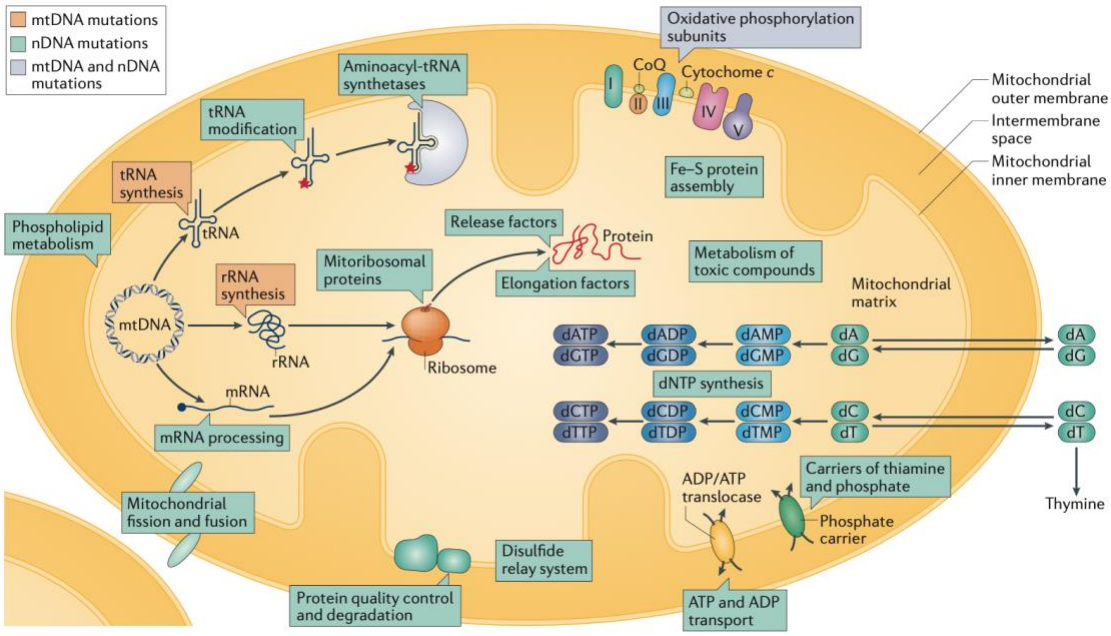

Figure 2. Mitochondrial diseases arise from mutations in both nuclear DNA and mitochondrial DNA.
Mutations in mtDNA genes can cause defects in oxidative phosphorylation subunits as well as the tRNAs and rRNAs necessary for transcription, translation, and replication of mitochondrial proteins. Mutations in nuclear DNA genes can cause defects in many mitochondrial function and biogenesis processes including oxidative phosphorylation, phospholipid metabolism, and fusion and fission (36).

Nuclear-encoded mitochondrial proteins are imported into mitochondria

Mitochondrial diseases may also arise from mutations and dysregulation of nuclear-encoded mitochondrial proteins (Figure 2). As mitochondria participate in many specialized functions, including oxidative phosphorylation, and must perform mitochondrial maintenance and replication, transcription, and translation of mtDNA, they rely heavily on the import of approximately 1700 nuclear-encoded protein products (60; 80). Nuclear-encoded mitochondrial proteins are synthesized on cytosolic ribosomes as mitochondrial precursor proteins and are subsequently imported into mitochondria through transporters on the mitochondria's outer and inner membranes in a process called

post-translational import (Figure 3A, (16)). Mitochondrial precursor proteins are directed to the appropriate mitochondrial compartment via the location of a mitochondrial targeting sequence within the precursor protein. After recognition of the targeting sequence by receptor proteins located in the TOM, translocase of the outer membrane, complex, precursor proteins are subsequently imported through the preprotein translocases located in the mitochondria's membranes, namely the TOM and TIM, translocase of the inner membrane, complexes (Figure 3B, (16)). Upon import, the mature peptides are delivered to their final destinations within the membranes, mitochondrial matrix, or inner membrane space. The TOM complex is required for the initial import of nearly all nuclear-encoded proteins (16; 60). The TOM complex also assists in inserting transmembrane proteins into the outer membrane (90). The TIM23 complex transports preproteins to the mitochondrial matrix and assists in inserting transmembrane proteins into the inner membrane (16; 60; 90). The TIM22 complex also assists in inserting those transmembrane proteins which are soluble metabolite carriers as well as TIM subunits into the inner membrane (16; 60; 90). As with mutations in mtDNA, mutations within the nuclear-encoded components of the import machinery itself will lead to mitochondrial disease and dysfunction through aberrant mitochondrial protein import (65).

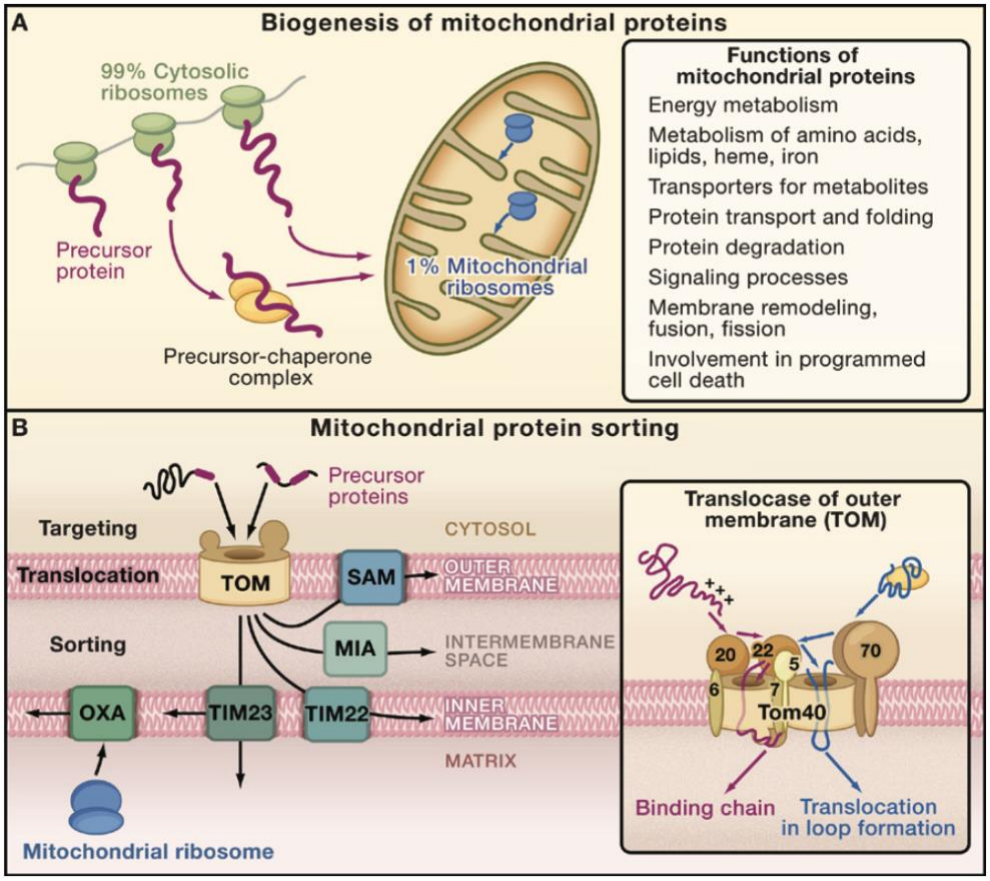

Figure 3. Mitochondrial biogenesis and function require import of nuclear encoded proteins.
(A) Most mitochondrial proteins are synthesized on cytosolic ribosomes as precursor proteins and imported into mitochondria. (B) Precursor proteins are imported via transporters in the mitochondrial membranes. The TOM (translocase of the outer membrane) complex is the initial entry point for all precursor proteins. Precursor proteins will further pass through the TIM (translocase of the inner membrane), MIA (mitochondrial inner membrane space assembly), and SAM (sorting and assembly machinery) complexes according to their final destination within the mitochondria (15).

Co-translational import model of nuclear-encoded mitochondrial proteins

In the post-translational import model, the mitochondrial preproteins are fully translated in the cytosol and then directed to mitochondria with the assistance of cytosolic chaperones (Figure 4, (2)) (1; 2; 35). Post-translational import is the best described

protein import mechanism for nuclear encoded mitochondrial import. However, multiple *in vitro* and *in vivo* studies have shown that at least a subset of nuclear-encoded mitochondrial proteins undergoes co-translational import with the assistance of cytosolic RNA-binding proteins (extensively reviewed in Ahmed and Fisher, (2)), though the mechanistic details are not well characterized. In this co-translational import model, localized translation and import of mitochondrial proteins may proceed via two pathways: 1) localization of translation competent mRNAs to the vicinity of the mitochondrial outer membrane and 2) physical association of cytosolic polysomes with the mitochondrial outer membrane (35). Genome-wide studies performed in yeast using DNA microarrays have shown that about half of the mRNAs of nuclear-encoded mitochondrial proteins are localized on mitochondrion-bound polysomes and that their 3' untranslated region is necessary for this localization (56; 74; 91). Saint-Georges et al. further identified Puf3p, a Pumilio family mRNA-binding protein in yeast, as being responsible for transporting mRNAs specifically encoding for mitochondrial proteins which contain a Puf3p binding motif in their 3' UTR region to the mitochondrial surface (2; 74). Puf3p binds to a subset of mRNAs which encode for mitochondrial proteins and is localized to the outer membrane (Figure 5a, (35)) (2; 33; 35). The association of cytosolic ribosomes with mitochondria in yeast is mediated through the nascent chain-associated complex (NAC) (2; 35; 50). The NAC facilitates the association of short nascent polypeptide chains still bound to the ribosome with mitochondria (Figure 5a, (35)). Additionally, the NAC associates with mitochondria through OM14, an outer mitochondrial membrane protein which was shown to support the co-translational import of mitochondrial proteins in yeast (49). For these reasons, both Puf3p and the NAC are

regarded as important factors in the co-translational import model of mitochondrial protein import in yeast. The proteins which mediate the localized translation and import of mitochondrial proteins in *Drosophila* and human cells are not as well characterized. Gehrke et al. showed a new role for PINK1 and Parkin, the mediators of mitophagy, in the localized translation of a group of nuclear-encoded respiratory chain components in *Drosophila* and human cells (32). PINK1 is localized to the mitochondrial outer membrane and directly interacts with mRNAs (Figure 5b, (35)). This interaction keeps the mRNAs translationally repressed until PINK1 interacts with Parkin. Upon interaction with Parkin, the translation repression is relieved, and the translation repressor Pumilio, another PUF family protein, is removed from the mRNA. Furthermore, the same study showed that both PINK1 and Pumilio interact with Tom20 in an RNA-dependent manner, and that Tom20 is also important for the localization of mRNAs to mitochondria (32; 35). Fazal et al. also recently showed that a significant number of mRNAs encoding for mitochondrial proteins are enriched at the mitochondrial outer membrane in HEK cells using APEX-seq proximity labeling (27). Though the exact mechanisms of how translation is locally regulated at the mitochondrial membrane have yet to be elucidated, these studies provide strong evidence that akin to yeast, select mitochondrial protein mRNAs are likely being targeted to and translationally regulated at the mitochondrial outer membrane in other eukaryotic cells via direct physical interactions or via still unknown RNA-binding proteins.

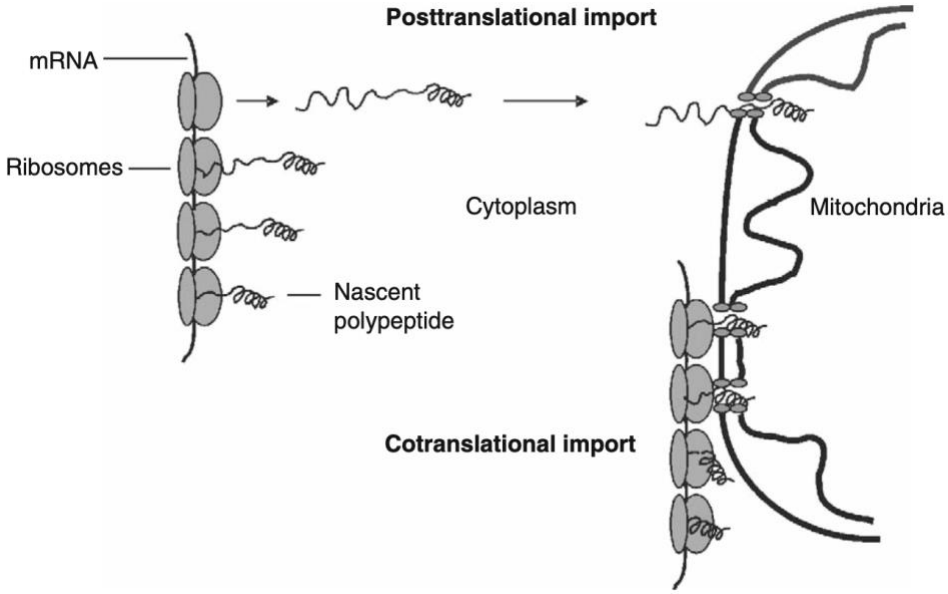

Figure 4. Post-translational import vs co-translational import into mitochondria. In the traditional post-translational import model, mitochondrial precursor proteins are fully synthesized on cytosolic ribosomes and then imported into mitochondria. In the co-translational import model, the precursor proteins are synthesized either very near or directly on the mitochondrial outer membrane and import proceeds as proteins are being translated (2).

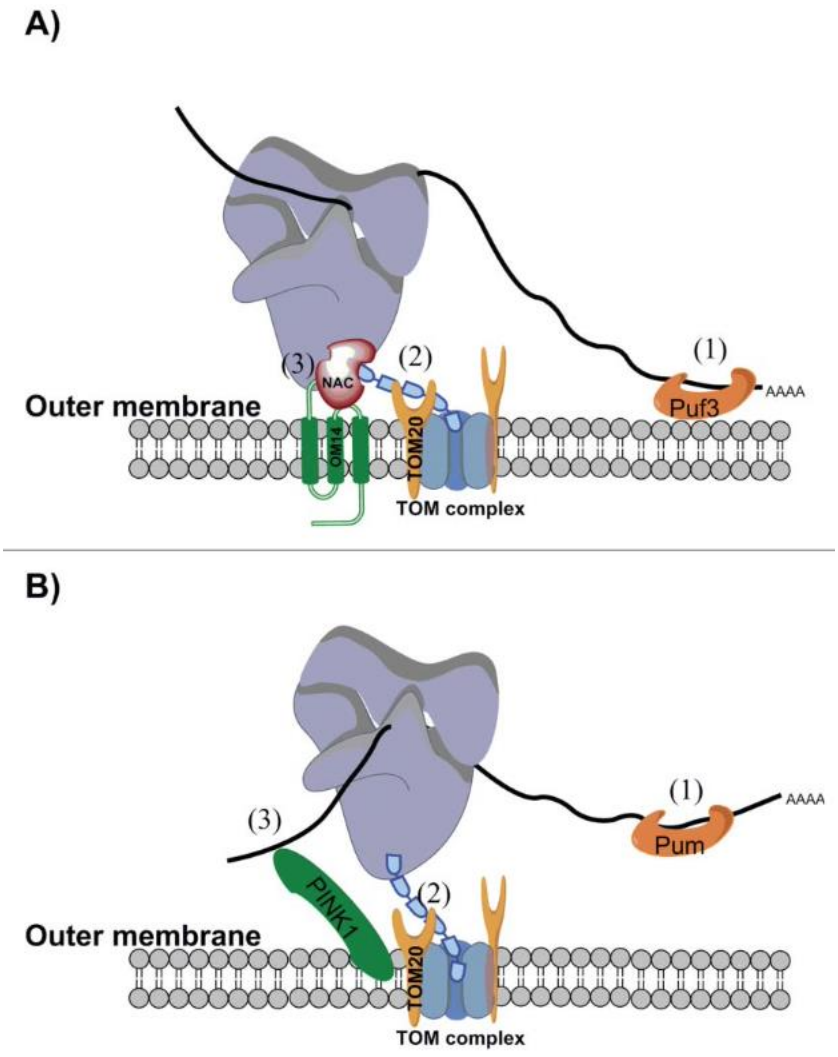

Figure 5. Localized translation near the mitochondria in yeast and *Drosophila*.
(A) The nascent chain-associated complex (NAC) and Puf3p assist in localized import of mitochondrial proteins in yeast. (B) PINK1 and Pumilio associate with mRNAs of respiratory chain components and keep them translationally repressed in *Drosophila* (50).

CLUELESS IS IMPORTANT FOR MITOCHONDRIAL FUNCTION

We have identified a nuclear-encoded gene *clueless (clu)* which is essential for proper mitochondria structure and function in *Drosophila* (21). Clueless is an RNA-binding protein which is conserved in yeast (Clu1p), *Drosophila* (Clu), humans (CLUH), and is named due to the mitochondrial clustering phenotype observed in *clu* mutants of multiple organisms (21). *Drosophila clueless* mutants have direct and systemic mitochondrial dysfunctions including reduced ATP and mitochondrial protein levels, mitochondria with abnormal morphology and clustered localization, drastically shortened lifespans, flight muscle defects, and sterility (21). These findings were also observed in *clu* larval neuroblasts which showed mitochondrial mislocalization and a significant decrease in eclosion rate but did not show a decrease in ATP levels or overall brain morphology (81). In addition, Clu binds mRNAs of proteins bound for import into the mitochondria, ribosomes present at the mitochondrial outer membrane, mitochondrial outer membrane transporters, and translation initiation and elongation factors (30; 79). Additionally, in humans, CLUH has been shown to post-transcriptionally regulate mitochondrial biogenesis by binding mitochondria-bound mRNAs (75). These characterizations signify that Clu may have a role in mitochondria-localized or co-translational import of nucleus-encoded proteins at the mitochondrial outer membrane.

Clu directly affects mitochondria and mitochondrial function

Clu is an abundant cytoplasmic protein which is required for proper mitochondrial function and morphology. Clu exists in cytoplasmic, mitochondria-associated aggregates ("particles") (Figure 6) (82). Clu directly affects mitochondria as shown by the systemic mitochondrial dysfunction phenotypes seen in *Drosophila clueless* mutants (21). Adult

flies are physically uncoordinated, shaky, and have upturned wings (Figure 7a). Their mitochondria are morphologically damaged as shown by electron microscopy and immunofluorescence (not shown), and the mitochondria improperly aggregate into clusters instead of evenly dispersing throughout the cytoplasm (Figure 7b). They also have reduced ATP levels upon eclosion and ATP levels continue to decrease until their early death after ~4 days (Figure 7c), increased mitochondrial oxidative damage (Figure 8d), and flight muscle defects (not shown) (21; 81). Loss of Clu and CLUH also leads to a decrease in the levels of mitochondrial proteins (Figure 8) (30; 82).

Clu is a conserved RNA-binding protein in yeast, *Drosophila*, and humans

Clueless is a ribonucleoprotein which is conserved in yeast (Clu1p), *Drosophila* (Clu), humans (CLUH). The protein contains a tetratricopeptide repeat (TPR) domain which shows 55% amino acid identity between Clu and CLUH and a Clu domain which shows 85% amino acid identity between Clu and Clu (Figure 9a) (79). The TPR domain was determined to be functionally important using domain deletion constructs of the protein. mRNA binding capability was measured using an oligo(dT) assay, and it was shown that Clu could no longer bind mRNA with the ΔTPR construct (Figure 9b). In addition, all of the other domains were shown to be essential as ectopic expression of the deletion constructs could not rescue survival of *clu* mutant adults, and loss of *clu* was only rescued by expression of full-length *Drosophila* Clu or Cluh (Figure 9c).

Human CLUH also binds mRNAs specifically bound for import into the mitochondria to post-transcriptionally regulate mitochondrial biogenesis (30). Several other Clu binding partners were identified via mass spectrometry, and select candidates were confirmed by co-immunoprecipitation. The binding partners included proteins

which compose the large and small ribosomal subunits (Figure 10b, 10d), the mitochondrial outer membrane transporters TOM20 and Porin (Figure 10c), and translation initiation and elongation factors (Figure 10d, Sen and Cox, unpublished) (79). Finally, the functional importance of the TPR domain in CLUH was demonstrated in a very recent study by Hémono et al (39). CLUH was shown to not only self-associate like Clu, but to also associate with nuclear-encoded mitochondrial proteins which are in close proximity to mitochondria as well as the corresponding mRNAs for these mitochondrial proteins which are localized near mitochondria. These interactions were also shown to be through CLUH's TPR domain.

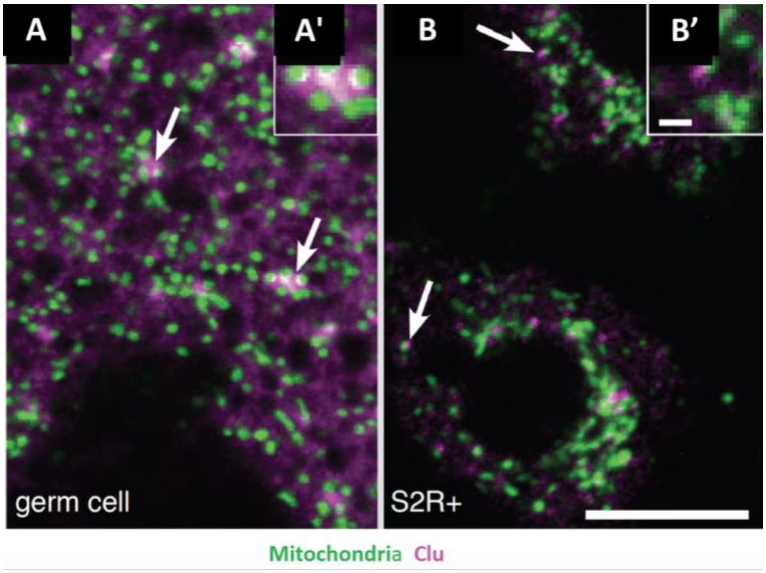

Figure 6. Clu forms cytoplasmic particles.
Clu forms mitochondria-associated particles (arrows) in germ cells (A, A') and in S2R+ cells (B, B') (82)

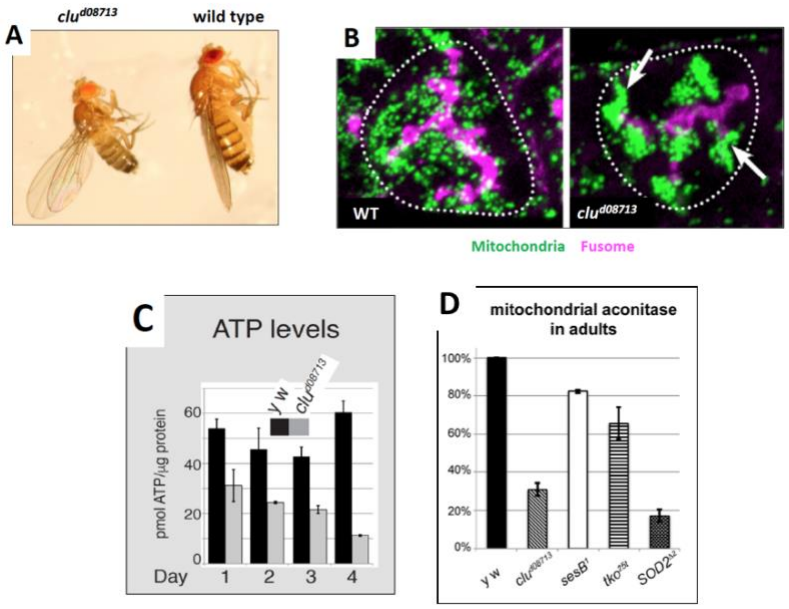

Figure 7. Loss of Clu affects mitochondrial localization and function.
Drosophila clu mutants are (A) uncoordinated, weak, and have upturned wings, (B) have mitochondria improperly aggregated into clusters (arrows) instead of evenly dispersed throughout the cytoplasm of germ cells, (C) have reduced levels of ATP upon eclosion which persists until early death, and (D) have reduced mitochondrial aconitase activity which denotes increased mitochondrial oxidative damage (21; 81).

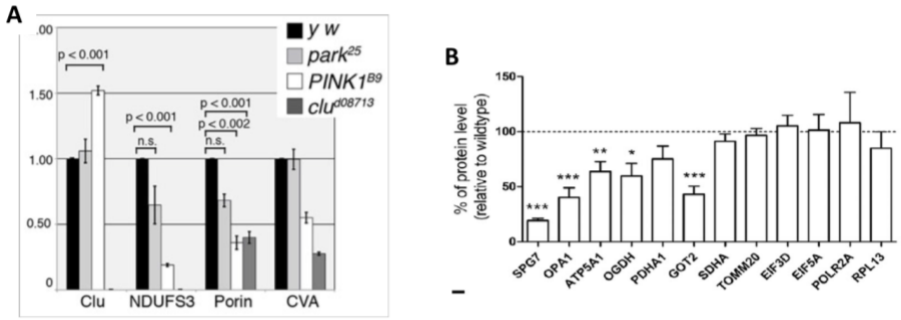

Figure 8. Loss of Clu affects mitochondrial protein levels.
(A) Quantification of Western blot analysis shows *Drosophila clu* mutants have reduced levels of the mitochondrial proteins NDUFS3, Porin, and ATP Synthase (CVA). (B) Quantification of the Western blot analysis shows *Cluh* knockout mouse embryonic fibroblasts also show decreased levels of mitochondrial proteins which are bound by CLUH (30; 82).

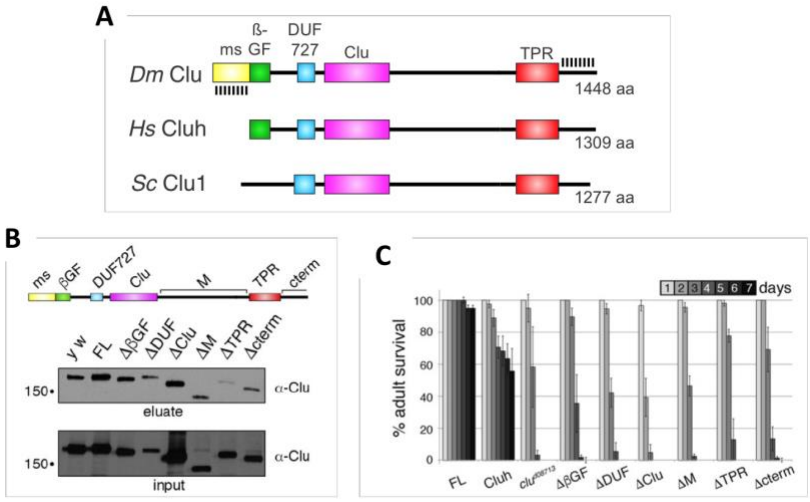

Figure 9. Clu is a conserved ribonucleoprotein.
(A) Clu is conserved from yeast to humans and contains multiple domains. (B) Deletion of the TPR domain diminishes mRNA binding in vivo. (C) Clu deletion constructs cannot rescue survival in *clu* mutants (79).

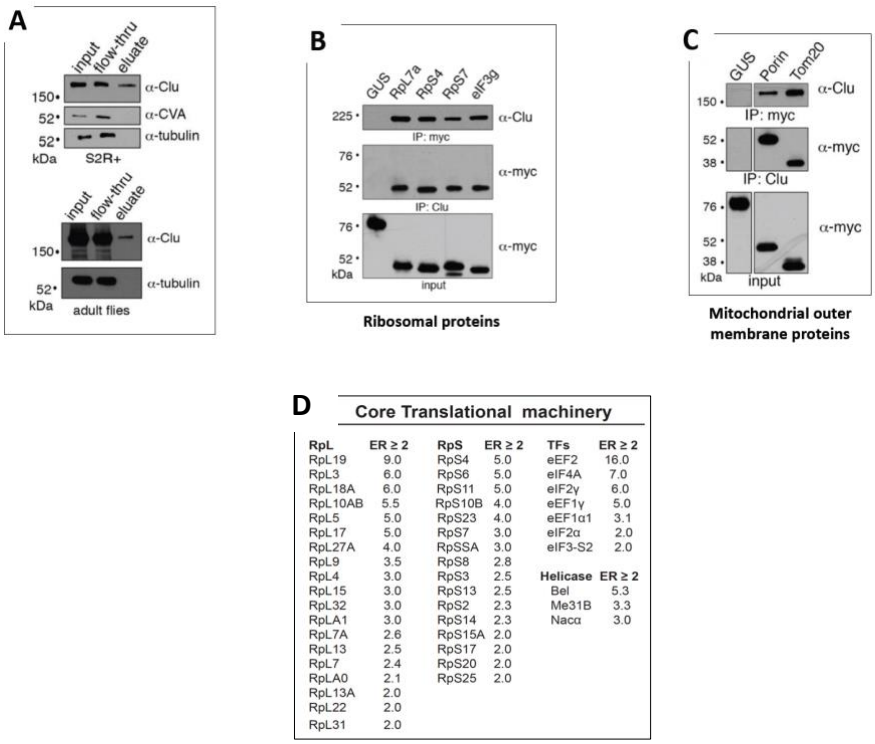

Figure 10. Clu binds mRNAs and ribosomal, mitochondrial proteins, and translation factors.
(A) An oligo(dT) column is able to retain Clu (elute) supporting that Clu binds mRNA in *Drosophila*. (B) Clu also co-IPs with ribosomal proteins and the translation initiation factor eIF3g and (C) Porin and TOM20 in transfected S2R+ cells (79; 82) (D) Mass spectrometry analysis shows that Clu associates with many ribosomal proteins and translation factors (Sen and Cox, unpublished).

CLU FORMS CYTOPLASMIC PARTICLES

Clu particles are dynamic and stress-responsive

A defining feature of Clu family members is the formation of cytoplasmic, mitochondria-associated aggregates ("particles"). The shape, size and cytoplasmic distribution of Clu particles are reminiscent of ribonucleoprotein (RNP) granules, cytoplasmic, non-membranous aggregates which function in temporal and spatial post-transcriptional regulation of their mRNA cargos (4; 5). RNP granules are present in

somatic and germ cells, and they serve to regulate gene expression by a variety of mechanisms. RNP granules in somatic cells regulate translation, mRNA decay, and gene silencing using miRNAs. RNP granules in germ cells regulate translation of maternal mRNAs and gene silencing using transmission of piRNAs (5). RNP granules have well-characterized roles in cellular stress responses, where regulation of transport, translation, and stability of mature mRNAs is an acute response to cellular stress (99). Non-translating mRNAs are redistributed to processing bodies (P-bodies) and stress granules, the two major types of RNP granules in the cytoplasm, for decay or storage under cellular stress (23; 59; 99). Wild-type flies show robust particles in germ cells (Figure 11a). Clu particles are also no visible in *pink1* and *parkin* mutant flies which are not able to complete mitophagy (Figures 11b and 11c) (21).

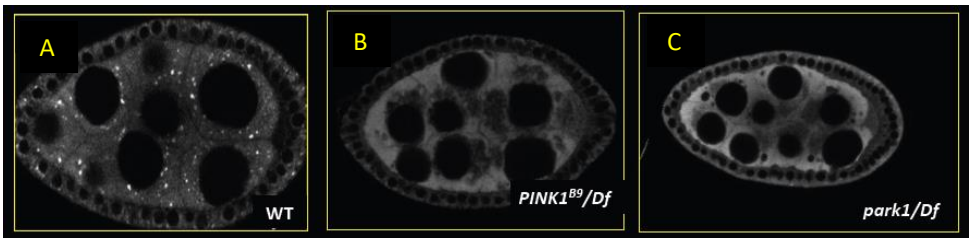

Figure 11. Clu particles are sensitive to mitochondrial stress.
(A) Wild-type flies form Clu particles in the cytoplasm. (B, C) Clu particles are absent in *parkin,* and *PINK1* mutants. (B, C) PTEN-induced putative kinase 1 (PINK1) senses oxidative stress using the membrane potential of the outer membrane and recruits Parkin (park1), an E3 ubiquitin ligase, to start mitophagy of compromised mitochondria.

Clu particles are reminiscent of other stress-responsive particles

Cells have evolved a variety of different responses to adapt to environmental fluctuations and stressors such as heat shock, oxidative stress, osmotic stress, nutritional

stress, and toxicity conditions (22; 55)**.** A prominent cellular response to stress is reorganization of the cell's transcriptome such that a set of global, environmental stress response genes and a set of stress-specific genes in yeast, *Drosophila*, and mammals are expressed as needed (22; 59; 99). The set of global genes are responsive to any environmental stress, and the set of stress-specific genes are only responsive to specific stressors. Genes involved in growth-related processes, RNA metabolism, protein synthesis, and ribosomal protein synthesis are typically downregulated, and genes involved in carbohydrate metabolism (energy production), transport and metabolism, detoxification and antioxidant production, protein metabolism (molecular chaperones and genes involved in ubiquitin-dependent degradation), intracellular signaling, and DNA damage repair are typically upregulated during stress responses (22; 31). An immediate mechanism to accomplish this gene regulation is localization of mRNA to RNP granules for post-transcriptional regulation, where the stress-responsive mRNAs are either selectively degraded or stabilized. Ribonucleoprotein granules regulate mRNA metabolism in somatic cell types and in the germ line (45; 77). *Drosophila* germ cells contain several RNP granules unique to the germ line which behave in the same manner as other known RNP granules during stress responses: they increase in number and size following stress, regulate mRNA decay and translation, they change in morphology, cellular localization, and composition. Furthermore, these changes are reversible upon removal of the stress. Maternal P-body-like granules in *Drosophila* oocytes are functionally comparable to somatic P-bodies and have a similar composition (45). Maternal RNP granules and P-bodies contain components of the 5'-3' mRNA decapping decay pathway as well as other proteins such as the translational repressor Trailerhitch

(Scd6p in yeast), the cap binding translation initiation factor eIF4E, and its repressor Cup (45; 77; 89). Clu particles also are large and robust in *Drosophila* germ cells, are responsive to mitochondrial stress, bind the translation initiation factor eIF3g as well as bind and post-transcriptionally regulate mitochondria-bound mRNAs. Both Clu and CLUH are cytosolic mRNA-binding proteins, with Clu binding ribosomes and mitochondrial outer membrane transporters and CLUH binding nuclear-encoded mRNAs bound for transport into the mitochondria. Schatton et al. further established that CLUH exerts its function through post-transcriptional regulation of mitochondrial protein expression, and Sen et al. proposed a working model in which mRNA- and ribosome-bound Clu particles associate with mitochondrial transporters at the mitochondrial outer membrane to function in co-translational import of mitochondrial proteins (75; 82). In brief, under stress-free cellular conditions, healthy mitochondria are co-translationally importing nuclear-encoded mitochondrial protein normally, and Clu particles may be localizing these proteins to mitochondrial outer membrane transporters (Figure 12a, (82)). Under stressed cellular conditions or when mitochondria are damaged, mitochondrial protein import is downregulated and Clu particles disperse (Figure 12b, (82)). Integrating our previous findings with the response of Clu particles to stress, the goal of this work is to investigate Clu particles as a novel mitochondria-associated ribonucleoprotein granule which supports mitochondrial function through regulation of mRNAs and proteins bound for co-translational import.

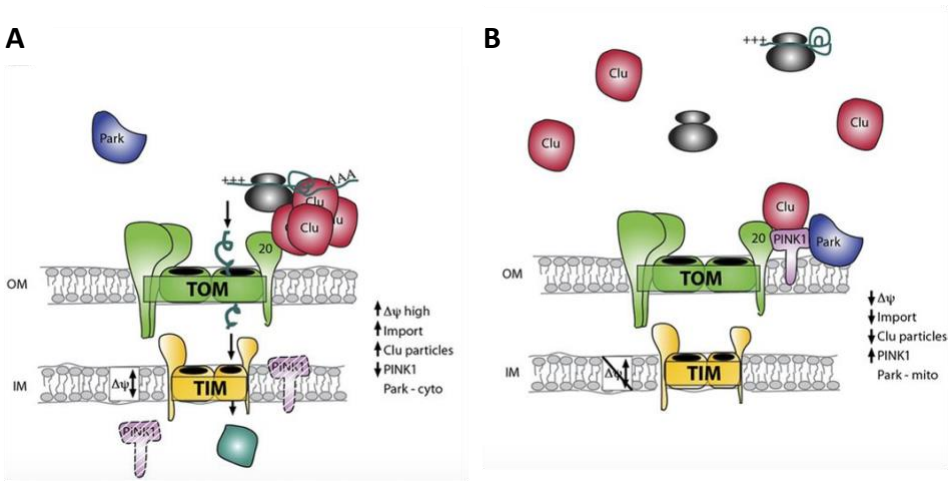

Figure 12. Working model of Clu particles' potential role in co-translational import of mitochondrial proteins.
(A) In healthy cellular conditions, Clu particles are present and mitochondrial proteins are co-translationally imported. (B) In stressed conditions, Clu particles disperse, translational machinery is not localized to the outer membrane, and co-translational import of mitochondrial proteins is impaired (82).

SIGNIFICANCE

The evidence amassed thus far shows that Clu is essential for proper mitochondrial structure and function and that it regulates mitochondrial function through regulation of mitochondrial mRNAs and proteins. However, we have yet to discover the nature of Clu interactions with mitochondria or how these interactions affect mitochondrial function. Clu particles possess many of the traits which define other RNP granules, with the exception of their contrasting reaction to stress. This work aims to define Clu particles as a new, highly conserved ribonucleoprotein particle which support mitochondrial function through post-transcriptional regulation of nuclear-encoded proteins. This is a significant goal as mitochondrial dysfunction is a major contributor to mitochondrial diseases and neurodegeneration. Better understanding this mechanism of regulating mitochondrial function will contribute knowledge to the pathology of

mitochondrial diseases and neurodegeneration resulting from mitochondrial dysfunction as well as improved means to treat these disorders.

HYPOTHESIS AND SPECIFIC AIMS

Mitochondria contain their own DNA whose products are required for ATP synthesis, and they also rely heavily on the import of approximately 1700 nuclear-encoded mitochondrial protein products necessary for mitochondrial maintenance, mtDNA replication, transcription, and translation, and specialized mitochondrial activities. Mutations in mtDNA and improperly functioning mitochondria have been implicated in severe mitochondrial diseases, with high-energy demand tissues such as the heart, brain, and muscles being affected most severely. Of note, mitochondrial dysfunction has also been linked to severe neurodegenerative disorders such as Parkinson's Disease. As such, it is paramount that healthy mitochondria are selected for and propagated through maternal inheritance and that there is also proper availability and regulation of the nuclear-encoded products which they depend upon.

We have shown that the nuclear-encoded gene *clueless (clu)* is important for properly functioning mitochondria. Several pieces of evidence show that Clu directly affects mitochondria: (1) it binds mRNAs bound for import into the mitochondria, ribosomes present at the mitochondrial outer membrane, and the mitochondrial outer membrane transport proteins TOM20 and Porin, (2) it genetically interacts with the mitophagy mediators PINK1 and Parkin, and (3) loss of *clu* in *Drosophila* leads to reduced ATP levels, physically damaged mitochondria, mitochondrial oxidative damage, and mislocalized mitochondria which aggregate into clusters. Clu exists in cytoplasmic, mitochondria-associated aggregates ("particles"). Clu particles are reminiscent of

ribonucleoprotein (RNP) granules, cytoplasmic, non-membranous aggregates which function in temporal and spatial post-transcriptional regulation of their mRNA cargos. Examples of RNPs include stress granules, processing bodies, and U bodies, three different RNPs which increase in number in response to cellular stress. In contrast to these examples, Clu particles are no longer visible under mitochondrial stress. Despite these findings, little is known about how Clu particles interact with mitochondria or how these interactions affect mitochondrial function. **We hypothesize that Clu particles are a novel mitochondria-associated ribonucleoprotein which affects mitochondrial function through regulation of mRNAs and proteins bound for mitochondrial import.** We propose to test this hypothesis through the following specific aims:

Aim 1. Determine the dynamics of Clu particles. Clu particles are dynamic, and they disperse and re-form under various conditions. We will use fixed- and live-imaging to visualize the real-time changes in Clu particles using female flies with and without particles.

Aim 2. Determine the effect of Clu particles on mitochondrial function. If Clu particles are sequestering mRNAs and proteins for mitochondrial import, we expect that the absence of particles will lead to differences in mitochondrial protein levels and mitochondrial function. We will use Western blotting and functional assays of mitochondria to determine how Clu particles affect mitochondria using female flies with and without particles.

CHAPTER 2: MANUSCRIPT 1 – "Visualizing the effects of oxidative damage on *Drosophila* egg chambers using live imaging"

Authors:

Kelsey M. Sheard[1] and Rachel T. Cox[1]

Affiliations:

[1]Department of Biochemistry and Molecular Biology, Uniformed Services University

SUMMARY

The objective of this protocol is to use live imaging to visualize the effects of oxidative damage on the localization and dynamics of subcellular structures in *Drosophila* ovaries.

ABSTRACT

Live imaging of *Drosophila melanogaster* ovaries has been instrumental in understanding a variety of basic cellular processes during development, including ribonucleoprotein particle movement, mRNA localization, organelle movement, and cytoskeletal dynamics. There are several methods for live imaging that have been developed. Due to the fact that each method involves dissecting individual ovarioles placed in media or halocarbon oil, cellular damage due to hypoxia and/or physical manipulation will inevitably occur over time. One downstream effect of hypoxia is to increase oxidative damage in the cells. The purpose of this protocol is to use live imaging to visualize the effects of oxidative damage on the localization and dynamics of subcellular structures in *Drosophila* ovaries after induction of controlled cellular damage. Here, we use hydrogen peroxide to induce cellular oxidative damage and give examples of the effects of such damage on two subcellular structures, mitochondria and Clu bliss particles. However, this method is applicable to any subcellular structure. The limitations are that hydrogen peroxide can only be added to aqueous media and would not work for imaging that uses halocarbon oil. The advantages are that hydrogen peroxide is readily available and inexpensive, acts quickly, its concentrations can be modulated, and oxidative damage is a good approximation of damage caused by hypoxia as well as general tissue damage due to manipulation.

INTRODUCTION

Multiple different cellular stressors may arise during the experimental culture and manipulation of tissues ex vivo, including heat shock, oxidative stress, osmotic stress, nutritional stress, and toxicity conditions. Live imaging is a powerful tool used to visualize real-time changes in ex vivo tissues after experimental treatment and manipulation. Fine tissue dissections and manipulation take practice, and the amount of time from dissection to imaging can vary depending on experience. The rationale for developing this method is based on the concern that preparing tissue for live imaging can cause cellular stress during dissection and imaging preparation. This could be particularly problematic for processes sensitive to changes in cellular metabolism and available oxygen levels, such as mitochondrial function. While having a parallel wild type sample is an important control, there is still the possibility that some or all observed changes in subcellular structures could be due to damage or cell stress from dissection and do not reflect normal physiology or the treatment or mutation being studied.

To address this potential problem, we use hydrogen peroxide addition during live imaging in order to induce cellular oxidative damage (106). The purpose of this method is to induce damage to tissues in order to monitor the effect on subcellular structures. This protocol is useful for two purposes: 1) determining whether changes in subcellular localization of the structure of interest is due to the stress caused by inexperienced dissection and 2) once the researcher is confident with the dissection techniques described to monitor the effect of controlled stress on the structure of interest. Here we show two examples of how increased oxidative damage causes changes in two subcellular structures, mitochondria and Clu bliss particles. To do this, we use the *Drosophila* ovary which is a common model for live imaging studies. The first example

examines mitochondrial localization. In our experience, normal mitochondrial localization in female germ cells is highly sensitive to perturbations and can act as a harbinger of cellular stress. Mitochondria in *Drosophila* female germ cells are normally evenly dispersed throughout the cytoplasm (19). Hydrogen peroxide addition causes the organelles to quickly mislocalize and cluster in a similar manner to various mutations (21; 82; 84). The second example are bliss particles formed by Clueless (Clu). Clu is a ribonucleoprotein which is diffuse throughout the cytoplasm; however, it also forms mitochondria-associated particles under optimal cellular conditions (84). Because the presence of Clu particles is dependent upon healthy cellular conditions, we have termed them "bliss" particles (21; 79; 84). Addition of hydrogen peroxide causes these particles to quickly disperse and become homogeneous in the cytoplasm (84). In the course of our studies, we have observed changes in localization of both of these subcellular structures, but only after performing live imaging studies could we fully appreciate the effect of cellular stress and oxidative damage on localization and dynamics of mitochondria and bliss particles.

The utility of this protocol as an addition to already established or alternative methods depends on several factors. First, the imaging protocol must be amenable to drug-addition. If the sample is mounted under a coverslip and in halocarbon oil, this method would not be possible (67). H_2O_2 addition causes a rapid rise in oxidative damage, therefore, this timescale may not be appropriate. Oxidative damage may be regarded as a proxy for hypoxia; however, it may be too harsh or too generalized to function as an appropriate control for damage for certain subcellular components. Finally, for imaging experiments that last hours such as those following a developmental process,

H_2O_2 addition may be too strong (for example, (58)). Testing a concentration curve may overcome this limitation.

PROTOCOL

Preparation of dissection and imaging media

Note: The media best suited for this live imaging experiment contains Schneider's *Drosophila* media containing 15% heat inactivated fetal bovine serum, 0.6X Pen-Strep, and 200 μg/mL bovine insulin, hereafter referred to as Complete Schneider's media.

1. Perform the media preparation under sterile conditions to ensure that it does not become contaminated. The media was developed to support *Drosophila* ovarioles for extended periods of time (70).

1.1. Add 15% heat inactivated fetal bovine serum, 0.6X Pen-Strep, and 200 μg/mL bovine insulin to the Schneider's media.

1.2. Mix the contents well and store at 4 °C overnight. Note: Insulin does not dissolve completely in the Complete Schneider's media, and you will notice a precipitate settle in the bottom of the tube.

1.3. Make aliquots of the media, being sure to leave the precipitate as it will interfere with imaging.

Note: This solution may be used within one month if stored in aliquots at 4 °C.

1. Collection of *Drosophila* for dissection

Note: Detailed *Drosophila* collection and dissection procedures may also be found in Weil et al. 2012 and Parker et al. 2017 (66; 104).

1. For optimal female germ cell imaging, first prepare a vial containing standard cornmeal fly food and a dab of wet yeast paste that is the consistency of peanut butter. This ensures the female flies are well-fed and will produce all follicle developmental stages for imaging.

2. For optimally healthy flies, collect 0-1 day old females and transfer with males into a fly food vial containing wet yeast paste. **Note:** Make sure the sleeping flies do not contact the yeast paste as they can stick to it.

2.1. Feed the flies 3-7 days, changing the vial and the yeast paste daily.

Note: Make sure the yeast paste contacts the fly food so it does not dry out.

2. *Drosophila* ovary dissection

Note: It is important to prepare the media solutions fresh because hydrogen peroxide is susceptible to oxidation and TMRE degrades over time.

1. Right before dissection, in Complete Schneider's media, prepare a fresh aliquot of 2 μM H_2O_2 solution, a fresh aliquot of 46 nM tetramethylrhodamine, ethyl ester (TMRE), and a fresh aliquot of a 46 nM TMRE solution containing 2μM H_2O_2.

2. For ovary dissection, you will need two pairs of fine forceps and a pair of

electrolytically sharpened tungsten needles (9). To dissect the ovaries, fill 2-3 wells of a glass bottom dissecting dish (watch glass) with Complete Schneider's that has been warmed to room temperature.

3. Anaesthetize the vial of fattened flies with carbon dioxide and segregate the desired number of female flies to be dissected.

3.1. Place a single fly in the media using forceps.

4. Under a dissecting microscope, gently grasp the fly by the thorax using one pair of fine forceps. With the other pair of forceps, grasp the posterior, and gently pull to remove the ovaries.

Note: if the ovaries do not come out smoothly using this method, the entire abdomen may also be removed from the fly, and the ovaries can be gently squeezed out of either end of the abdomen using forceps.

5. Remove any extraneous cuticle or tissue, then transfer the ovaries to a new well containing fresh media. **Note:** the ovaries should still be moving from the surrounding muscle sheath.

3. Preparing ovarioles for imaging

1. Using sharpened tungsten needles, gently tease the ovarioles apart, taking care to remove the surrounding muscle sheath. (Figure 1)

2. Gently tease away any muscle sheath and nerve fibers attached to the isolated ovarioles. (Figure 2) Note: If the muscle sheath is not removed, the ovariole will twitch and move, causing problems with image acquisition. (Video 1)

3. If the subcellular structures of interest are endogenously labeled, proceed to Step 3.4.

If the structures of interest will be labeled with a fluorescent dye, proceed to Section 4.

4. Once the ovarioles have been cleanly dissected, using a micropipette, transfer them in a 100 µL drop of Complete Schneider's imaging media into the glass depression of a MatTek glass bottom dish. The individual ovarioles will sink to the bottom of the droplet.

5. Proceed to Section 5 for imaging.

Note: For imaging mitochondria and Clu bliss particles, no more than five-ten minutes should elapse from the start of dissection to imaging.

4. Staining mitochondria with TMRE

Note: Additional detailed procedures on live staining of mitochondria with fluorescent dyes may be found in Parker et al. 2017 (6).

1. After step 3.3, transfer the isolated ovarioles in a 100 µL drop of 46 nM TMRE media into the glass depression of a MatTek glass bottom dish. The individual ovarioles will sink to the bottom of the droplet.

2. Incubate at room temperature for 20 minutes. Place the lid onto the glass-bottom dish and place the dish into a covered box for the duration of the experiment to protect from light. Note: After incubation, samples can be imaged directly with no washes.

Note: Repeat steps 1 and 2 to prepare at least two dishes of TMRE-labeled ovarioles, one to serve as an experimental group and one to serve as a control.

5. Live image acquisition

1. Once the ovarioles are mounted, place one of the glass bottom dishes onto the

microscope and configure the imaging parameters as necessary. The optimum excitation/emission wavelengths for the TMRE used here are 549nm/574nm (AnaSpec Inc., Fremont, CA).

2. After locating the desired field of view, acquire still images or brief videos of one or more ovarioles as desired as a record of pre-treatment conditions.

6. Addition of hydrogen peroxide during imaging

1. Pause live imaging, remove the lid from the glass bottom dish, and carefully add 100 µL of the 2 µM H_2O_2 solution to the dish using a micropipette if imaging endogenously labeled structures. If imaging mitochondria, carefully add 100 µL of the 46 nM TMRE + 2 µM H_2O_2 solution to the dish using a micropipette (Video 2). Note: Avoid breaking the surface of the existing media droplet or adding the solution too quickly so as not to displace the ovarioles resting on the bottom of the dish (Video 2).

2. Replace the dish lid (dish cover), relocate and refocus the desired field of view if necessary, and resume imaging (Video 3, Video 4, Figure 3, Figure 4). Note: Take care to resume imaging as quickly as possible after H_2O_2 addition as the experimental treatment is time-sensitive (Video 5).

3. Acquire still images or brief videos of one or more ovarioles as desired. This will serve as a record of post-treatment conditions.

4. For the control, place the second glass bottom dish onto the microscope and repeat Section 5

5. Repeat step 6.1, this time adding 100 µL of TMRE-only media to the dish. If imaging endogenously labeled structures, add 100 µL of the Complete Schneider's media-only solution.

6. Repeat steps 6.2 and 6.3 to acquire data for the control group.

Note: For imaging mitochondria and Clu bliss particles, no more than three-five minutes should elapse from the addition of hydrogen peroxide to imaging.

REPRESENTATIVE RESULTS

The described protocols can be used to study the effects of hydrogen peroxide during live imaging of *Drosophila* ovaries. As shown in Figure 3 and Figure 4 and Video 3 and Video 4, this procedure provides an effective means to visualize tissue changes and dynamics after experimental treatment in real-time. Importantly, this protocol is specific for the addition of H_2O_2 to ovarioles while imaging; however, it may be adapted for the exogenous addition of other drugs or reagents of interest. In addition, follicles may be labeled with any fluorescent dyes of interest (e.g. tetramethylrhodamine (TMRE), LysoTracker) prior to imaging (Video 3). The most critical steps to obtaining clear imaging results are 1) the proper dissection and isolation of single ovarioles with all contractile elements removed (Figure 1 and Figure 2) and 2) the speed at which imaging is restarted after hydrogen peroxide addition. Video 4 is an illustration of a properly dissected follicle which remains steady throughout the imaging duration as compared to Video 1, which illustrates a poorly dissected follicle exiting the field of view during imaging. Video 5 is an illustration in which the H_2O_2 effects on TMRE-labeled mitochondria have already progressed prior to the start of imaging as a result of too much elapsed time. As compared to Video 3 in which imaging was restarted immediately after hydrogen peroxide addition (time 0) and intact, dispersed mitochondria are still visible, the mitochondria in Video 5 have already began to visibly clump and lose their

membrane potential upon the restart of imaging. This issue is mostly attributed to disruption of the sample positions during H_2O_2 addition and can be alleviated by following the technique to keep the imaging media and sample position intact (Video 2). Of note, in control experiments performed without H_2O_2 added to the media, the mitochondria in follicles remains properly dispersed, and the TMRE dye remains sequestered in the mitochondria.

DISCUSSION

This protocol could be a useful addition as a control for artifacts due to ovary dissection and tissue incubation for any live imaging experiment. The critical steps are similar to those found for other live imaging protocols. Learning how to dissect whole *Drosophila* ovaries takes practice; however, this skill can usually be learned fairly quickly with the appropriate dissection tools. More difficult to master is removing the muscle enveloping the ovaries and each ovariole (44). This must be done to ensure muscle contractions do not interfere with image acquisition. If using sharpened tungsten needles to do this does not prove successful, the germarium at the tip of the ovariole can be grasped with forceps and the ovariole pulled from the muscle sheath. However, this technique is problematic if the earliest developmental stages are to be examined because they can become damaged. Another key step is to not dislodge the ovarioles resting on the bottom of the dish when adding H_2O_2. An additional important aspect is shared by all live imaging: the researcher should ensure that the structure of interest is fluorescently well-labeled before treatment. The dishes used here (MatTek Life Sciences, Ashland, MA) are commonly used for live imaging; however, any dish or slide with a glass coverslip on the bottom or even a large glass coverslip should work as long as the drop of

media can be covered to prevent media evaporation. While we use a particular microscope, any inverted microscope with an objective of sufficient magnification to see the subcellular structure in question and an attached camera that has sufficient resolution and image capture rate should work.

While our laboratory is primarily interested in mitochondrial function, this method could be helpful examining the dynamics and localization of any subcellular structure or organelle, such as the nucleus, cytoskeleton or endoplasmic reticulum. However, this method has limitations. In order to add hydrogen peroxide, the tissue must be in an aqueous media. An alternative method for live imaging is to use halocarbon oil, which has been instrumental in describing many important processes in *Drosophila* ovarioles including the first example of dynamic movement of GFP in a model organism (67; 100). In addition, adding hydrogen peroxide to the media causes wide-spread oxidative damage which may be too general an insult to the tissue to be informative for the cellular process of interest, particularly for longer experiments examining development. Though it may not be feasible to perform experiments which require visualizing the cell over long periods of time due to this rapid, extensive, and likely irreversible oxidative damage, we have seen that the acute hydrogen peroxide treatment we have described is applicable to most stages of oogenesis as we are able to see the same effects in most stages within the imaging time period. Given the low cost and ease of the protocol, it may be a useful control for damage and can be used as a treatment before fixation and antibody labeling as well.

In our hands, H_2O_2 treatment mimics the changes in mitochondrial mislocalization and Clu bliss particle dispersion that we see in various *Drosophila*

mutants. It also mimics results we see for new researchers in the lab learning dissection techniques. Therefore, this method clearly revealed that sample preparation and general cellular stress can lead to unexpected and previously unexplained changes to mitochondrial mislocalization and the presence of bliss particles. Moving this technique forward, hydrogen peroxide concentrations could be modulated using a higher or lower concentration. If a cellular effect is seen using a lower concentration, it is possible the stress phenotype may be reversible by replacing the media with Complete Schneider's. Different cell stressors such as carbonyl cyanide m-chlorophenyl hydrazone (CCCP), arsenite or simple heat shock might prove useful for general cellular stress for other subcellular structures. Since live imaging of ex vivo tissues requires manual manipulation and incubation in different media, this control should be a useful addition to ensure any observations are as close to normal physiology as possible.

ACKNOWLEDGEMENTS

We would like to thank Dr. Jeremy Smyth for imaging support and Ann C. Shenk for illustrations, production and videography. This work was supported by the National Institutes of Health (1R01GM127938 to R.T.C.).

MAIN FIGURES

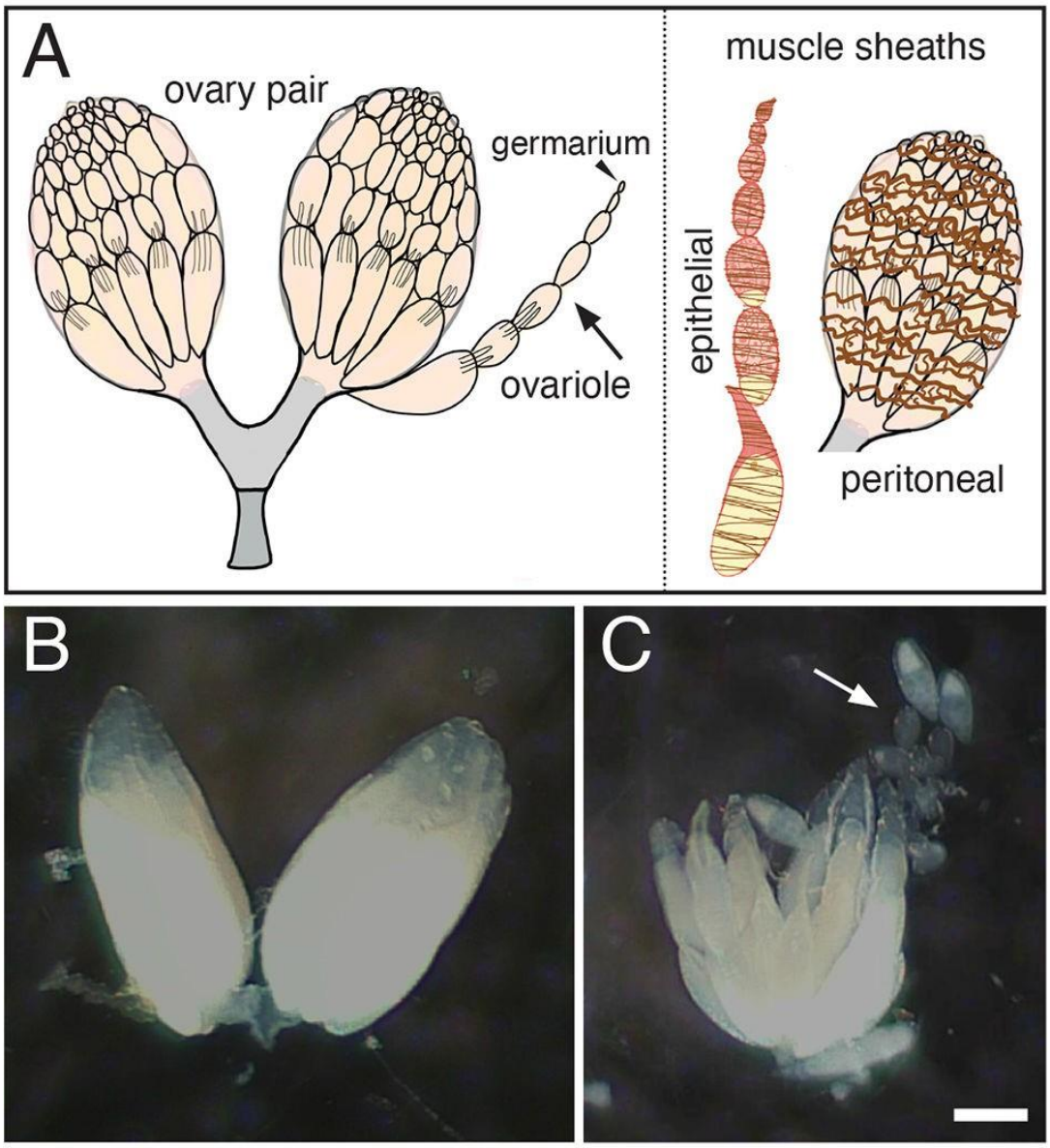

Figure 1. Isolation of single ovarioles from *Drosophila* ovaries.
(A) Cartoon indicating a pair of ovaries, a single ovariole (arrow) with the germarium at the tip (arrowhead) and the two muscle sheaths that surround the ovariole (brown, epithelial) and the ovary (brown, peritoneal). (B) Dissected *Drosophila* ovary. (C) Subsequent separation of the teased ovary into individual ovarioles (arrow). Scale bar = 100 uM

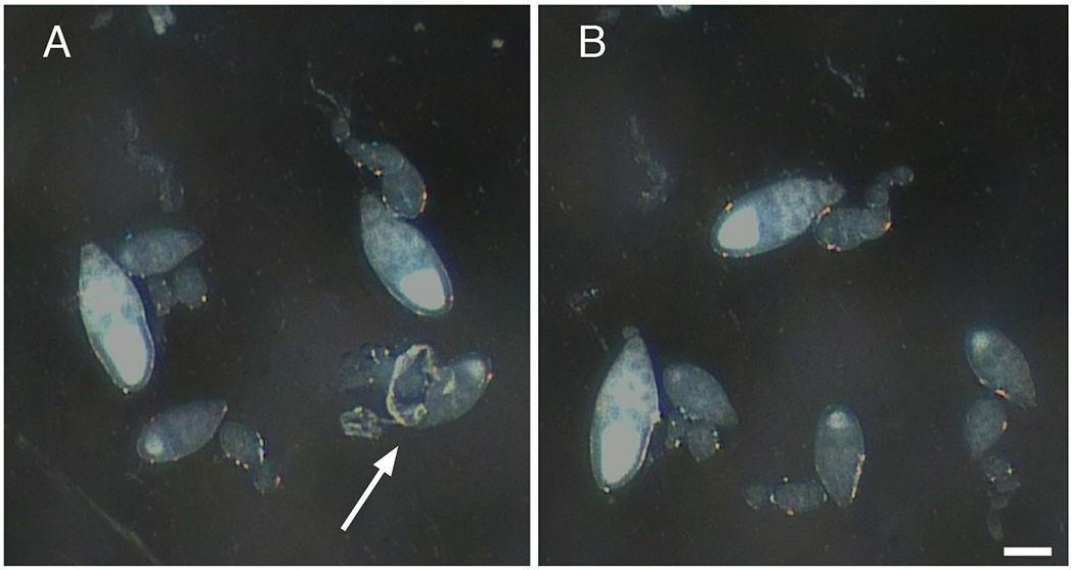

Figure 2. Removal of nerve fibers and contractile elements from single ovarioles. (A) Single ovariole with remnants of nerve tissue and the muscle sheath still attached (arrow). (B) Gentle removal of all remaining tissue attached to ovariole in A (arrow). Scale bar = 100 μm

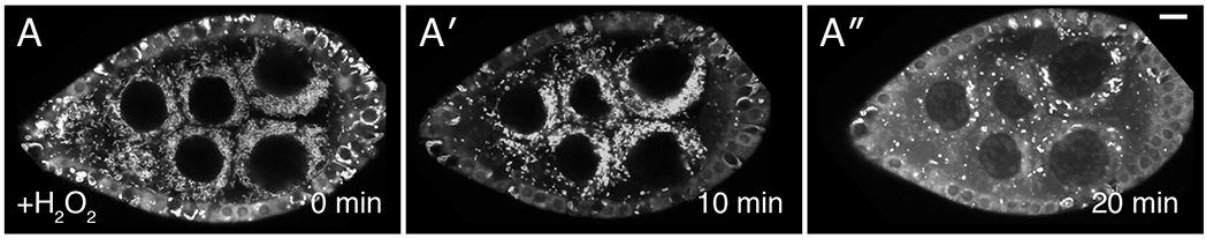

Figure 3. H_2O_2 causes mitochondrial mislocalization.
(A-A″) Live-image stills of a well-fed *clu*^{CA06604} (Clu::GFP flies) follicle. Addition of H_2O_2 causes mitochondria to clump over the duration of imaging. TMRE labeling of mitochondria indicates that mitochondria are initially dispersed at time 0 (A), and that mitochondria start to clump after H_2O_2 addition (A′) At a later time-point, the TMRE labeling becomes spotty due to mitochondria losing their membrane potential and therefore their ability to sequester the dye (A″). White = TMRE (A-A″). Scale bars: 10 μm in A for A-A″ (84).

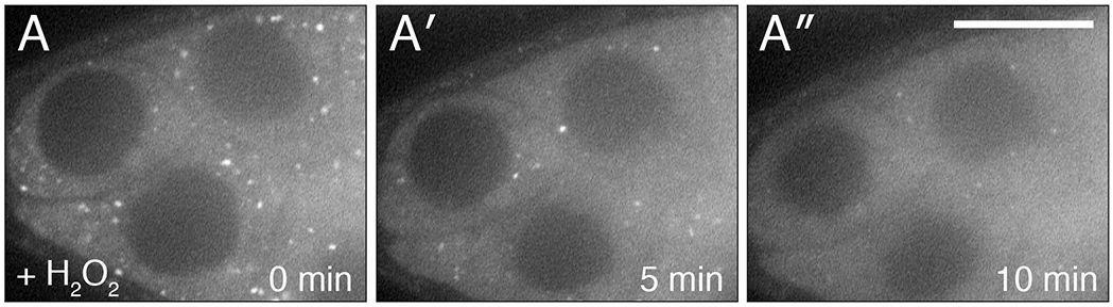

Figure 4. H_2O_2 disperses Clu.
(A-A″) Live-image stills of a well-fed *clu*^{CA06604} follicle. Addition of H_2O_2 causes particles to disperse and come homogeneous in the cytoplasm over the duration of imaging. White = Clu::GFP (A-A″). Scale bar: 40μm in A″ for A-A″ (84).

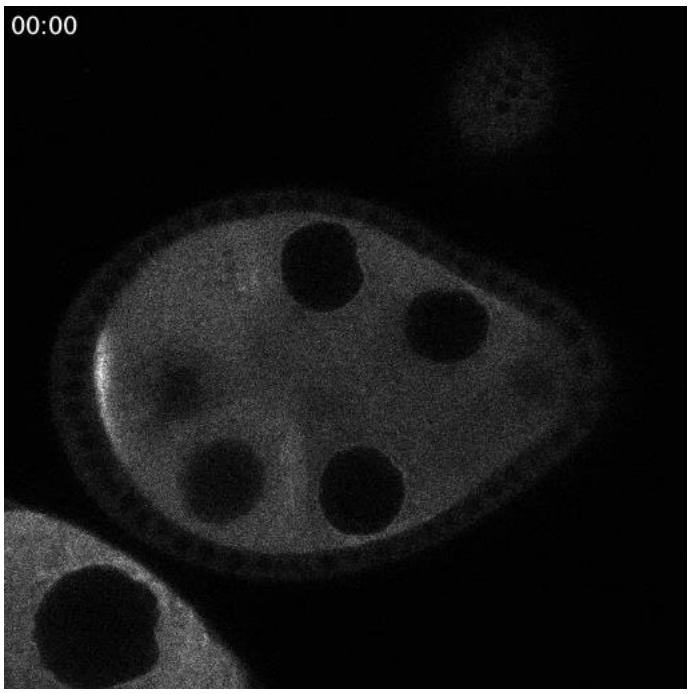

Video 1.

Follicle from a *clu*^{CA06604} female. As described in Figure 2, failure to remove nerve fiber contractile elements from single ovarioles will cause marked drifting and movement of the ovarioles during imaging and subsequent inability to analyze imaging data. White = Clu::GFP.

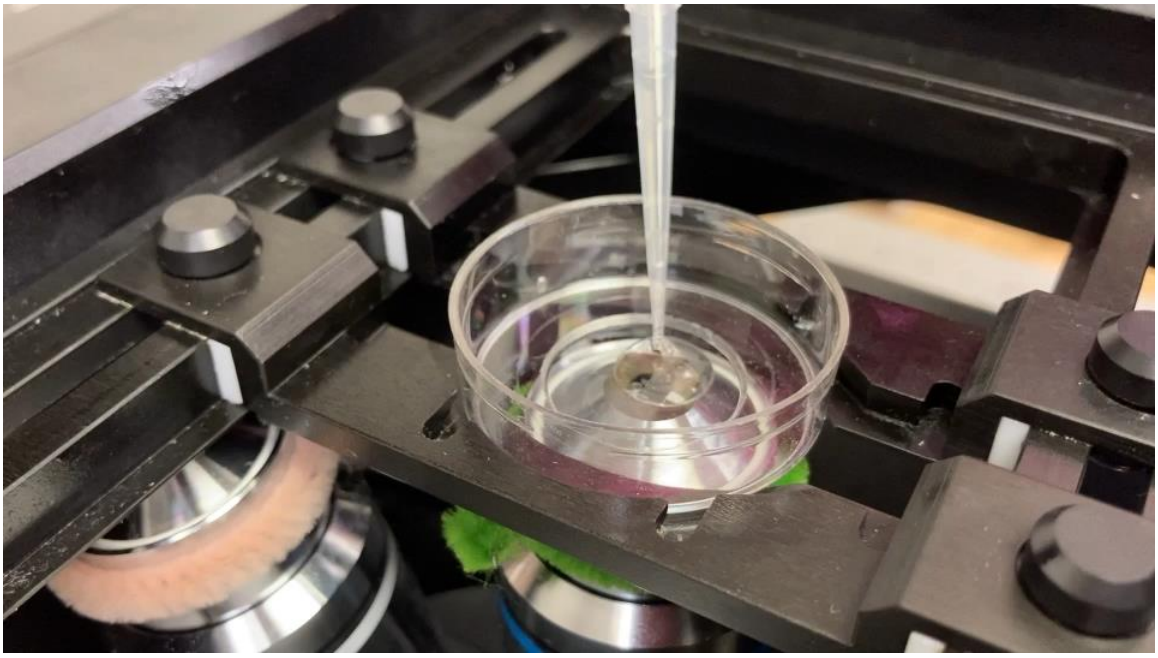

Video 2. Proper addition of H_2O_2 to sample dish.
Hydrogen peroxide should be added to the sample dish using an appropriately sized micropipette. Dispensing H_2O_2 without breaking media surface. Care is taken to avoid breaking the surface of the imaging media to minimize sample drift during hydrogen peroxide addition.

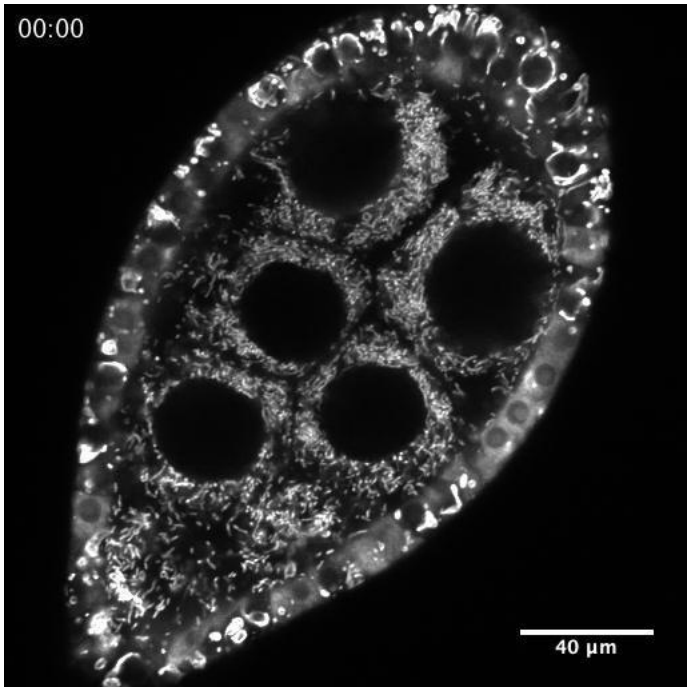

Video 3. H_2O_2 addition during imaging of TMRE labeled follicles.
Follicle from a *clu*^{CA06604} female stained with TMRE. H_2O_2 causes mitochondrial mislocalization in *Drosophila* follicles. White = TMRE dye. Imaged one frame per 15 s for 20 min, and the video is 10 frames per second (84).

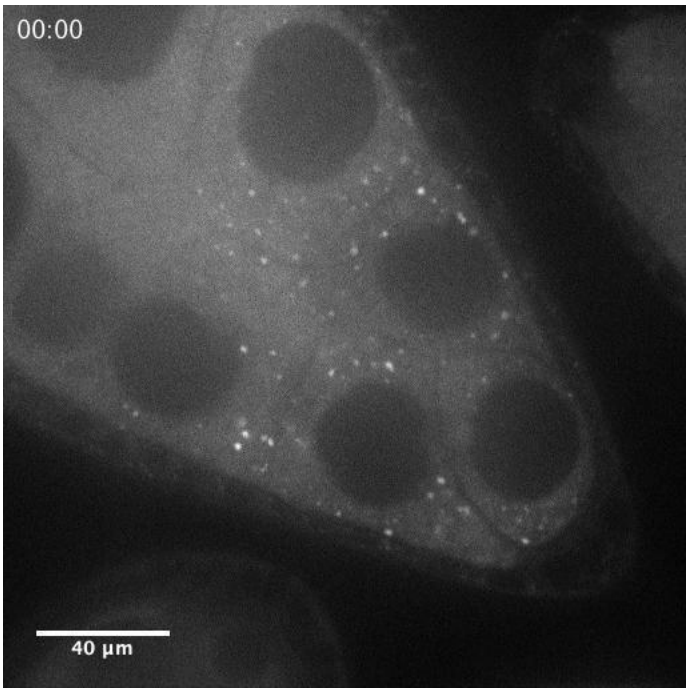

Video 4. H_2O_2 addition during imaging of Clu::GFP follicles.
Follicle from a *clu*^{CA06604} female. H_2O_2 disperses Clu particles as described in Figure 4. White = Clu::GFP. Imaged one frame per 15 s for 15 mins, and the video is 10 frames per second (84).

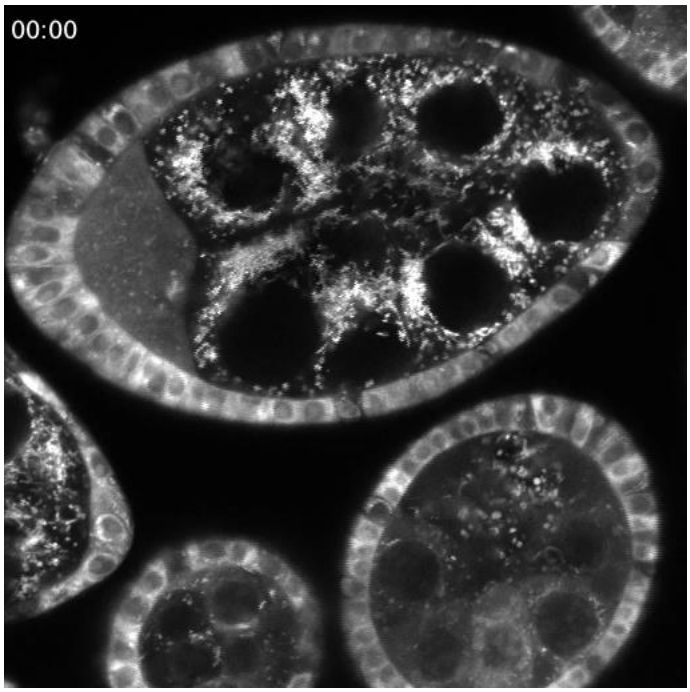

Video 5. Delayed imaging after H_2O_2 addition.
Follicle from a *clu*^{CA06604} female. Addition of hydrogen-peroxide to follicles is a time-sensitive treatment. The restart of imaging was delayed in this video as a result of sample displacement during H_2O_2 addition. The mitochondria have already begun to visibly clump and lose their membrane potential upon the restart of imaging at time 0 (as compared to time 0 in Video 3). Failure to resume imaging quickly after treatment will result in inaccurate and unusable results as the early experimental effects will be missed prior time imaging. White = TMRE. Imaged one frame per 15 s for 20 mins, and the video is 10 frames per second.

TABLES

Name of Material/ Equipment	Company	Catalog Number	Comments/Description
Active dry yeast	Red Star®		
CO_2 gas			99.9% purity
CO_2 pad			
Dissecting microscope, Nikon SMZ645 model	Nikon		
Dissecting needles - PrecisionGlide needles	BD	305165	B-D 21G1 size
Dissecting needles - PrecisionGlide syringes	BD	309657	Luer-Lok tip, 3 mL size
Dissecting needles - tungsten wire	Electron Microscopy Sciences	73800	
Dumont #5 forceps (2 pairs)	Fine Science Tools	11251-10	
NI-150 High Intensity Illuminator	Nikon Instruments Inc.		
Gibco Fetal Bovine Serum, Heat Inactivated	Fisher Scientific	10082-147	
Gibco Schneider's Drosophila Media	Sigma-Aldrich	21720-024	
Hydrogen peroxide solution, 30% (w/w) in H2O	Sigma-Aldrich	H1009	
Insulin from bovine pancreas	Sigma-Aldrich	I6634	
Spinning disk microscope	Nikon		Equivalent scopes may also be used
Lonza BioWhittaker Antibiotics: Penicillin-Streptomycin mixtures	Fisher Scientific	17-602E	
MatTek Corporation Glass Bottom Dishes, 35 mm	Fisher Scientific	NC9344527	
Micropipettes and tips of appropiate size	Eppendorf		
Microcentrifuge tubes, 1.7 mL	VWR	87003-294	
Tetramethylrhodamine, Ethyl Ester, Perchlorate (TMRE)	AnaSpec	AS-88061	
w[1118]	Bloomington Drosophila Stock Center	5905	Wild-type flies
y w; clu[CA06604]		Available upon request.	Clu::GFP trap flies

Table 1. Table of Materials.

CHAPTER 3: MANUSCRIPT 2 – "Clueless forms dynamic, insulin-responsive bliss particles sensitive to stress"

Authors:

Sheard[1,3], K.M., Thibault-Sennett[1,3,4], S.A., Sen[3], A., Shewmaker[2,5], F., and Cox[3], R.T.

Affiliations:

[3]Department of Biochemistry and Molecular Biology

[2]Department of Pharmacology and Molecular Therapeutics

[4]current address: The Association for Molecular Pathology, Rockville, MD 20852

[5]current address: Department of Biochemistry and Molecular Biology

Uniformed Services University

Bethesda, MD 20814

[1]these authors contributed equally

ABSTRACT

Drosophila Clueless (Clu) is a ribonucleoprotein that directly affects mitochondrial function. Loss of *clu* causes mitochondrial damage, and Clu associates with proteins on the mitochondrial outer membrane. Clu's subcellular pattern is diffuse throughout the cytoplasm, but Clu also forms large mitochondria-associated particles. Clu particles are reminiscent of ribonucleoprotein particles such as stress granules and processing bodies. Ribonucleoprotein particles play critical roles in the cell by regulating mRNAs spatially and temporally. Here, we show that Clu particles are unique, highly dynamic and rapidly disperse in response to stress in contrast to processing bodies and autophagosomes. In addition, Clu particle formation is dependent on diet as ovaries from starved females no longer contain Clu particles, and insulin signaling is necessary and sufficient for Clu particle formation. Oxidative stress also disperses particles. Since Clu particles are only present under optimal conditions, we have termed them "bliss particles". We also demonstrate that many aspects of Clu function are conserved in the yeast homolog Clu1p. These observations identify Clu particles as stress-sensitive cytoplasmic particles whose absence corresponds with altered cell stress and mitochondrial localization.

INTRODUCTION

Clu encodes a large multi-domain protein that is directly involved in regulating mitochondrial function, although the molecular mechanisms are still not completely understood (21; 79; 82). Loss of *clu* in *Drosophila* is adult lethal, with flies surviving only 4-7 days post-eclosion(79; 81). *clu* mutants are male and female sterile, and mitochondria in female germ cells are clumped, mislocalized, and morphologically

swollen which is a phenotypic hallmark of damaged, nonfunctional mitochondria (21). *Drosophila* Clu also physically and genetically interacts with the PINK1/Parkin mitophagy complex and thus may play a role as a sensor linking mitochondrial function with mitophagy although what role Clu plays in mitophagy is not yet clear (82). Clu, CLUH and Clu1p, the *Drosophila*, human and yeast homologs, respectively, are ribonucleoproteins (30; 75; 79). Clu and Clu1p bind to mRNA in *Drosophila* and yeast, respectively, and *Drosophila* Clu was shown to associate with the ribosome in *Drosophila*, potentially at the mitochondrial outer membrane (79). CLUH binds to and regulates mRNAs encoding proteins that will be imported into mitochondria and CLUH deficiency alters metabolism (30; 75; 98).

Ribonucleoprotein (RNP) granules are cytoplasmic, non-membranous aggregates which function in temporal and spatial post-transcriptional regulation of their mRNA cargos (4; 5). RNP granules are present in somatic and germ cells, and they serve to regulate gene expression by a variety of mechanisms (5). Processing bodies (P-bodies) and stress granules, two major types of RNP granules in the cytoplasm, have well-characterized roles in cellular stress responses. During stress, both become more abundant in order to regulate the transport, translation, and stability of mature mRNAs (23; 59; 99).

Clu forms large particles in *Drosophila* female germ cells that are closely juxtaposed with mitochondria (21). Particles are also found in the surrounding somatic follicle cells, larval neuroblasts and other neuronal cell types and larval muscle (81; 102). The Arabidopsis thaliana homolog, *friendly mitochondria* (*FMT*), forms particles, which are

also found in close proximity to mitochondria (26). In addition, the vertebrate homolog CLUH has a granular cytoplasmic pattern in cultured COS7 cells (30).

Here, we examine the dynamic nature of Clu particle formation and disaggregation using live-imaging to show that Clu forms previously undescribed and highly stress-sensitive cytoplasmic particles. Clu particles are dynamic and require an intact microtubule cytoskeleton in order to move processively. The oocyte does not contain particles and has very low levels of Clu protein relative to the connected germ cells (called nurse cells). Clu particles do not colocalize with other well described cytoplasmic components that form under stress; thus, we believe these particles uniquely respond to stress by disaggregating. Additionally, we demonstrate a conserved role for Clu in *Saccharomyces cerevisiae*. Yeast Clu1p also forms particles, *clu1* deletion causes decreased growth on a non-fermentable carbon source and increased petite colony formation, and Clu1p binds the ribosomal protein RpL3p. Clu particles in fly ovaries are highly sensitive to nutrition and insulin. Starved follicles no longer have particles in germ cells and surrounding somatic follicle cells even though Clu protein levels remain the same. This effect is at least partly regulated by insulin, as insulin is both necessary and sufficient for particle formation. Nutritional stress is not the only particle disruptor, as increased mitochondrial oxidation also causes particles to disperse. We have named Clu

particles “bliss particles” because they are only present under stress-free, well-fed optimal conditions, unlike stress granules and processing bodies. Finally, we show mitochondrial localization in germ cells is completely dependent on well-fed, stress-free conditions, as any of the aforementioned stressors cause clumping and mislocalization. These observations shed light on how Clu’s subcellular localization is highly dependent on the cell’s nutritional status and this localization changes in response to insulin signaling.

RESULTS

Clu particles are abundant and highly dynamic

Clu protein forms particles in the cytoplasm of many cell types. Female germ cells have been an excellent tissue in which to study Clu particles as they are highly metabolically active, are very large and have abundant particles (45). To better understand Clu’s role in the cell, we used live-imaging to dissect Clu particle dynamics. To do this, we imaged Clu::GFP in the GFP trap line *clueless*^{CA06604} and compared these results to our previous observations in fixed, wild-type ovaries labeled with anti-Clu antibodies (21; 81; 82). *clu*^{CA06604} is homozygous viable with no apparent defects in oogenesis or lifespan (14; 21). Extract from *clu*^{CA06604} probed with anti-Clu antibody had only one higher migrating band indicating all Clu in the cells is GFP labeled (Fig. 1A). Clu particles appeared more abundant using live-imaging compared to the abundance of particles seen using anti-Clu antibody in fixed germ cells (Movie 1 vs. Fig. 4, (21)). During live-imaging, Clu::GFP showed a mix of apparently random and directed movement. At any given time, approximately 12% of the particles appeared to move in a

directed manner over the course of 200 seconds (Fig. 1B-B″ , yellow arrows, Movie 1). For particles that move quickly, kymographic analysis supported that the average particle velocity is 1.5 μm/sec (Fig. 1C, D, E). The rest of the particles were either fairly stationary or appear to move randomly in the cytoplasm. Adding the microtubule destabilizer colcemide disrupted the microtubule cytoskeleton as expected and caused particles and mitochondria to remain stationary, indicating that particle movement is microtubule-based (Fig. S1, Movie 2, 3, 4). Clu particles were present in the surrounding somatic follicle cells, but did not appear to move as much, likely due to the restrictive size of the cells (Fig. 1F, Movie 5). In addition, Clu::GFP protein levels were very low in the oocyte relative to the nurse cells, and we never observed Clu::GFP particles in the oocyte (Fig. 1G, dotted line).

Clu particles do not colocalize with many known structures

As we have previously shown, Clu particles tightly associate, but do not co-localize, with mitochondria (Fig. 2A) (21). Every large particle associates with several mitochondria in fixed tissues, but many of the mitochondria present are not associated with particles. Initially, we thought this mitochondrial association may be due to Clu being involved in autophagosome formation and mitophagy (47). However, in germ cells labeled with anti-Clu antibody, Clu did not co-localize with the LC3 homolog Atg8a, a marker of autophagosomes whose number increases in response to stress. Clu particles also did not co-localize with a second stress-associated cytoplasmic body, processing bodies (Fig. 2B and 2C). Finally, it appeared that Clu associated with ER-exit sites in *Drosophila* larval muscle (103). However, we did not observe any co-localization with

components of the secretory pathway. Clu particles did not show any particular association with endoplasmic reticulum in the germ cells (Fig. 2D). Antibodies used to determine colocalization with components of ER exit sites/COPII vesicles, cis Golgi, and trans Golgi labeled surrounding follicle cells, but did not penetrate the female germ cells well (Fig. 2E-G). Thus, we examined the surrounding follicle cells for co-localization. In somatic follicle cells, Clu particles were distinct from ER exit sites/COPII vesicles (Fig. 2E), cis Golgi (Fig. 2F) and trans Golgi (Fig. 2G). Therefore, we believe Clu forms previously undescribed particles in the cytoplasm specific to mitochondrial function.

Clu particles are conserved

Clu has homologs in many species, including the poorly characterized Clu1p in *Saccharomyces cerevisiae*. Clu1p shares 39% amino acid identity overall with *Drosophila* Clu, 31% between the tetratricopeptide repeat (TPR) domains, and 32% between the Clu domains (Fig. 3A). Since Clu directly affects mitochondrial function in *Drosophila*, we tested whether a *clu1*Δ knockout yeast strain shows defects associated with mitochondrial dysfunction including loss of ability to grow on a non-fermentable carbon source and spontaneous petite colony formation. Wild type yeast normally use fermentation and grow well on glucose (Fig. 3B). *clu1*Δ grew equally as well as wild type yeast on media containing glucose (Fig. 3B). However, when grown on the non-fermentable carbon source glycerol which forces the cells to rely on oxidative phosphorylation, *clu1*Δ showed decreased growth compared to wild type (Fig. 3B and 3C). This was true in two different wild type backgrounds (BY4741 and W303) with three re-derived *clu1::KANMX* deletions (Fig. S2). The poor growth and small colonies

could be readily seen after growing a small number of cells on glycerol for over a week (Fig. 3C). Petite colony formation occurs in mutants that are defective for oxidative phosphorylation even when they are grown on a fermentable carbon source. Newly derived *clu1*Δ in a BY4741 background had a significantly higher percent (~15%) petite formation vs wild type BY4741 (~2%) when grown on Yeast Extract-Peptone-Dextrose (YPDextrose) (Fig. 3D, E). The *clu1:CLU1-GFP* strain contains a GFP insertion at the endogenous *CLU1* locus (Huh et al., 2003). Anti-GFP antibody labeling of this strain showed that Clu1p, similar to Clu, was punctate in the cytoplasm (Fig. 3F, arrows). As with *Drosophila* Clu, yeast Clu1p also associated with a ribosomal protein, RpL3p (Fig. 3G, H (79)). *Drosophila* Clu sediments in the heavier fractions on a sucrose gradient (Fig. 3I (79)). Yeast Clu1p had a similar sedimentation pattern (Fig. 3I). Thus, many aspects of yeast Clu1p recapitulate those found in *Drosophila*, supporting a conserved function between the two species.

Clu particles are sensitive to nutritional stress

In *Drosophila*, we have observed that only well-fed females reproducibly have robust Clu particles. This suggests that ample access to yeast is important and that the distribution of Clu is sensitive to nutritional stress. To analyze the effect of nutritional stress on Clu particle dynamics, we starved and refed wild type flies then labeled the ovaries with anti-Clu antibodies. Wild type females fed wet yeast paste always had robust Clu particles (Fig. 4A′-A″). However, starving the same well-fattened flies for five hours on water completely abolished particles, resulting in dispersed Clu (Fig. 4B′-B″). Re-feeding yeast paste for as little as two hours completely reversed this effect (Fig. 4C′-

C″ , G). These results were the same for the surrounding somatic follicle cells (Fig. 4D-F ″). The short five-hour starvation (typical starvation protocols last >24 hours (7; 62) did not result in any behavioral defects and levels of ATP remained the same (Fig. 4H). Particle disaggregation was not due to protein degradation as Clu protein levels remained the same for all three conditions (Fig. 4I, J). These results support nutrition as an important regulator of Clu particle formation, and that their formation and disaggregation are highly dynamic and reversible.

After starvation, Clu protein levels remain the same (Fig. 4I, J) but Clu particles disperse. To confirm that dispersed cytoplasmic Clu levels increase when particles disperse, we measured the amount of diffuse Clu in the nurse cell cytoplasm and compared this to a protein found in processing bodies. Trailer hitch (Tral) is a ribonucleoprotein that is a component of processing bodies (6; 105). Under well-fed conditions, *tral*^{CA06517} follicles expressing Tral::GFP and subsequently labeled with anti-GFP antibody formed characteristic small Tral-containing particles in the cytoplasm (Fig. 5A). Tral labeling was also concentrated at the anterior of the oocyte and was diffusely cytoplasmic (Fig. 5A) (105). In the same follicle, anti-Clu antibody labeling showed Clu particles (Fig. 5B). Similar to our result using live-imaging, Clu protein levels were very low in the oocyte relative to the nurse cells, and we never observed Clu particles in the oocyte (Fig. 5B, dotted line). After five-hour starvation, Tral::GFP formed very large processing bodies in the nurse cells and oocyte with a significant decrease in the diffuse cytoplasmic staining (Fig. 5A′ , C′, F) (13). In contrast, in the same follicle Clu particles

dispersed completely with a significant rise in diffuse cytoplasmic staining (Fig. 5B′ ,C ′ , E).

Insulin is sufficient and necessary to induce Clu particle formation

Since nutrition availability affects Clu particle formation, we examined the role of insulin signaling on this process. To determine if insulin is sufficient to induce particle formation, we used live-imaging. Well-fed Clu::GFP expressing $clu^{CA06604}$ females were transferred to either standard food (no yeast paste) or H_20 for five hours, followed by dissection in insulin-free media. Insulin addition caused robust Clu particle formation within ten minutes, with 80% of the follicles containing particles after 15 minutes (Fig. 6A-A‴, B, Movie 6). The percentage of individual follicles that formed particles in response to insulin was similar whether the females were starved on water or fed only standard food (no yeast paste) (Fig. 6B) and was also similar to fixed samples from well-fed females (Fig. 6B vs 4G). Using this technique, both starvation conditions resulted in a baseline of 20% individual follicles with particles (Fig. 6B, 0 µg/mL insulin bars). These results support that insulin is sufficient to induce particle formation.

To further assess the role of insulin in Clu particle regulation, we used clonal analysis to increase and decrease insulin signaling in the surrounding somatic follicle cells. In a FRT82B control wild type background, GFP- and GFP+ clones contained particles indicating the presence or absence of GFP has no effect on Clu particle formation (Fig. 6C-C″ , dotted outline, F). To determine whether an increase in insulin signaling affects Clu particle formation, we made follicle cell clones mutant for $TSC1^{Q87X}$, a negative effector of insulin signaling. *TSC1* mutant clones contained

particles at the same frequency as the sibling *TSC1*/+ control clones (Fig. 6D- D″ , dotted outlines, F). To test if insulin signaling is necessary for Clu particle formation, we made clones for two alleles of the *Insulin-like Receptor* (*InR*). *InR* mutant cells divide slowly and our heat shock protocol was short from clone induction to dissection, thus follicle cell clone size and frequency were small (17; 63; 64). Loss of *InR* resulted in a loss of Clu particles in the mutant clones compared to *InR*/+ sibling clones (Fig. 6E-E″ , dotted outlines, F, Fig. S3). These results support that upregulating insulin signaling does not affect Clu particle formation and that loss of insulin signaling causes loss of particles, indicating insulin is required for particle formation.

Clu particle formation is sensitive to mitochondrial oxidative stress

Nutritional stress and lack of insulin caused particles to disaggregate. To determine whether more general oxidative stress has the same effect, we examined *Superoxide Dismutase 2* (*SOD2*) mutants. SOD2 scavenges the free-radical superoxide in the mitochondrial matrix (29). Loss of SOD2 causes an increase in mitochondrial oxidation (68; 81). *SOD2* mutant flies eclose at normal numbers and appear healthy upon eclosion, but die within 24 hours (68; 81). Their ovaries appeared to develop relatively normally; however, they completely lacked Clu particles (Fig. 7A, B). We have shown previously that *SOD2* mutant adults have low levels of ATP (Fig. 7C) (81). However, Clu levels were not reduced (Fig. 7D). *SOD2* mutants test the effect of systemic loss of an important free-radical scavenging enzyme throughout development. However, superoxide is known to function in multiple cell signaling pathways and loss of *SOD2* in *Drosophila* has been shown to cause defects in behavior, axonal targeting and neurodegeneration (15;

101). To determine if the effect of *SOD2* loss on Clu particles is due to increased oxidative damage, we added H_20_2 to insulin-containing culture media on follicles dissected from $clu^{CA06604}$ well-fed females. Clu::GFP particles started to disaggregate in as quickly as five minutes after addition of H_20_2 indicating acute oxidative stress can quickly disperse Clu particles (Fig. 7E-E″ , Movie 7).

Mitochondrial mislocalization in *Drosophila* female germ cells is downstream of stress

We have shown that mitochondria mislocalize in female germ cells due to a variety of mitochondrial dysfunction, including loss of *clu*, *PINK1* and *parkin (21; 82)*. Under well-fed conditions, mitochondria are evenly dispersed in developing follicles in the ovary as previously described (100%: 68/68 individual follicles) (Fig. 8A) (19). However, after five-hour starvation, mitochondria clumped in the nurse cell cytoplasm in a manner reminiscent of *clu* mutants (82%: 75/92 individual follicles) (Fig. 8B, arrow, F). After two hours re-feeding, mitochondria evenly dispersed back to the pattern seen in well-fed flies (70%: 67/97 individual follicles) (Fig. 8C).

SOD2 mutants also showed a similar mitochondrial clumping phenotype (100%: n = 44/44) compared to wild type *SOD2/+* siblings (0% clumped: n = 51/51) (Fig. 8D, E, arrow). To examine the effect of oxidative damage on mitochondrial localization using live-imaging, we utilized TMRE, a cell-permeant cationic dye that preferentially sequesters in mitochondria with high membrane potential. At time zero, TMRE-labeled mitochondria were evenly distributed and thin and rod-shaped (Fig. 8G, Movie 8). After incubating follicles in H_20_2 for five minutes, mitochondria started to clump in the

cytoplasm and became more swollen and rounded (Fig. 8G′). After ten minutes, oxidative damage had accumulated to a level where most mitochondria are quite dim with only a small subset still fluorescing (Fig. 8G″). These results indicate that once the cells undergo stress including oxidative damage, nutritional stress, or the presence of mutations causing mitochondrial dysfunction, mitochondria no longer retain their proper dispersion and localization. This effect occurs quite quickly, and with respect to nutrition, can be readily reversed.

DISCUSSION

Here, we show that Clu bliss particles are dynamic cytoplasmic bodies whose formation and dispersal is highly dependent on nutritional and oxidative stress. Dynamic cytoplasmic movement is a common feature of RNP particles (reviewed in (76)). Clu particle processive movement occurs at a speed consistent with mitochondrial movement in neurons (3; 41; 52). The 12% directed Clu particle movement we observed is likely an under-estimate since we only examined one focal plane during live-imaging. Mitochondria are highly dynamic in *Drosophila* nurse cells; however, neither the changes in mitochondrial movement during development and cell stress nor their cytoplasmic localization has been systematically investigated using live-imaging. A potential function of Clu particles is to sequester mRNAs and proteins that are required for mitochondrial oxidative phosphorylation. For processively moving Clu particles, co- transport of Clu particles with mitochondria could be directed to parts of the cytoplasm with high ATP requirements. As smaller and larger Clu particles appeared to move in a directed fashion, size does not seem to dictate particle movement (Movie 1). The directed movement

appears to rely on the microtubule cytoskeleton, as disruption from colcemide treatment causes particles to become stationary (Fig. S1, Movie 4). Clu particles also appear to undergo random movement similar to what has been observed for other proteins at this developmental stage (85). Furthermore, Clu protein labeling is low in the oocyte, and Clu particles are never observed there (Fig. 1G, 5A). This finding may be due to the metabolic differences between the oocyte and nurse cells (86). It also suggests that either Clu is not moving into the oocyte from the nurse cells during follicle development or that it may be actively degraded in the oocyte during these stages.

There are several well-described RNP particles in the cytoplasm, including stress granules and processing bodies, which are known to regulate mRNA biology (11; 38). These RNP particles generally respond to stress by becoming larger and more plentiful (Fig. 5B', (13)). Here, we demonstrate Clu particles have the opposite response. The dispersion of Clu particles is complete upon nutritional stress and reversible. Re-feeding flies yeast paste or adding insulin to the culture media quickly induces particle reformation. Our live-imaging and clonal analysis indicates insulin is both necessary and sufficient for Clu particle formation (Fig. 6). Upregulated insulin signaling did not appear to affect Clu particle formation however follicle cell clonal analysis of *InR* mutant clones indicated loss of Clu particles (Fig. 6). The standard method used by the field to induce germline stem cell clones (3x heat shock, 7-10 days on yeast paste before dissection) produced mutant germline clones but did not show consistent, reproducible Clu particles in the germ cells of controls. Thus, the results were not interpretable and we did not use this protocol (see Materials and Methods). We assume the inconsistent Clu particle loss

in the controls using the standard longer protocol was due to stress from the addition heat shock combined with aging. Instead, we reduced the number of heat shocks and the time after heat shock for dissection, which resulted in small *InR* follicle cell clones. In addition, visualizing Clu particles live without insulin resulted in a higher percentage of follicles with particles compared to dissecting and fixing wild type starved flies (20% vs 0%) (Fig. 6B vs 4G). This difference is likely due to the fact that we counted individual follicles at high magnification using live-imaging whereas with fixed imaging we used a high-throughput method and counted ovarioles (strings of developing follicles). Oxidative stress also causes particles to disperse in addition to nutritional stress. Producing oxidative stress systemically using *SOD2* mutants or acutely with the addition of H_20_2 causes either a complete lack of Clu particles (Fig. 7B) or real-time particle dispersion (Fig. 7F- F", Movie 7). In all the conditions we tested, the change in cytoplasmic localization with altered nutrition and increased oxidative stress is independent of Clu protein levels and is thus not due to protein degradation (Fig. 4I, J). This is the first time to our knowledge that this dynamic for a cytoplasmic particle has been described.

Clu directly effects mitochondrial function. Clu particles are closely associated with mitochondria in the cytoplasm (Fig. 2A, (21)), Clu associates with mitochondrial outer membrane proteins (79; 82), and it associates with at least one ribosomal protein preferentially in mitochondrial fractions (79). Clu particles do not co-localize with processing bodies or autophagosomes (Fig. 2). This was surprising to us because Clu genetically and physically interacts with the PINK1/Parkin mitophagy complex (82; 102).

Since only a subset of Clu particles associates with mitochondria in fixed antibody-labeled tissues, we expected particles would increase in response to stress, and perhaps be involved in autophagosome formation and culling damaged mitochondria (47). However, to our surprise, the opposite occurs. Thus, not only do Clu particles have a previously undescribed dynamic, they are also a novel cytoplasmic particle consisting of a protein with a direct effect on, and an association with, mitochondria. Given that their presence is strictly dependent on stress-free conditions, we have named them "bliss particles" to differentiate their cytoplasmic dynamic from the many other RNP particles that form in response to stress.

Clu and Clu1p bind mRNA, and CLUH preferentially binds transcripts encoding proteins destined for mitochondrial import (30; 79). There is evidence that in the absence of CLUH, target mRNAs undergo increased degradation, suggesting that CLUH is required for mRNA stability (75). Clu and Clu1p both bind ribosomal proteins and eukaryotic initiation factors (Fig. 3, (79; 97). Because insulin and nutrition regulate Clu particle formation, this supports the notion that the presence or absence of Clu particles could also affect mitochondrial function and perhaps translation and import of mitochondrial proteins.

Clu contains multiple putative domains based on sequence alignment between species and literature searches (Fig. 3A) (21; 82). The protein contains tetratricopeptide repeats (TPR) and Clu domains which show 55% and 85% amino acid identity, respectively, between Clu and CLUH (79). Based on several available online algorithms (Iupred2a and Globplot), the M domain is not predicted to have structure and does not

contain any sequences associated with intrinsically disordered domains (IDDs). IDD-containing proteins have been shown to be involved in liquid-liquid phase separation as well as mRNA association, two traits that control membrane-less organelle formation, including some RNP particles (93). For Clu, the TPR domain, not the M domain, was determined to be functionally important for mRNA binding (82). We have previously shown that ectopically expressing deletion constructs for each of Clu's domains in a *clu* null mutant background does not rescue pupation delays, adult lethality, mitochondrial localization defects, or reduced ATP levels (79). The resulting adults that hatch die within approximately four days and are as weak and sick as *clu* null adult flies. Thus, we were unable to assess which Clu domain, including the M domain, is required for Clu particle formation in vivo as the flies are systemically stressed. *clu* mutant phenotypes were only rescued by expressing full-length *Drosophila* Clu, melanogaster specific (ms) domain deletion, or CLUH. Furthermore, Clu associates with itself, further complicating deletion analysis to determine which domain is necessary for Clu particle formation (79).

Mitochondria are plentiful in the cytoplasm of developing germ cells, and they undergo characteristic localization, shape, and number changes during oogenesis (19; 20). In well-fed wild type females, mitochondria in the germ cells are evenly dispersed throughout the cytoplasm. Through mutation analysis, we previously described that mitochondria mislocalize into clumps in *clu*, *PINK1* and *parkin* mutant germ cells (21; 82). Fields et al. also showed evidence that Clu1p influences mitochondrial distribution and morphology, and in a large screen examining mitochondrial localization Dimmer et al. showed that clu1Δ knockout yeast have mislocalized and aggregated mitochondria

(24; 28). In this work, we demonstrate this clumping is present in *SOD2* mutants and starvation causes the same mislocalization. From these data, it is clear that mitochondrial mislocalization in germ cells is likely an indirect, downstream effect of general cellular stress. Thus, experiments examining mitochondrial localization in germ cells should take into account the culture and fixation conditions in order to ensure that low-stress conditions and normal mitochondrial distribution are maintained.

Drosophila Clu and vertebrate CLUH are ribonucleoproteins, and CLUH was shown to preferentially bind mRNAs encoding nucleus-encoded mitochondrial proteins. Loss of Clu/CLUH disrupts mitochondrial function by reducing ATP levels, causing improper mitochondria localization and mitochondrial ultrastructural changes, and by altering metabolism (21; 30; 75; 79; 98). *Drosophila* Clu associates with the ribosome and the mitochondrial outer membrane proteins TOM20 and Porin, suggesting it may have a role in site-specific or co-translational import of nucleus-encoded proteins (79). Since the particles respond quickly to nutritional cues, they may also represent an additional acute control of mRNA translation, with differing translation rates in the presence and absence of particles. We do not yet know if Clu particles are the sites of translation for Clu-bound mRNAs, or whether they are enriched with mRNAs and/or ribosomes. This hypothesis remains to be tested. Clu associates with TOM20 and Porin and also self-associates; however, it is unclear how Clu particles associate with mitochondria, whether they directly associate with microtubules, and how this association changes with stress (82). Attempts to simultaneously visualize mitochondria and Clu particles using live-imaging have been stymied by sensitivity to TMRE addition (the Clu

particles disperse); however, there is evidence that Clu particles do move with mitochondria in Arabidopsis (26).

There have not yet been patients identified with mitochondrial disorders who harbor mutations in *CLUH*. This may be because any perturbations in CLUH are either not compatible with life or cause very early lethality. This is supported by evidence that in mice knockout of the vertebrate homolog CLUH causes post-natal lethality between P0-1, with no apparent respiratory failure and a concomitant 10-15% decrease in weight (75). Schatton et al found post-natal death is due to metabolic disruption in hepatocytes which have mislocalized mitochondria and are depleted of key enzymes used in catabolic energy pathways (75). Additionally, in human development, comparison of preterm to term newborn umbilical cord mesenchymal stem cells shows that changes in CLUH expression correspond with changes in the mitochondrial network and cellular metabolic changes in response to an oxygen- rich environment (71). Nonetheless, given that Clu forms dynamic cytoplasmic particles highly sensitive to stress and that it is an important RNP critical for directly affecting mitochondrial function and biogenesis, understanding Clu's molecular role and how its mRNA binding is related to cytoplasmic localization will be important in the future.

MATERIALS AND METHODS

Fly stocks: The following stocks were used for experiments: w^{1118}, $clueless^{d08713}$/*CyO P(ActGFP)JMR1 (21), trailer hitch*^{CA06517}, *Sec61*α*CC00735*, $clueless^{CA06604}$ *(14)*, $SOD2^{2}$/ *CyO P(ActGFP)JMR1*, *P(ry[+t7.2]=neoFR)82B ry[506]*, *w*; P(ry[+t7.2]=neoFRT}82B P(w[+mC]=Ubi-GFP.D)83* (Bloomington *Drosophila* Stock Center), *FRT82B* $TSC1^{Q87X}$/

TM3 (92), *FRT82B* InR^{339}/TM3, FRT82B InR^{E19}/ *TM3 (48)*, *Ubi-GFP::tubulin/ CyO; Pri/TM6, Tb (72)*. Flies were reared on either standard cornmeal fly media or standard cornmeal fly media supplemented with yeast paste at 22° or 25° C.

Clone generation: 0-24hr females of the appropriate genotype were fed yeast paste for 24 hr, then heat shocked 2x 1 hour in a 37℃ water bath, morning and evening. Except for during heat shock, the flies were kept undisturbed on a quiet shelf at room temperature. After heat shock, the flies were fed for an additional 24 hr, then 3x ten flies were dissected in parallel with controls and fixed and labeled as described below. Clones were distinguished by absence of GFP antibody labeling.

Fixed image immunofluorescence: 0-24 hr flies were fattened with yeast paste for 3-7 days. 60 female flies were then transferred to an empty vial containing a Kimwipe soaked in water for five hours to induce starvation. 30 starved flies were then transferred back to a vial with fresh fly food and yeast paste for two hours for re-feeding. 30 female flies remained feeding on yeast paste throughout as controls. From each condition, 3x 10 flies were then dissected at room temperature (RT) in Grace's Insect Medium (modified) (BioWhittaker, Lonza, Cologne, Germany). Ovaries were fixed for 20 minutes in 4% paraformaldehyde and 20mM formic acid solution (Sigma, St. Louis, MO) made in Grace's. Tissues were washed two times (40 minutes each) with Antibody wash buffer (Ab) (1X PBS:0.1% Triton X-100:1% BSA), then incubated in primary antibody over night at 4°C. They were then washed two times (40 minutes each) and incubated

overnight at 4°C in secondary antibody. After washing, DAPI (1:1000) was added for five minutes then removed, and Vectashield (Vector Laboratories, Inc., Burlingame, CA) was added. For yeast staining, log phase Clu1p::GFP yeast grown in Yeast-Peptone-Dextrose (YPD). 20% paraformaldehyde was added to the culture to a final concentration of 4% for 20 min. The cells were spun, washed with 1.2M sorbitol, 50mM KPOH, spun twice, then resuspended in 500 uL of the same buffer. The cells were treated with Zymolase 100T (MP Biomedicals, LLC, Irving CA), for 35 min at 37℃, then very gently washed 2x with Ab wash, followed by a 2 hour incubation with α-GFP sitting at room temperature with occasional gentle inversion. The cells were then washed 2x with Ab wash, incubated with α-rabbit Alexa-488 in Ab wash for 1 hour, then washed gently 2x with DAPI addition in the second wash. The cells were then mounted in Vectashield and imaged using a Leica AF6000 Time-lapse Imaging System. The following primary antibodies were used: guinea pig anti-Clu N-terminus (1:2000) (21), mouse anti-Complex V (ATP synthase (CVA)) (1:1000, AbCam, Cambridge, MA, cat# ab14748), rabbit anti-GFP (1:2000, AbCam, Cambridge, MA, cat# ab290), chicken anti-GFP (1:1000, AbCam, Cambridge, MA, cat# ab13970), GABARAP (Atg8a) (1:200, AbCam, Cambridge, MA, cat# ab109364), Sec23 (1:500), GMAP (1:1000, Developmental Studies Hybridoma Bank, Iowa City, Iowa), Golgin245 (1:1000, Developmental Studies Hybridoma Bank, Iowa City, Iowa), . The following secondary antibodies were used: goat anti-mouse IgG_{2b} Alexa 568 (1:500), goat anti-guinea pig Alexa 488 (1:1000), and goat anti-chicken Alexa 568 (1:1000) (Invitrogen, Waltham, MA), donkey anti-guinea pig Cy3 (1:1000) and donkey anti- rabbit Alexa 488 (1:500) (Jackson ImmunoResearch Laboratories, Inc, West

Grove, PA). Samples were imaged using a Zeiss 700 confocal microscope and 63x Plan Apo NA 1.4 lens.

Image quantification: For Clu particle quantification, slides were scanned at 40x using a Zeiss Axio Scan.Z1 slide scanner. The number of ovarioles per slide was counted (87-170 ovarioles per slide, average = 132±16 ovarioles) using the Cell Counter tool in ImageJ. Each ovariole on a slide was subsequently scored using the Zeiss Zen blue software; an ovariole was scored as having particles if at least one follicle in the ovariole contained particles and as having no particles if no follicles contained particles. The mean percentage of ovarioles with particles in each experiment (n = 6 groups of 10 flies for well-fed group, n = 3 groups of 10 flies for starved group, n = 3 groups of 10 flies for refed group) is represented in the graph with error bars representing mean ±SD. The amount of Clu::GFP and Trailer hitch::GFP was quantified by measuring the fluorescence intensity (integrated density) using ImageJ (n = 6 images, (same images for both)). Taking care to avoid Clu and Tral particles three equally sized ROIs were randomly placed within the nurse cells. Significance was calculated using an unpaired t-test with Welch's correlation. Kymographs were generated using ImageJ from videos of *clueless*^{CA06604} well-fed follicles taken at 60x, with one frame captured every second for 200 seconds. To measure average particle velocity, six randomly chosen particles which showed processive movement were analyzed from four follicles (n = 24 particles). A representative image was used in the figure (1D). For quantification of the percentage of clones with particles in control FRT82B clones, *TSC1* mutant clones and *InR*^{339} mutant

clones, samples were imaged using a Zeiss 700 confocal microscope and 63x Plan Apo NA 1.4 lens. Twenty clones (FRT82B, *TSC1*) and 11 clones (InR^{339}) from individual images were scored for the presence or absence of particles in the GFP- and GFP+ regions to generate the graph.

Live Imaging Microscopy for Drosophila Tissue Samples: $clueless^{CA06604}$ females that had been either fattened with yeast paste, fed only standard cornmeal fly media (no yeast paste), or starved on water for 5 hours were dissected at room temperature (RT) in either Complete Schneider's Media (Schneider's *Drosophila* media (ThermoFisher Scientific, Waltham, MA) with 15% Fetal Bovine Serum and 0.6X Pen-Strep solution) or Complete Schneider's Media supplemented with 200 µg/mL of insulin (insulin which did not readily dissolve in media was allowed to settle overnight at 4°C prior to use). Ovaries were removed and further teased apart into single, isolated ovarioles. Ovarioles were then loaded onto a glass bottom 35mm dish (MatTek Corporation, Ashland, MA) and live videos of a single focal plane were collected using a Nikon spinning disk/TIRF/3D-STORM microscope at 60x at room temperature. For experiments with insulin addition, ovarioles were prepared as above in Complete Schneider's Media. Complete Schneider's Media containing 400 µg/mL insulin would be added to the dish with a 3mL syringe to dilute the sample 1:1, resulting in an insulin concentration of 200 µg/mL. For the Insulin response graph, flies were dissected in Complete Schneider's Media containing the amount of insulin indicated and viewed on the Nikon spinning disk microscope as described above. Individual follicles were counted (16-62 follicles per experiment, n

values below) to either have particles (if at least one nurse cell in follicle had particles) or no particles after focusing throughout entire follicle. The mean percentage of total number of follicles with particles in each culture condition is represented in the graph with error bars representing mean ±S.E. The following follicles counted per experiment:

Non-fattened flies in plus 200ug/mL insulin – 16, 39 and 62;

Non-fattened flies plus 100ug/mL insulin – 27, 39, and 39;

Non-fattened flies plus 50ug/mL insulin – 29, 27, and 26;

Non-fattened flies in 0ug/mL insulin – 34 and 16;

Starved flies in 0ug/mL insulin – 19 and 23;

Starved flies plus 200ug/mL insulin – 29 and 26.

For colcemide treatment, follicles were dissected in Complete Schneider's Media plus 200µg/mL insulin and 100 µg/mL colcemide (Sigma-Aldrich, St. Louis, MO) then incubated for 3 hours at room temperature before imaging. Tetramethylrhodamine, ethyl ester, perchlorate (TMRE, AnaSpec cat# AS88061, ThermoFisher, Waltham, MA, 100 mM stock in DMSO) was used at a concentration of 1:10,000. Follicles were dissected in Complete Schneider's Media plus 200µg/mL insulin and TMRE, incubated for 20 min then directly imaged with no washes. For H_2O_2 treatments, follicles were dissected in Complete Schneider's Media plus 200µg/mL insulin and transferred to 100 µL of the same media in a MatTek dish (MatTek Corporation, Ashland, MA). 100 µL of additional media + 2mM H_2O_2 was added during imaging to make the final concentration 1mM. Treatment lasted for 15 minutes while filming. To determine the percent Clu particles that undergo directed vs apparently random movement, Clu-particle containing follicles

were imaged in the presence of insulin for 200 seconds and particles were counted by hand in each frame for three movies. Each movie contained 4 complete or partial nurse cells. Upon overlaying the image with a 1.5 μm by 1.5 μm grid, a particle was scored as having moving directionally if it moved in one direction across two boxes over a minimal of 6 frames. These parameters were chosen based on the maximum, minimum and average particle speed (Fig. 1E). This analysis gave an average of 12% moving particles from an average of 174 total particles per follicle (moving particles/total particles per follicle: 24/152, 12/170, & 30/200). To analyze the effect of nutrition on mitochondrial mislocalization, control (well-fed) and experimental (starved on water and refed) ovaries were labeled for mitochondria (anti-ATP synthase) and anti-Clu. All ovarioles on the slide were imaged through three Z-sections. Using just the mitochondria channel, each follicle in the ovariole was scored for completely dispersed or clumped mitochondria.

Yeast Growth Assays: Saccharomyces cerevisiae strain BY4741 (*his3 leu2 met15 ura3*) and two clu1Δ derivatives (*clu1::kanMX*; strain numbers FPS674 and FPS675) were used in this study. *clu1* deletions were generated using the S288C-derived BY4741 strain background (*MATa his3Δ leu2Δ met15Δ ura3Δ clu1::kanMX*) (34) obtained from Horizon Discovery, Cambridge, UK, (formally Open Biosystems). Yeast chromosomal DNA was purified from strain BY4741 using the YeaStar Genomic DNA Kit (Zymo Research, Irvine, CA), according to the manufacturer's protocol. The *clu1::kanMX* cassette was then PCR-amplified using the following primers, which are respectively approximately 250 base pairs up- and down-stream of the cassette:

GTGTAACGGCTATCACATC (CLU1-250F) and CTTTAGAGGGAACTCTTGCG (CLU1-250R). Amplified DNA was purified using the GeneJET PCR Purification Kit (ThermoFisher, Waltham, MA), according to the manufacturer's protocol. The purified DNA was used to freshly delete CLU1 in strain backgrounds BY4741(*MATa his3Δ leu2Δ met15Δ ura3Δ*) and W303 (*leu2 ade2-1 ura3 can1 trp1 his3*) using a previously described method (8). For percent petite colony formation, cells from each yeast strain were dispersed on Yeast-Peptone-Dextrose (YPD) plates (~500 cells per plate; performed in quadruplicate) and grown at 30° C for ~1 week. Total normal (rho+) and petite (rho-) colonies were counted. For the glycerol growth assay, log-phase BY4741 wild type and *clu1Δ* strains were grown overnight in YPGlucose, then diluted and grown the next morning until log-phase. Approximately the same number of cells was spotted on YPGlycerol and allowed to grow for a week before imaging.

ATP Assays: 0-24 hr flies were fattened with yeast paste for 3-7 days. 30 female flies were then transferred for five hours to an empty vial containing a Kimwipe soaked in water. 15 starved flies were then transferred back to a vial with fresh fly food and yeast paste for two hours for re-feeding. 15 female flies continued feeding on yeast paste throughout as a control. Flies were then homogenized in extraction buffer (100 mM Tris-Cl, pH 8.0, 4 mM EDTA, pH 8.0; 6 M guanidine hydrochloride) (3 groups of 5 flies/50 µL extraction buffer), boiled for 4 minutes, then centrifuged at 8000 g for 5 minutes at RT. The protein concentration of the samples was determined using a Bradford assay. The ATP concentration was determined using an ATP Determination Kit (Molecular

Probes, Invitrogen, Waltham, MA) according to the manufacturer's directions. 100 µL assays were performed in a 96 well plate and the luminescence was measured using a BioTek Synergy H1 luminometer (BioTek Instruments, Winooski, VT). Each sample was read in triplicate. The amount of ATP was normalized against protein concentration.

Western blotting and Immunoprecipitation: 0-24 hr flies were fattened with yeast paste for 3-7 days. 30 female flies were then transferred for five hours to an empty vial containing a Kimwipe soaked in water. 15 starved flies were then transferred back to a vial with fresh fly food and yeast paste for two hours for re-feeding. 15 female flies continued feeding on yeast paste throughout as a control. Ovaries were then removed at room temperature (RT) in Grace's Insect Medium (modified) (BioWhittaker, Lonza, Cologne, Germany). Ovaries were homogenized in 150 µL of sample buffer and the extract run on a 4-20% polyacrylamide gel using a standard SDS-PAGE protocol for Western blotting. After electrophoresis, proteins were transferred onto a Hybond- ECL nitrocellulose membrane (GE Healthsciences, Inc., Chicago, IL) then soaked with Ponceau S for 10 min and briefly rinsed. Blots were exposed to the following antibodies: anti-Clu (1:20,000) (21) and anti-α-tubulin (1:5000, AA4.3, Developmental Studies Hybridoma Bank, University of Iowa, Iowa City). Quantification of Western blots was performed with ImageJ, and the amount of Clu protein was normalized against α--tubulin (n = 3). Immunoprecipitation (IP) from adult flies was performed as previously described (82). For IP from yeast, an equal volume of silica beads and 1X PBS was added to the yeast pellet. The tube was vortexed frequently for up to 5 minutes. The slurry was

resuspended in IP buffer (20 mM HEPES, pH 7.4; 50 mM KCl, 0.02% Triton X-100, 1% NP-40 (sub), 1 mM EDTA, 0.5 mM EGTA, 5% glycerol) supplemented with 1 mM DTT and Protease inhibitor cocktail (Roche, Basel, Switzerland). The following antibodies were used for IP and western blots from yeast samples; anti-ScRPL3 (1:1000, Developmental Studies Hybridoma Bank, University of Iowa, Iowa city), anti-ELO3 (1:2500, a gift from Dr. Teresa Dunn, Uniformed Services University). For the anti-ELO3 blot, the IP was done using GFP-Trap magnetic beads (ChromoTek GmbH, Planegg-Martinsried, Germany) not anti-GFP antibody since ELO3 migrates at a similar position to IgG heavy chain.

Sucrose gradients: Sucrose gradients for fly extract were performed as previously described (79). The modifications for yeast were the following: yeast from a 5 ml YPD overnight culture was pelleted and transferred to an Eppendorf tube. An equal volume of silica beads was added to the pellet plus 50 µL of 1X mDXB (25 mM HEPES pH 6.8, 50 mM KCl, 1 mM MgCl2, 125 mM Sucrose, 1 mM DTT and 1x protease inhibitor cocktail). The tube was vortexed frequently for up to 5 minutes. 300 µL 1X mDXB was added to the mixture and spun at 2000g, twice for 5 minutes to collect the supernatant. Half the supernatant was loaded on the sucrose column.

ACKNOWLEDGEMENTS

We would like to thank the USUHS Biomedical Instrumentation Core and Dr. Dennis McDaniel for imaging support and The Developmental Studies Hybridoma Bank, created by the NICHD of the NIH and maintained at The University of Iowa, Department of

Biology. We thank Ms. Hala Wyne, Department of Biochemistry, USU, for assistance with the yeast petite colony assay. This work was supported by the National Institutes of Health (1R21NS085730 and 1R01GM127938 to R.T.C. and 1R35GM119790-01 to F.S.) and Uniformed Services University (USUHS BIO-71- 3019) to R.T.C.

MAIN FIGURES

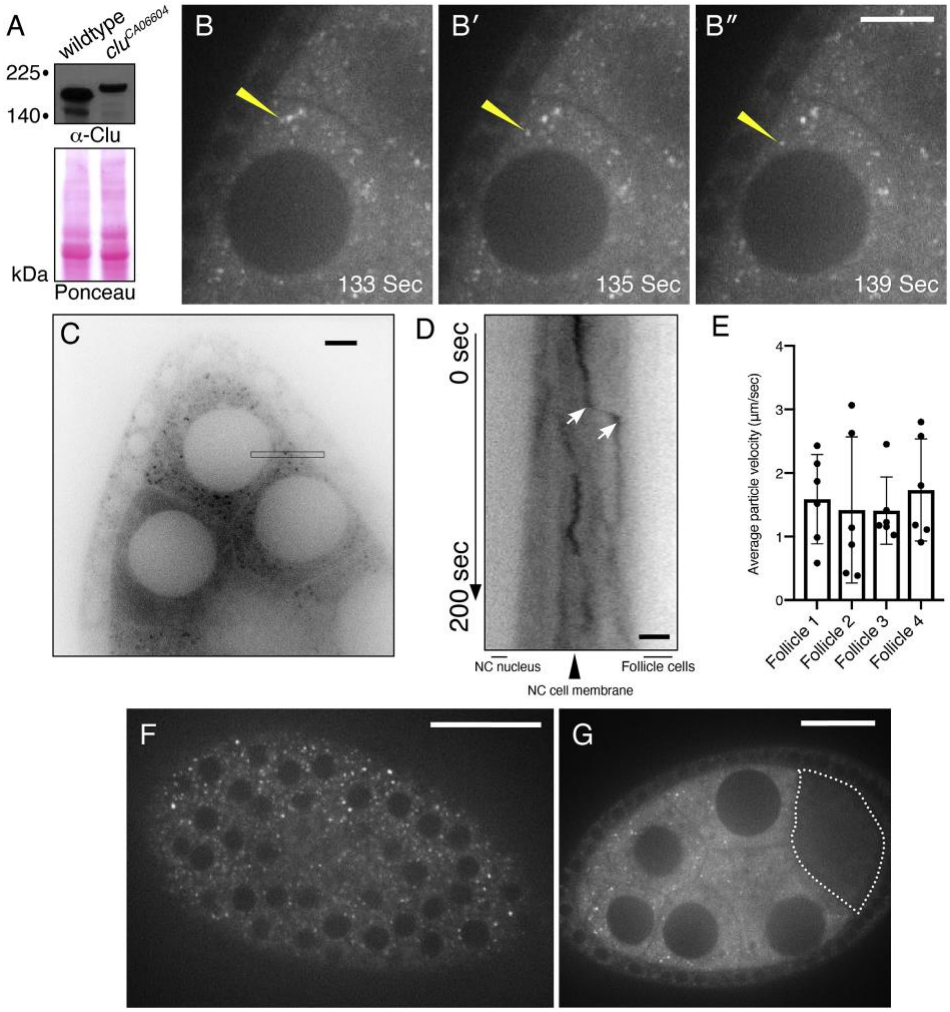

Figure 1. Clu::GFP live-imaging shows robust, dynamic particles in germ cells and surrounding follicle cells. Follicle from a *clu*^{CA06604} female. Addition of hydrogen-peroxide to follicles is a time-sensitive treatment. The restart of imaging was delayed in this video as a result of sample displacement during H_2O_2 addition. The mitochondria have already begun to visibly clump and lose their membrane potential upon the restart of imaging at time 0 (as compared to time 0 in Video 3). Failure to resume imaging quickly after treatment will result in inaccurate and unusable results as the early experimental effects will be missed prior time imaging. White = TMRE. Imaged one frame per 15 s for 20 mins, and the video is 10 frames per second.

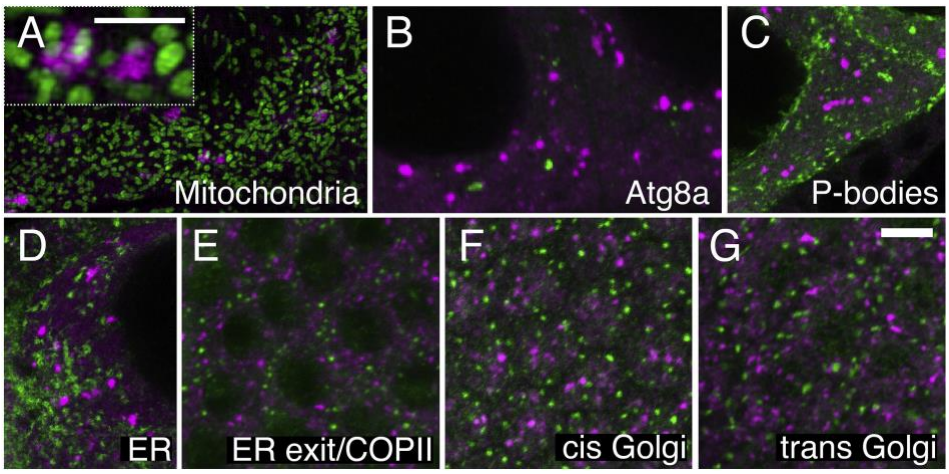

Figure 2. Clu particles are unique.

(A) Structured illumination micrograph. Clu particles are granular and touch mitochondria in germ cells (inset), as previously shown. (B, C) Clu particles do not co-localize with autolysosomes (B) or Processing bodies (C) in germ cells. (D-G) Clu particles do not appear to associate with ER in germ cells (D), nor with ER-exit sites (E), cis-Golgi (F) or trans-Golgi (G) in surrounding somatic follicle cells. Green = ATP synthase (A), Atg8a (B), Tral::GFP (C), Sec61α::GFP (D), Sec23 (E), GMAP (F), and Golgin245 (G). Magenta = Clu (A-G). Scale bar: 5 µm in G for A-G, 2.5µm in A for inset.

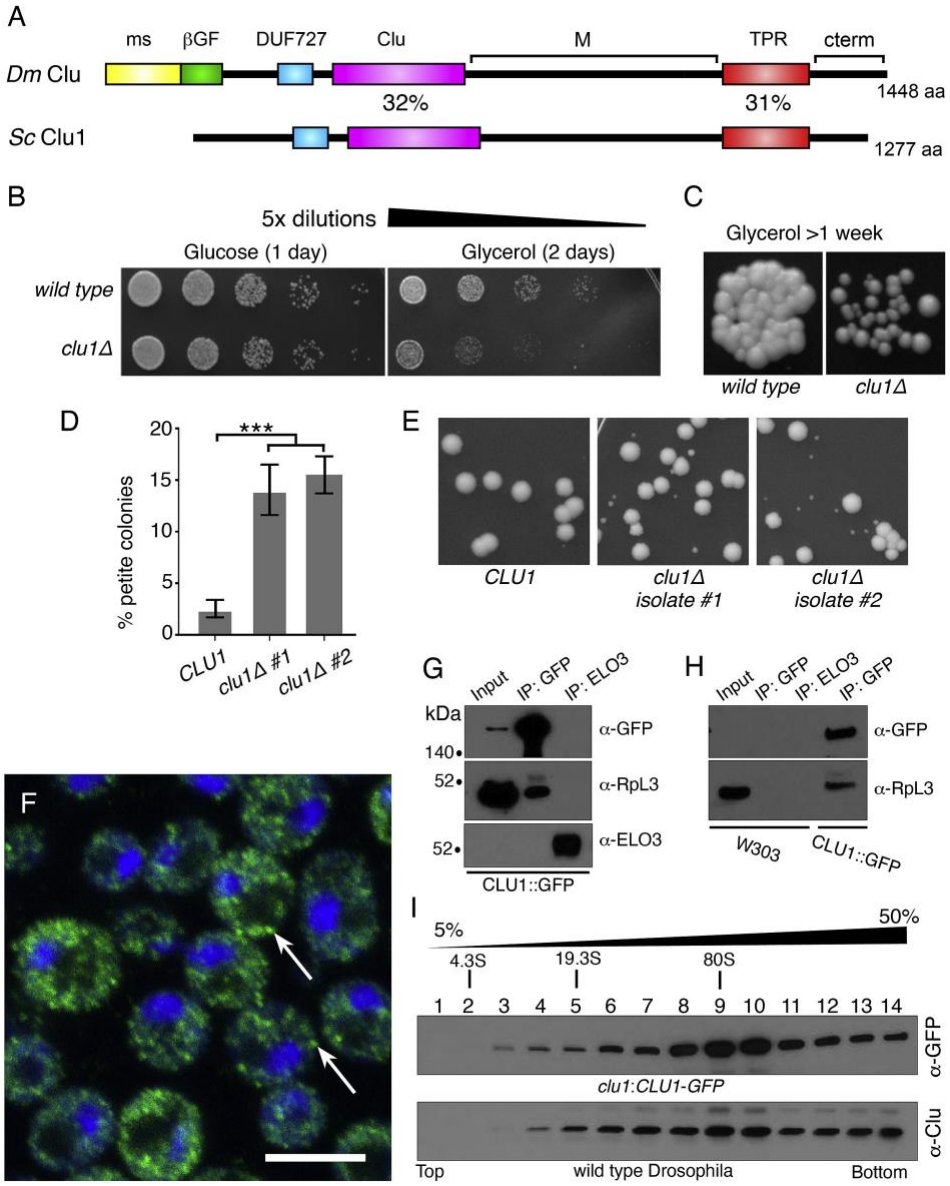

Figure 3. Yeast Clu1p accumulates as cytoplasmic particles and associate with RpL3p. (A) A cartoon diagram of the shared domain structure between *Drosophila* Clu (Dm) and yeast Clu1p (Sc). (B) Serially diluted *clu1*Δ cultures grow normally on glucose, but not on glycerol. (C) *clu1*Δ forms small colonies after one week of growth on glycerol compared to its parental wild type strain. (D) Two independent isolates of *clu1Δ* (BY4741 genetic background) form significantly higher percentages of petite colonies. (E) Representative micrographs showing petite colony formation. (F) Fixed and anti-GFP labeled log-phase yeast cells of *strain clu1::CLU1-GFP*. Clu1p puncta are indicated by arrows. (G) Co-immunoprecipitation shows that Clu1p associates with the ribosomal protein

RpL3. Elongation of fatty acids protein 3 (Elo3p) serves as a negative control. Pulldowns were from *clu1::CLU1-GFP* extract. (H) The anti-GFP antibody is specific for *clu1::CLU1-GFP*. GFP pulldown from a wild type strain (W303) indicates there is no non-specific cross-reactivity. (I) Sucrose gradient using extract from yeast strain *clu1::CLU1-GFP* (top) and *Drosophila* wild type ovaries (bottom). Green = Clu1p::GFP, blue = DAPI. Scale bar: 5 μm in F for F. For D, $p < 0.001$ using a two-way ANOVA test.

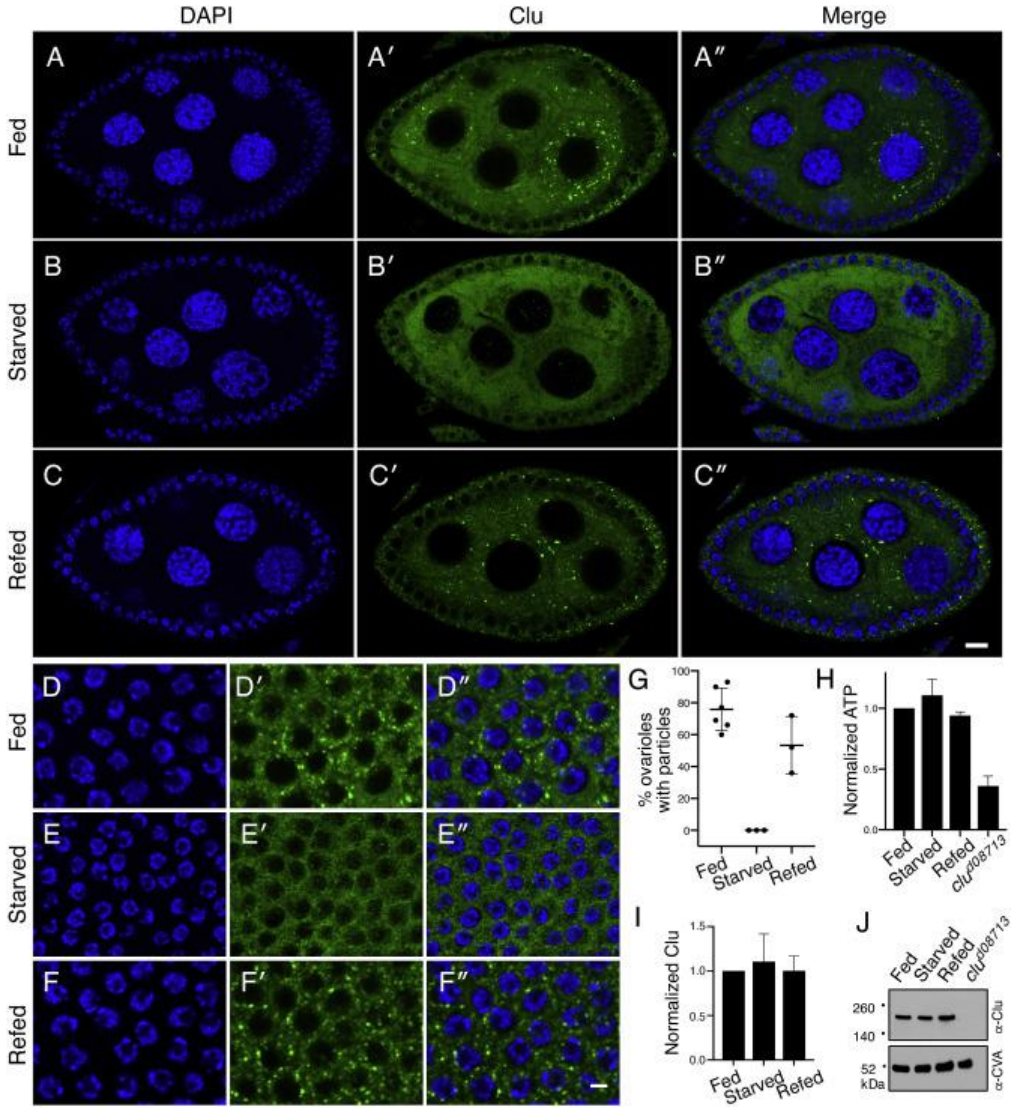

Figure 4. Clu particles disaggregate in response to starvation.
(A-C″). Follicles from w1118 females. Well-fed follicles contain many large particles in the germ cells (A′). Starvation for 5 hours on H_20 causes the particles to disaggregate (B′). Re-feeding starved females causes Clu particles to reform (C′). Quantification is shown in (G). (D-F″) Surrounding somatic follicle cells show the same dynamic as the germ cells. ATP levels (H) and Clu levels (I, J) remain the same for all three conditions. clu^{d08713} is a positive control. Details of n values are in the materials and methods. Error bars are S.E.M. Green = Clu (A-F″) and blue = DAPI (A-F″). Scale bar: 10 μm in C″ for A-C″ and in F″ for D-F″.

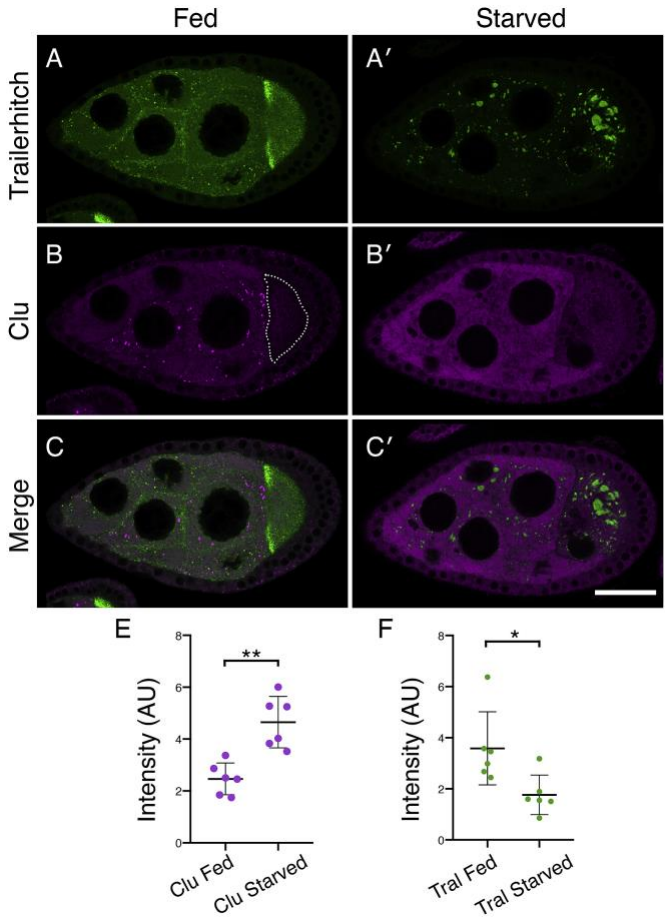

Figure 5. Clu particles and the Processing body component Trailer hitch respond oppositely to starvation. (A-C′) Follicles from Tral::GFP females. (A, C) Tral::GFP forms small aggregates in the nurse cells, homogeneous dispersed staining, and is concentrated at the anterior of the oocyte (A). Upon starvation, Tral::GFP forms very large processing bodies, the diffuse Tral signal decreases (A′, C′), whereas Clu particles disaggregate with Clu becoming diffuse (B′, C′). The dotted line indicates the oocyte (B). (E) Quantification of homogeneously dispersed Clu intensity in nurse cells under fed and starved conditions. (F) Quantification of Tral::GFP homogeneously dispersed intensity in nurse cells under fed and starved conditions. Details of n values are in the materials and methods. Green = Tral::GFP (A-A′, C-C′), magenta = Clu (B-B′, C-C′). Scale bar: 40µm in C′ for A-C′. Error bars are S.E.M. * p = 0.015, ** p = 0.0016 using a Student's t-test with Welch's correlation.

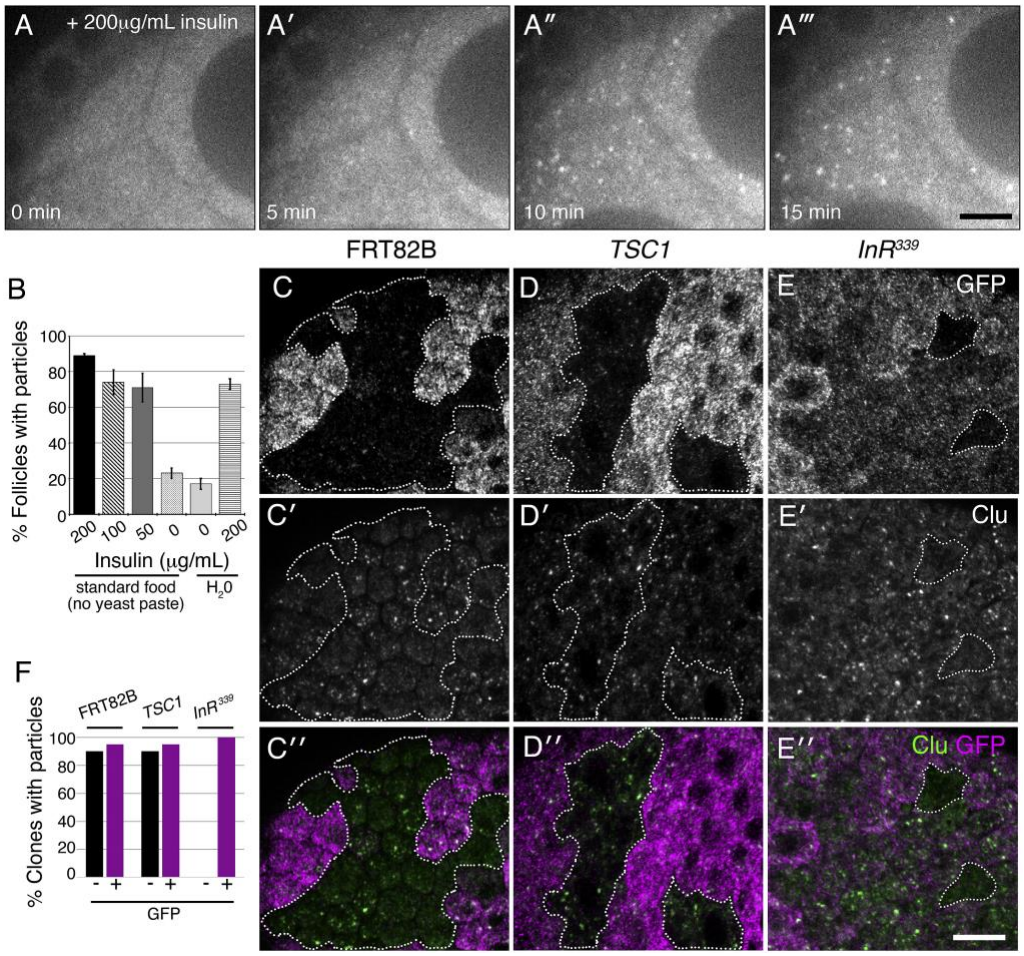

Figure 6. Insulin is necessary and sufficient for Cu particle formation.
(A-A‴) Stills from live imaging of starved *clu*^{CA06604} germ cells expressing Clu::GFP. Females were raised on standard fly food (no yeast paste) and dissected in Complete Schneider's. After adding insulin at time zero (A), particles start forming within five minutes (A′). (B) Quantification of the percent single follicles containing Clu particles for females starved on standard food (no yeast paste) or H_2O. (C-E″) Clonal analysis in follicle cells. Wild type control clones (FRT82B, GFP-, dotted white line) have Clu particles as expected (C-C″). Clones mutant for *TSC1*^{Q87X} also have Clu particles (D-D″, dotted white lines). Clones mutant for *InR*^{339} lack particles (dotted white lines) (E-E″). (F) Quantification of the number of GFP+ and GFP- clones containing particles for control FRT82B (n = 20), TSC1 (n = 20), and *InR*^{339} (n = 11) mutant clones. White = Clu::GFP (A-A‴), GFP (C, D, E), and Clu, (C′, D′, E′), green = Clu, magenta = GFP. For B, error bars = S.D. Scale bars: 20 µm in A‴ for A-A‴, 10 µm in E″ for C-E′.

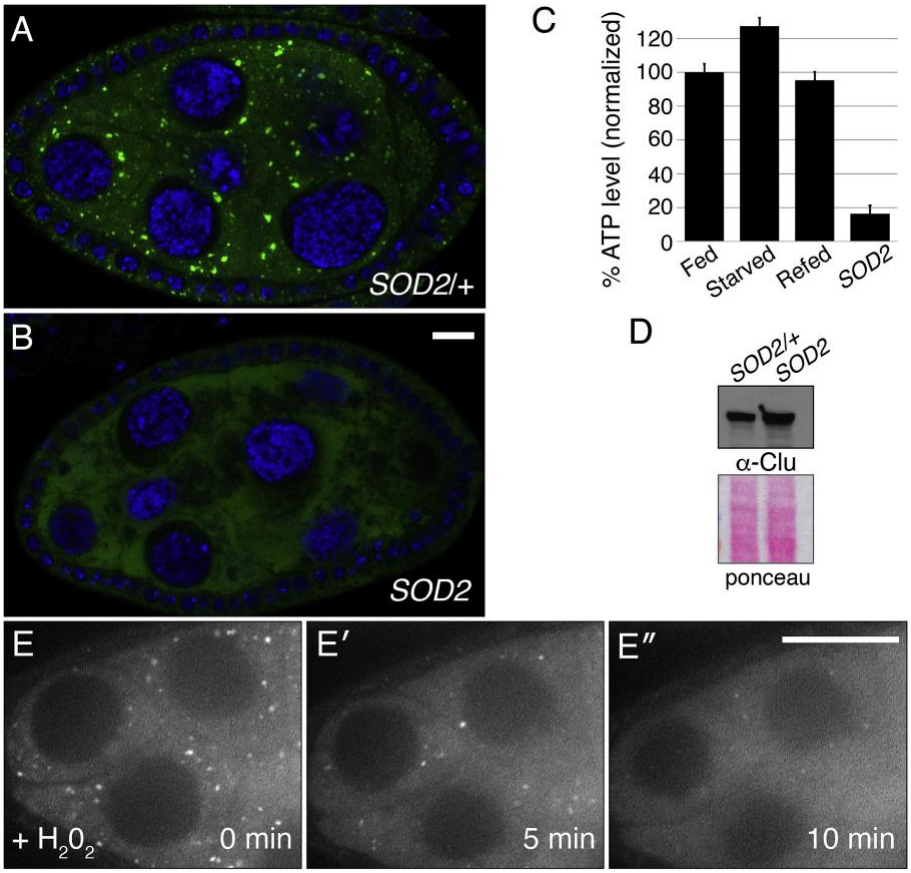

Figure 7. Oxidative stress disperses Clu particles.

(A, B) Clu particles are always present in wild type siblings (n = 44) (A) but always missing in *SOD2* mutant follicles (n = 51). (C, D) *SOD2* mutants have decreased levels of ATP (C), but not decreased levels of Clu protein (D). (E-E″) Live-image stills of a well-fed $clu^{CA06604}$ follicle. Addition of H_20_2 causes particles to disperse (n = 11). Green = Clu (A, B), blue = DAPI (A, B), white = Clu::GFP (E-E″). Error bars are S.E.M. Scale bar: 10µm in B for A, B, 40µm in E″ for E-E″.

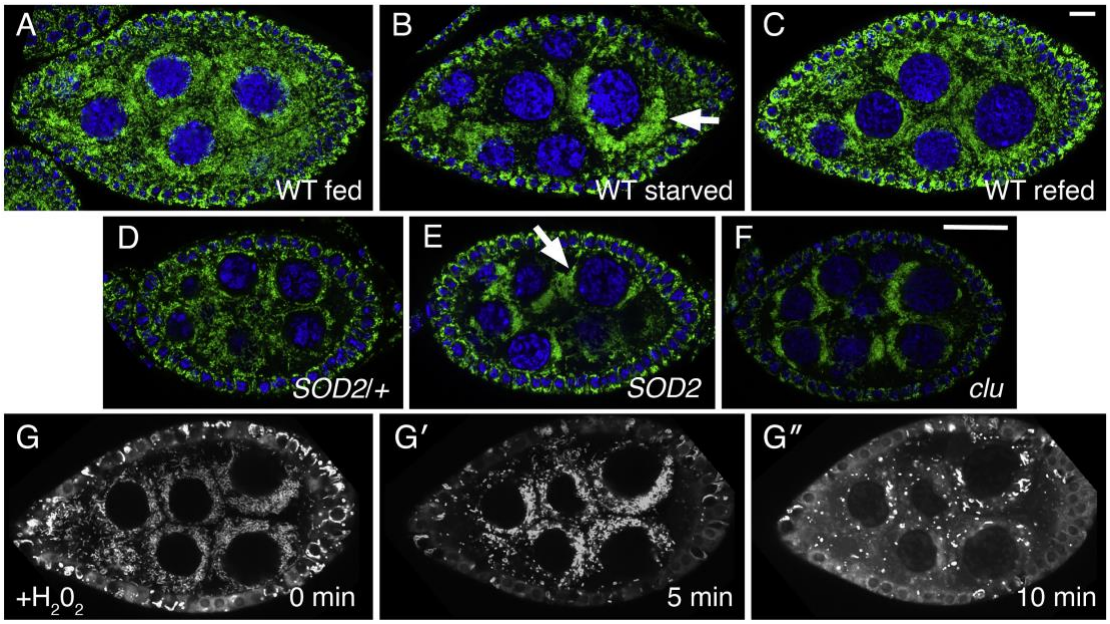

Figure 8. Stress causes mitochondrial mislocalization in *Drosophila* germ cells. (A-C) Follicles from w^{1118} females. Well-fed females have evenly dispersed mitochondria in germ cells (A). Starvation causes mitochondria to clump (arrow) (B). Refeeding yeast paste for two hours post starvation causes mitochondria to disperse (C). (D, E) Mitochondria in *SOD2* mutant germ cells also form clumps (E, arrow) compared to wild type *SOD2/+* sibling follicles (D). This clumping is reminiscent of loss of Clu, as previously published (F). (G- G″) Stills from live-imaging well-fed $clu^{CA06604}$. Adding H_2O_2 during imaging to initiate oxidative stress also causes mitochondria to clump. TMRE labeling of mitochondria indicates that mitochondria are initially dispersed at time zero (G), and that mitochondria start to clump after H_2O_2 addition (G′) (n = 6). At a later time-point, the TMRE labeling becomes spotty due to mitochondria losing their membrane potential and therefore their ability to sequester the dye (G″). Green = ATP synthase (A-F), blue = DAPI (A-F), white = TMRE (G-G″). Scale bars: 10 µm in C for A-C, G-G″, 10 µm in F for D-F.

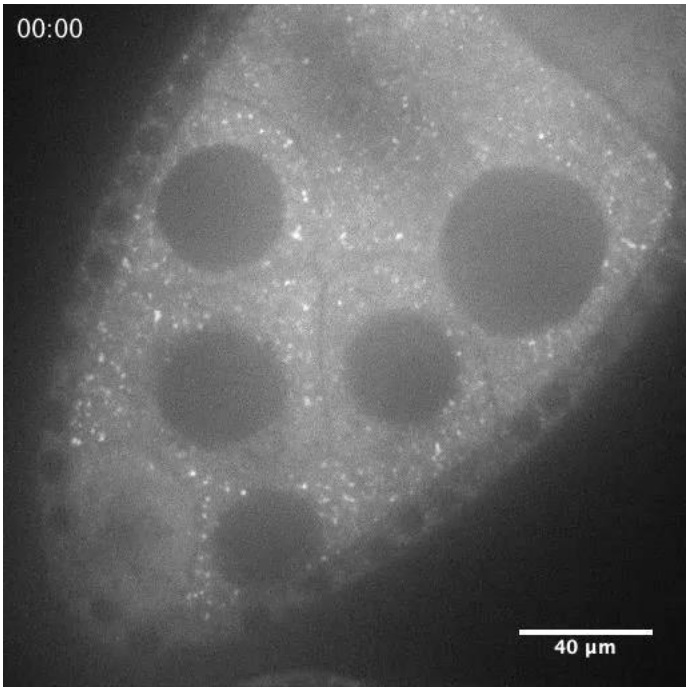

Movie 1. Clu live-imaging shows robust, dynamic particles in germ cells.
Follicle from *clu*^{CA06604} (Clu-GFP) female. Imaged one frame per second for 200 seconds. Video is 36 frames per second.

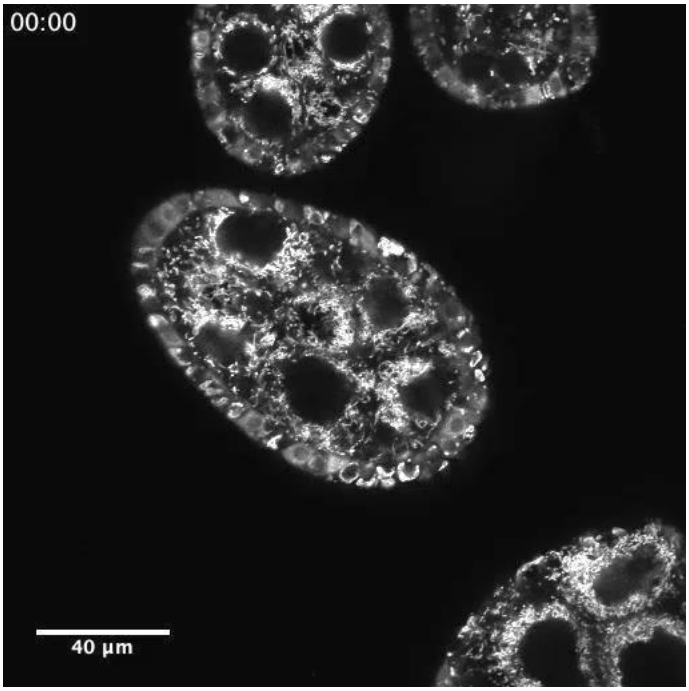

Movie 2. Mitochondria movement is normal without colcemide treatment.
Follicle from cluCA06604 (Clu-GFP) female treated with TMRE. Imaged one frame per second for 120 seconds. Video is 10 frames per second.

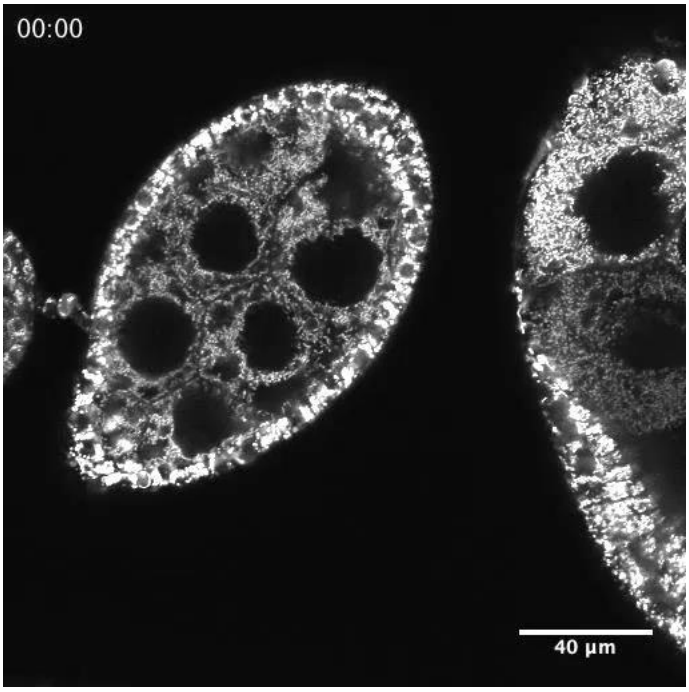

Movie 3. Mitochondria movement ceases with treatment of the microtubule destabilizer colcemide. Follicle from *clu*^{CA06604} (Clu-GFP) female treated with TMRE. Imaged one frame per second for 120 seconds. Video is 10 frames per second.

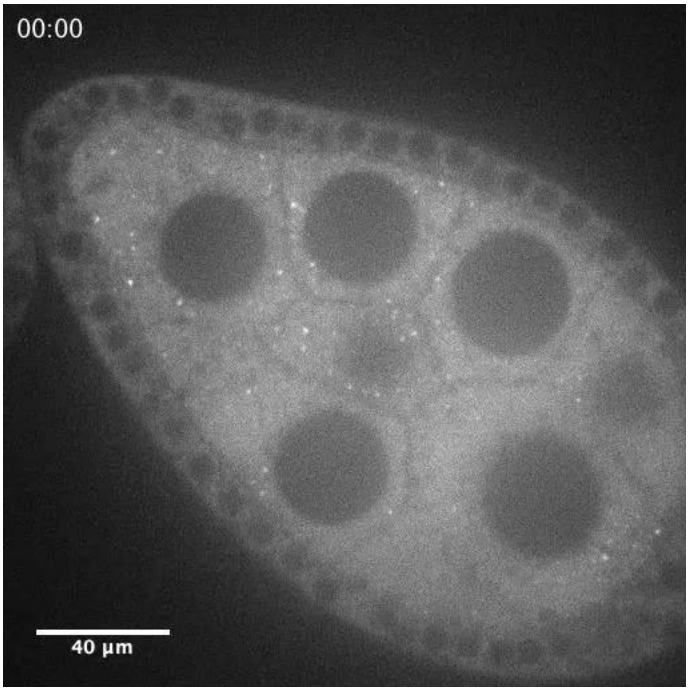

Movie 4. Clu particle movement ceases with treatment of the microtubule destabilizer colcemide. Follicle from *clu*^{CA06604} (Clu-GFP) female. Imaged one frame per second for 120 seconds. Video is 24 frames per second.

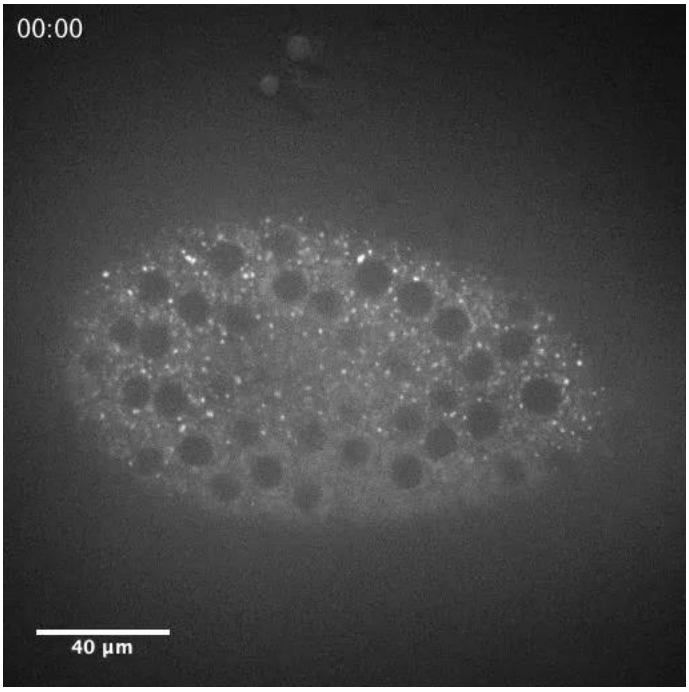

Movie 5. Clu particles in the surrounding follicle cells are more stationary than in germ cells. Follicle from *clu*^{CA06604} (Clu-GFP) female. Imaged one frame per second for 120 seconds. Video is 24 frames per second.

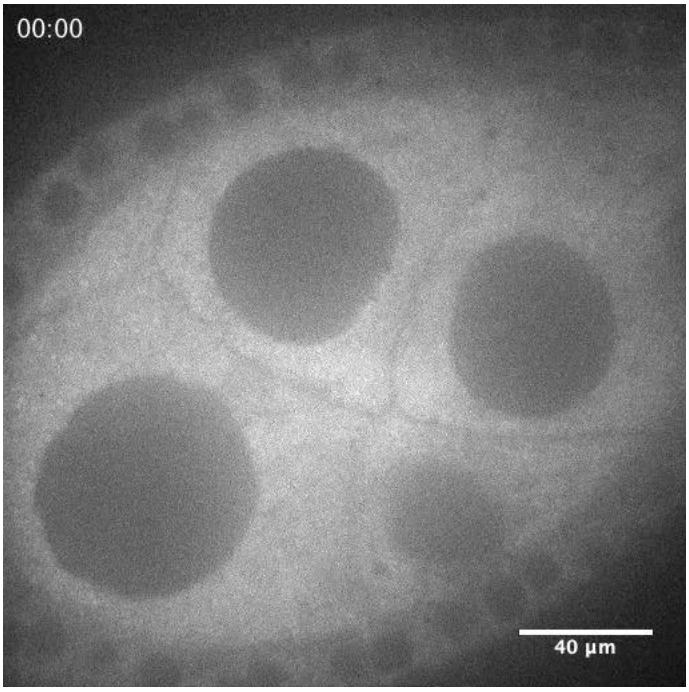

Movie 6. Clu particle formation is induced with insulin.
Follicle from *clu*^{CA06604} (Clu-GFP) female. Imaged one frame per minute for 45 minutes. Video is 10 frames per second.

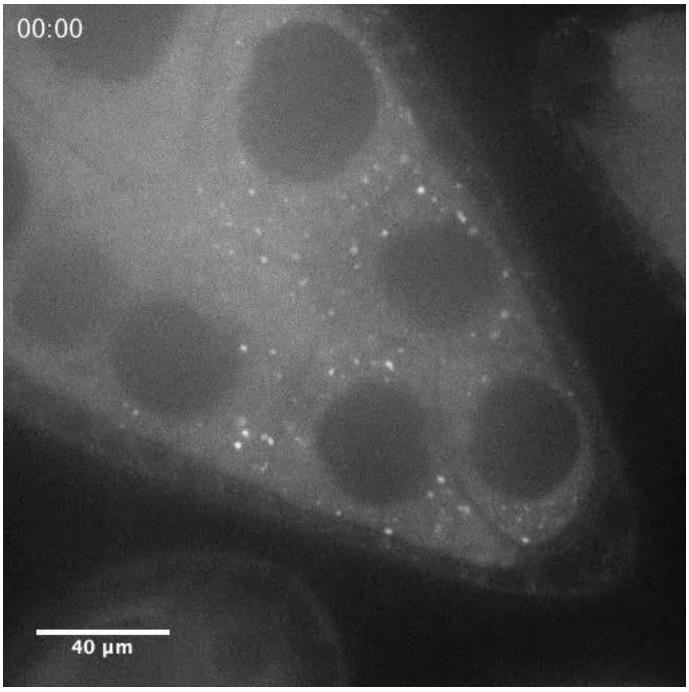

Movie 7. Oxidative stress disperses Clu particles.
Follicle from *clu*^{CA06604} (Clu-GFP) female. Imaged one frame per 15 seconds for 15 minutes. Video is 10 frames per second.

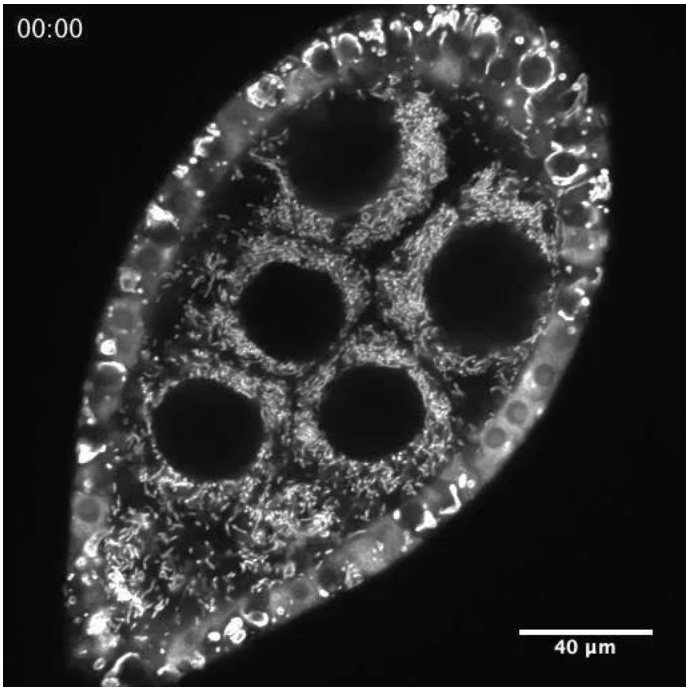

Movie 8. Oxidative stress causes mitochondrial mislocalization in *Drosophila* germ cells. Follicle from *clu*^{CA06604} (Clu-GFP) female. Imaged one frame per 15 seconds for 20 minutes. Video is 10 frames per second.

SUPPLEMENTAL FIGURES

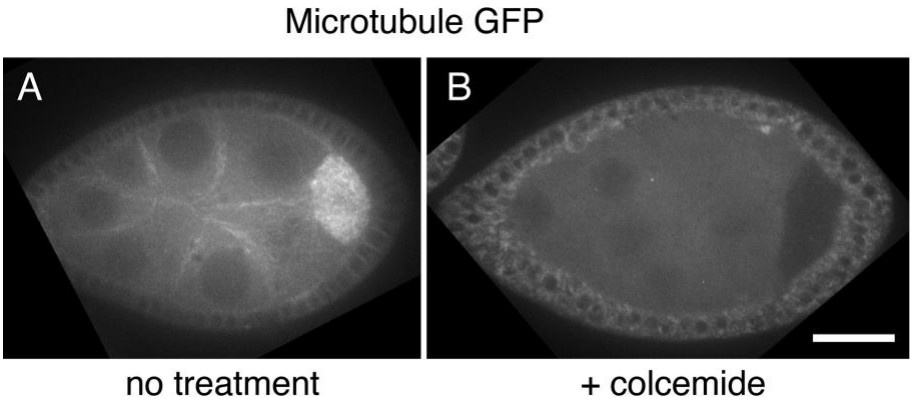

Figure S1. Colcemide treatment disrupts microtubules. *Ubi-GFP::tubulin* expressing follicles. Follicles cultured in Complete Schneider's Media supplemented with 200 µg/mL of insulin display an intact microtubule cytoskeleton (A). Follicles after colcemide treatment show the microtubule cytoskeleton has been disrupted (B). Scale bar: 40µm in B for A, B.

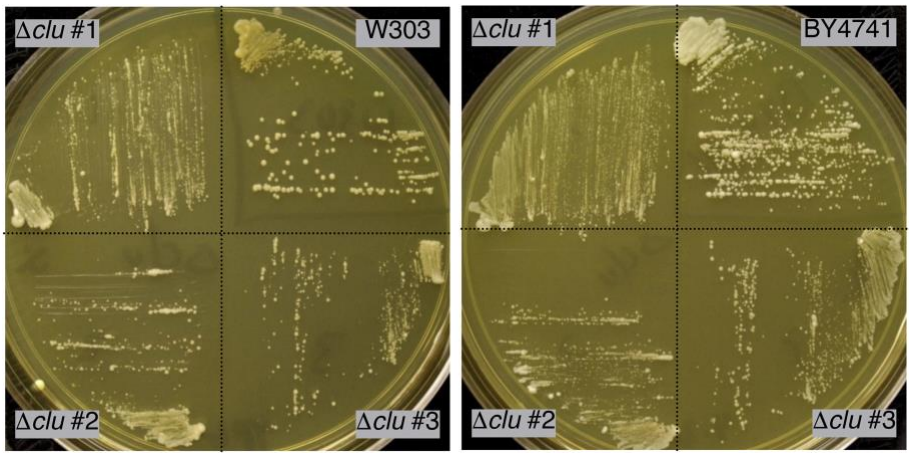

Figure S2. Multiple *Δclu1* strains derived in two different wild type genetic backgrounds have reduced growth on glycerol. Each plate shows three newly generated deletions of *CLU1* (*clu1::KanMX*) in two wild type strain backgrounds (W303, left plate and BY4741, right plate). After one week on glycerol, the wild type strain grows at a normal rate whereas colonies of three newly *Δclu1* derived strains are smaller and less robust.

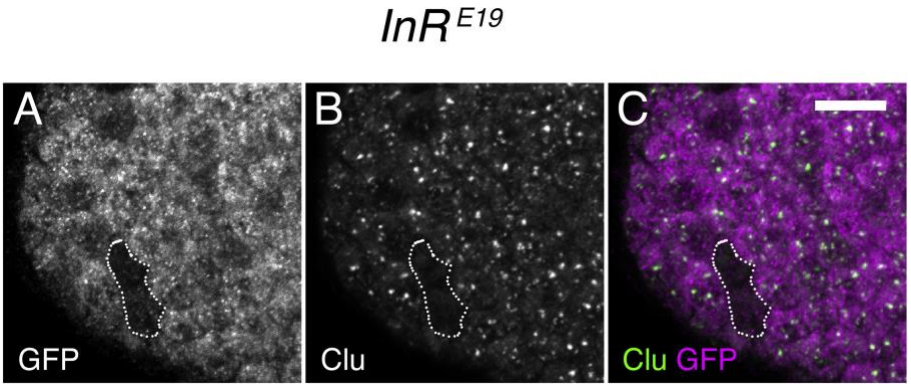

Figure S3. *InR*^{E19} mutant follicle cell clones do not contain Clu particles.
(A-C) The surrounding somatic follicle cells of a follicle. The mutant cells are indicated by lack of GFP antibody labeling (dotted outline, A). Clu particles are not present in cells mutant for *InR*^{E19} (dotted outline, B, C). White = GFP (A) and Clu (B). Magenta = GFP (C). Green = Clu (C). Scale bar = 10 μm in C for A-C. n=7.

CHAPTER 4: Elucidating how translation affects Clu particle dynamics

INTRODUCTION

Clu is necessary for proper mitochondrial function and morphology. *clu* mutant flies have decreased levels of ATP and mitochondrial proteins, increased levels of mitochondrial oxidative damage, and physically damaged and mislocalized mitochondria (21; 79; 81). *Cluh* knockout mouse embryonic fibroblasts have reduced levels of mitochondrial proteins (30). Furthermore, we have shown that under stress conditions where particles disperse, Clu protein levels do not decrease, signifying that Clu particles specifically are responsive to stress (21; 84). Therefore, we believe that Clu's effects on mitochondria are specific to the presence of Clu particles. In Specific Aim 1, we established that Clu particles are unique, dynamic, stress-responsive cytoplasmic particles. Following, the goal of Specific Aim 2 is to characterize how these particle dynamics may be impacting mitochondrial function, specifically through Clu's role in translation.

We have previously shown that Clu is a ribonucleoprotein that peripherally associates with mitochondria. In an oligo(dT) binding assay using deletion domain constructs of Clu protein, the Clu-mRNA binding was only abolished when the TPR domain was absent, signifying that Clu binds mRNAs through this domain (79). We also found through immunoprecipitation and mass spectrometry analysis that Clu interacts with the outer mitochondrial membrane transporters Porin and TOM20, and this was confirmed with co-IPs (82). An unbiased CLUH-RIP experiment further shows that CLUH specifically associates with mRNAs of a subset of nucleus-encoded mitochondrial proteins (30). Data from mass spectrometry experiments shows that Clu associates with ribosomal proteins of the large and small subunits, translation initiation and elongation

factors, and notably, the translation initiation factor eIF3g, and this was confirmed by co-IP (79). eIF3g is a member of the eIF3 complex which is present during active translation (94). This suggests that Clu associates with ribosomes when mRNAs are being actively translated. Another piece of evidence that Clu directly affects mitochondria is that mitochondrial protein levels are reduced in *clu* mutant flies and in *Cluh* knockout mice where there were reduced protein levels of several of the mRNAs shown to be enriched in CLUH binding in a CLUH-RIP analysis (75; 82).

Taken together, the data that Clu binds mRNAs, ribosomes, translation factors, and TOM20 and Porin and that the absence of Clu leads to reduced mitochondrial protein levels, this suggests that Clu may function in the translation and import of mitochondrial proteins. Traditional post-translational mitochondrial import involves mRNAs being transcribed and translated in the cytoplasm and then imported into the mitochondria through transporters in the outer membrane (see Introduction, Figure 3 and 4). In co-translational import, nascent polypeptides are imported immediately after translation (Introduction, Figure 4). Clu particles may be the sites of localized translation for Clu-bound mRNAs, or they may assist in localizing mRNAs of mitochondrial proteins to the mitochondrial outer membrane similar to Puf3p in yeast (2; 74). In Sheard et al., we identified a signaling mechanism which is responsible for the nutritional stress response we observed in Clu particles. We showed that insulin signaling is both necessary and sufficient to induce Clu particle formation using clonal analysis, and that exogenous addition of insulin to the culture media of follicles from starved flies rapidly induces particle formation (84). As such, we have proposed an updated working model in which

Clu particles regulate mRNAs to control mitochondrial output in response to nutritional cues. The aim of this work is to determine if the presence and absence of Clu particles affects translation of mitochondrial proteins. RNP granules, stress granules in particular, function in translational regulation and reprogramming (46; 61). Clu also associates with ribosomal proteins, eIF3g, and mRNAs. These findings bring forth three specific questions: 1) whether the presence and absence of Clu particles affect global translation, 2) whether the presence and absence of particles affect the synthesis rate of mitochondrial proteins, and 3) whether stalling translation has an effect on Clu particle stability. We employed cycloheximide-based approaches to begin addressing these questions. The antibiotic cycloheximide is a protein translation inhibitor which works by physically hindering the exit site of ribosomes in a manner that blocks the elongating polypeptide chain in the neighboring elongation site (Figure 1, (78)). Consequently, translation stalls, but the mRNA-ribosome-nascent polypeptide chain complex remains intact. Cycloheximide chase followed by Western blotting is an effective method to study translation kinetics since any changes in protein abundance are a result of protein degradation, and any differences in the recovery rate of proteins may be attributed to the presence and absence of particles (12).

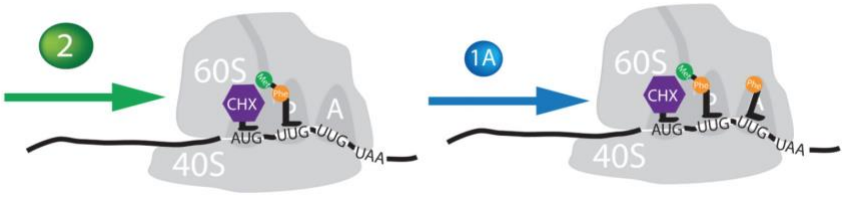

Figure 1. Mechanism of cycloheximide inhibition on translation.
Cycloheximide inhibits translation elongation by binding to the exit (E) site in a manner which physically hinders the elongating polypeptide in the elongation (P) site (78).

MATERIALS AND METHODS

Fly stocks: The following stocks were used for experiments: w^{1118}, *clueless*^{d08713}/*CyO P(ActGFP)JMR1 (21), trailer hitch*^{CA06517}, *Sec61*α*CC00735*, *clueless*^{CA06604} *(14)*, (Bloomington *Drosophila* Stock Center). Flies were reared on either standard cornmeal fly media or standard cornmeal fly media supplemented with yeast paste at 22° or 25° C.

Cycloheximide feeding: Fresh aliquots of wet yeast paste spiked with cycloheximide (Sigma, St. Louis, MO) were prepared immediately prior to each experiment. Cycloheximide aliquots of the desired concentration were prepared in by dissolving the cycloheximide in distilled water, aliquoting into 1.7mL microcentrifuge tubes, and storing at -20° C until use. Active dry yeast aliquots were prepared by adding active dry yeast (Red Star Yeast, Milwaukee, WI) 0.38 grams of yeast to a 1.7mL centrifuge tube

and storing at 4° C until use. To prepare an aliquot of wet yeast paste, 500µL of thawed cycloheximide solution was added to one tube of dry yeast and mixed into a paste.

Blue dye feeding and quantification: Blue-dye feeding and quantification was performed as described in Wong et al. (107). 0-24 hr flies were fattened with yeast paste for 3-7 days. All wet yeast paste sources were prepared with 2.5% (w/v) of FD&C Blue Dye no. 1 (Sigma, St. Louis, MO). 30 female flies were then transferred to a vial with fresh fly food and wet yeast paste (controls) or fresh fly food and yeast paste spiked with cycloheximide (Sigma, St. Louis, MO) for 24 or 48 h. The absorbance of the samples was measured at 629 nm on a BioTek Synergy H1 hybrid multi-mode reader (BioTek Instruments, Winooski, VT) as described.

Fixed image immunofluorescence: 0-24 hr flies were fattened with yeast paste for 3-7 days. 30 female flies were then transferred to a vial with fresh fly food and yeast paste spiked with cycloheximide (Sigma, St. Louis, MO) for 24 hr. 30 female flies remained feeding on yeast paste throughout as controls. From each condition, 3x10 flies were then dissected at room temperature (RT) in Grace's Insect Medium (modified) (BioWhittaker, Lonza, Cologne, Germany). Ovaries were fixed for 20 minutes in 4% paraformaldehyde and 20mM formic acid solution (Sigma, St. Louis, MO) made in Grace's. Tissues were washed two times (40 minutes each) with Antibody wash buffer (Ab) (1X PBS:0.1% Triton X-100:1% BSA), then incubated in primary antibody over night at 4°C. They were then washed two times (40 minutes each) and incubated overnight at 4°C in secondary

antibody. After washing, DAPI (1:1000) was added for five minutes then removed, and Vectashield (Vector Laboratories, Inc., Burlingame, CA) was added. The following primary antibodies were used: guinea pig anti-Clu N-terminus (1:2000) (21), mouse anti-Complex V (ATP synthase (CVA)) (1:1000, AbCam, Cambridge, MA, cat# ab14748). The following secondary antibodies were used: goat anti-mouse IgG_{2b} Alexa 568 (1:500), goat anti-guinea pig Alexa 488 (1:1000). Samples were imaged using a Zeiss 700 confocal microscope and 63x Plan Apo NA 1.4 lens.

Live Imaging Microscopy for Drosophila Tissue Samples: *clueless*^{CA06604} females that had been fattened with yeast paste were dissected at room temperature (RT) in Complete Schneider's (CS) Media (Schneider's *Drosophila* media (ThermoFisher Scientific, Waltham, MA) with 15% Fetal Bovine Serum and 0.6X Pen-Strep solution) supplemented with 200 µg/mL of insulin (insulin which did not readily dissolve in media was allowed to settle overnight at 4°C prior to use) or CS supplemented with 7.0 mM cycloheximide (Sigma, St. Louis, MO). Ovaries were removed and further teased apart into single, isolated ovarioles. Ovarioles were then loaded onto a glass bottom 35mm dish (MatTek Corporation, Ashland, MA) and live videos of a single focal plane were collected using a Nikon spinning disk/TIRF/3D-STORM microscope at 60x at room temperature. For experiments with cycloheximide addition, ovarioles were prepared as above in Complete Schneider's Media with 200 µg/mL of insulin. Complete Schneider's Media containing 7.0 mM cycloheximide would be added to the dish with a pipette to dilute the sample 1:1, resulting in an insulin concentration of 100 µg/mL and a

cycloheximide concentration of 3.5 mM. For subsequent H_2O_2 treatments, additional Complete Schneider's Media containing 100 µg/mL of insulin, 3.5 mM cycloheximide media, and 4mM H_2O_2 was added during imaging to make the final concentration 2 mM H_2O_2. Treatment lasted for 20 minutes while filming.

Western blotting and Immunoprecipitation: 0-24 hr flies were fattened with yeast paste for 3-7 days. 30 female flies were then transferred to a vial with fresh fly food and yeast paste spiked with cycloheximide (Sigma, St. Louis, MO) for 24 hr. 30 female flies remained feeding on yeast paste throughout as controls. From each condition, 3 groups of 7 flies (n = 21) flies were then dissected at room temperature (RT) in Grace's Insect Medium (modified) (BioWhittaker, Lonza, Cologne, Germany). The ovaries were dissected out, and the remaining carcasses were retained separately. Seven ovaries were homogenized in 170 µL of sample buffer, and the corresponding 7 carcasses were also homogenized in 170 µL of sample buffer. The sample extracts were weighed on an analytical balance (Mettler-Toledo, model AL54, Columbus, OH) for normalization purposes. The sample extracts were run on a 4-20% polyacrylamide gel using a standard SDS-PAGE protocol for Western blotting. After electrophoresis, proteins were transferred onto a Hybond- ECL nitrocellulose membrane (GE Healthsciences, Inc., Chicago, IL) then soaked with Ponceau S for 10 min and briefly rinsed. Blots were exposed to the following antibodies: guinea pig anti-Clu N-terminus (1:30,000) (21), mouse anti-Complex V (ATP synthase (CVA)) (1:10,000, AbCam, Cambridge, MA, cat#

ab14748), and anti-α-tubulin (1:5000, AA4.3, Developmental Studies Hybridoma Bank, University of Iowa, Iowa City).

Egg laying and adult survival measurements: Egg-laying was performed based on a modified procedure from Drummond-Barbosa and Spradling (25). 0-24 hr flies were fattened with yeast paste for 1 day in plastic bottles containing agar-corn syrup plates. After 1 day, five pairs of flies (5 females and 5 males) x 3 replicates were transferred to a bottle with a fresh agar-corn syrup plate containing either a layer of wet yeast paste (controls) or a layer of wet yeast paste spiked with cycloheximide. The number of eggs laid was counted every 24 h, and the flies were subsequently transferred to a fresh agar-corn syrup plate containing a fresh layer of wet yeast paste or wet yeast paste spiked with cycloheximide. Adult survival was performed based on a modified procedure from Sen et. al (81). 0-24 hr flies were fattened with yeast paste for 3-7 days. 3 groups of 20 female flies (n = 60) were then transferred to vials with fresh fly food and yeast paste spiked with cycloheximide (Sigma, St. Louis, MO) or vials with fresh fly food and yeast paste as controls. The number of dead flies was counted every 24 h, and the flies were subsequently transferred to a fresh vial containing fresh fly food and wet yeast paste or wet yeast paste spiked with cycloheximide. This procedure was also repeated for 3 groups of 20 male flies.

RESULTS

Cycloheximide feeding detrimentally affects *Drosophila* development and oogenesis

To determine if cycloheximide feeding was an effective means of delivering the drug to flies, we first fed flies wet yeast paste spiked with increasing concentrations of cycloheximide for 1-2 days as modified from Marcos et al (57). As a control to verify that the flies were ingesting the cycloheximide-spiked food, the food was dyed blue with FD&C blue no. 1 (Figure 1a, right side), and the amount of blue food ingested was quantified using a spectrophotometer (Figure 1c). As a visual confirmation, blue food is also visible in the guts of female flies at every cycloheximide concentration tested after both 24 and 48 hours of feeding (Figure 1b, arrow). The protein levels of Clu, ATP synthase, and α-tubulin in the ovaries were also measured to determine if there was a change in protein levels after cycloheximide feeding. Western blot analysis shows that the protein levels of Clu, ATP Synthase, and α-tubulin are all reduced as expected, signifying that cycloheximide feeding is an effective means of drug delivery (Figure 1d).

Notably, the ovary sizes in female flies are visibly smaller after cycloheximide feeding as illustrated in Figure 1b, and this decrease in size is exaggerated with increasing concentrations of cycloheximide in the wet yeast paste (Figure 2a). Flies fed yeast paste containing increasing concentrations of cycloheximide also produce decreased numbers of larvae (Figure 2b). Due to the effects on ovary size that we observed, we next sought to determine if cycloheximide feeding results in any other developmental effects on flies by measuring female fertility and survival of both males and females. As measured by an egg-laying assay, there is an expected overall increase in the number of eggs per female per day for each group; however, the cycloheximide-fed females show decreases in the number of eggs laid compared to the controls, and this

effect is also dose-dependent (Figure 2c). There was virtually no difference between the survival of females fed normal yeast paste compared to females fed yeast paste spike with 3.5 mM cycloheximide within a three-week time span (Figure 2d). However, there was a marked difference in the groups of males within the same time span, with cycloheximide-fed males showing about a 40% decrease in survival (Figure 2d). These results support that adult flies readily ingest cycloheximide at various concentrations and that this treatment decreases ovary size in a dose-dependent manner. Furthermore, the doses that caused decreased ovaries did not have a lethal effect on females over the time period we tested, thus has the greatest effect in the ovary which is a highly metabolically active tissue.

Cycloheximide feeding does not disrupt particle formation or stability

Because particles are very sensitive to cellular stress and other drug treatments, we next determined whether cycloheximide feeding would disrupt particle formation and stability. To achieve this, we fed wild-type flies wet yeast paste spiked with 3.5 mM cycloheximide for 1 day and then labeled the ovaries with anti-Clu and anti-CVA (ATP synthase) antibodies. Clu particles are present, and mitochondria are properly dispersed (Figure 3a – 3a″) in these flies. This result is consistent with data showing that treatment with cycloheximide does not disrupt CLUH granules in HeLa cells (69). Stalling translation does not disperse Clu particles though there is a decrease in Clu protein levels (Figure 1d) and the ovaries are smaller (Figure 2a). Based on this observation, the next question we aimed to address was whether the cycloheximide treatment was stabilizing particles on the translational machinery. Follicles from flies which are starved on water

only for 5 hours do not have particles (84). To address this question, we next starved the flies first on water only for five hours and then fed them wet yeast paste spiked with 3.5 mM cycloheximide for 1 day. Clu particles still reform, and the mitochondria are properly dispersed in the presence of cycloheximide (Figure 3b – 3b″) in these flies. These results show that Clu particles can reform when translation is stalled, suggesting that particle formation is independent of active translation.

Characterization of effects mitochondrial proteins after cycloheximide feeding

If Clu particles are localizing mRNAs of mitochondrial proteins and mitochondrial proteins for mitochondrial translation and import, we expect that the absence of particles will lead to changes in mitochondrial protein levels and mitochondrial function. The ultimate goal of this experiment is to measure the recovery rate of selected mitochondrial proteins after cycloheximide feeding and subsequent re-feeding or starvation. As a first step towards this goal, we measured the protein levels of Clu, ATP synthase, and α-tubulin in ovaries from wild-type flies which were fed wet yeast paste spiked with increasing concentrations of cycloheximide for 1-2 days to visualize the baseline effects of cycloheximide feeding on protein levels. Western blot analysis of the ovaries does not show a noticeable change in Clu levels at the 3.5 mM and 7.0 mM concentrations at 24 hours, but there is a small decrease in the Clu level at the 10.0 mM concentration at 24 hours (Figure 3c). There also appears to be further decreases in the Clu protein levels at all concentrations at the 48-hour timepoint compared to the 24-hour timepoint. There does not appear to be a noticeable difference of ATP synthase levels either within (0, 3.5, 7, 10 mM cycloheximide) or between (24-hour

vs 48-hour) any of the groups in the ovaries (Figure 3c). However, there is a marked decrease in the α-tubulin levels at all concentrations at both the 24- and 48-hour timepoints (Figure 3c). As a control, we analyzed the carcasses from which the ovaries were dissected. As expected, the protein levels of Clu and α-tubulin were mostly consistent within (0, 3.5, 7, 10 mM cycloheximide) and between each group (24-hour vs 48-hour) (Figure 3d). These results are preliminary and therefore are not yet conclusive. Moving forward, these experiments must be replicated in order to accurately quantify the protein levels at each cycloheximide concentration.

Live-imaging in combination with cycloheximide and insulin addition to determine whether particles are translation independent

Next, we moved on to live imaging studies to determine whether Clu particles are involved in global translation. We have previously shown that adding insulin to the imaging media of follicles induces particle formation in starved flies (84). Follicles from starved Clu-GFP flies in which insulin is added to the media at time 0 are able to reform Clu particles within 5 minutes of insulin addition, signifying that insulin is sufficient to induce particle formation. To visualize the effects of stalling translation on Clu particles using live-imaging, follicles from Clu-GFP flies were dissected in insulin-containing media and treated with cycloheximide during imaging. Cycloheximide addition does not cause Clu particles to disperse over the course of 20 minutes (Video 1b) compared to the baseline (Video 1a). This result is consistent with the results seen with fixed imaging in which cycloheximide feeding does not cause particles to disperse (Figure 3a).

Hydrogen peroxide treatment does not abolish cycloheximide-treated particles

Due to our observations that treatment with cycloheximide does not cause particles to disperse, we next sought to determine if subsequent treatment with hydrogen peroxide (H_2O_2) could disperse the particles after cycloheximide treatment. We have previously shown that adding hydrogen peroxide to imaging media of follicles induces oxidative stress in flies and causes particles to disperse (83; 84). H_2O_2 is added during imaging to follicles from Clu-GFP flies which were dissected in insulin-containing media, and Clu particles disperse within 20 minutes of imaging, signifying that induction of oxidative stress is detrimental to particles. To visualize the effects of adding H_2O_2 to cycloheximide-treated follicles, follicles from Clu-GFP flies were dissected in insulin-containing media, then treated with cycloheximide during imaging, and further treated with H_2O_2 following the cycloheximide treatment. H_2O_2 addition still does not cause Clu particles to disperse over the course of 20 minutes (Video 1c) compared to the baseline (Video 1a).

DISCUSSION AND LIMITATIONS OF THE STUDY

Drosophila Clu and vertebrate CLUH are ribonucleoproteins. CLUH was also shown to bind both mitochondrial proteins and their corresponding mRNAs in close proximity to mitochondria. Loss of Clu and CLUH disrupts mitochondrial function by reducing ATP levels, causing improper mitochondria localization and mitochondrial ultrastructural changes, and by altering metabolism (21; 30; 75; 79; 98). *Drosophila* Clu associates with many different ribosomal proteins, the mitochondrial outer membrane proteins TOM20 and Porin, and translation initiation and elongation factors, suggesting it may have a role in mitochondria-localized or co-translational import of nucleus-encoded

proteins (79). Here, we have begun to test the hypothesis of whether Clu particles are the sites of translation for nuclear-encoded mitochondrial proteins using biochemical and live-imaging approaches. Traditional pulse-chase analyses which are used to visualize protein degradation and protein synthesis kinetics require the use of radioisotopes, fluorescent dyes, or fluorescent reporter genes. Because of this, we sought to use potentially simpler and more time-efficient approaches, the cycloheximide chase followed by Western blotting as well as acute cycloheximide treatment in culture media. We have shown that cycloheximide feeding is an effective method of drug delivery to the flies (Figure 1). However, upon 1-2 days of cycloheximide feeding, we did observe noticeable defects at every *Drosophila* developmental stage. We have not yet determined if or how these developmental defects may impact our results in these studies.

We did not observe any differences in the survival rates of females with 3.5 mM cycloheximide feeding, and the survival rate of males began to decrease after one week of feeding (Figure 2d). These results are consistent with previously published data in which it was shown that sensitivity differences between the sexes is less apparent at low concentrations of cycloheximide (1 mM and 3 mM), and that male survival is more sensitive at higher concentrations (10 mM and 15 mM) (57). Of note, this study also found that the survival of both sexes significantly decreases at every cycloheximide concentration within 4 days. This is in contrast to our findings which did not show significant decreases in survival at the 3.5 mM concentration over a three-week time span. This discrepancy may be attributed to differences in the drug delivery method; Marcos et al. performed cycloheximide feeding using a 5% sucrose solution (a poor food

source) as compared to our feeding which used wet yeast paste (a rich food source) (57). Moving forward, we will include both the 7.0 mM and 10.0 mM cycloheximide concentrations into our survival assays to assess whether the same general trend is present within the females as well as whether male survival further decreases.

We observed that the ovary sizes in females progressively decreased with increasing cycloheximide concentrations (Figure 1b, Figure 2a). It is important to note that this finding presented a challenge when performing the Western blot analyses. We did not know whether the decrease in protein levels (Figure 1d) was due to the smaller ovary size or due to the decrease in protein production over the 24-hour feeding period. Therefore, it was necessary to normalize the amount of each sample by weight. As the α-tubulin levels in the samples were inconsistent (Figure 3c) and there were also smaller than expected decreases in the protein levels compared to earlier, non-normalized blots (Figure 1d), this normalization by weight may be unexpectedly over-correcting the results. Moving forward, in order to determine the source of the smaller sizes, we will label the ovaries with anti-Vasa antibodies and DAPI to determine whether this finding is due to shrinking of the follicle sizes or whether the ovariole may be missing specific stages. As previously mentioned, if Clu particles do function in translation of mitochondrial proteins, we expect that the recovery rate of mitochondrial proteins in starved flies after a cycloheximide chase will be slower when compared to fed flies. As such, another important future step will be to select mitochondrial proteins for analyses which are both short- and long-lived (95; 96). An unstable protein or one with a short half-life will decrease in abundance after cycloheximide treatment, and a stable protein or

one with a long half-life will remain consistent in abundance (12). Utilizing mitochondrial proteins with different turnover rates will further allow us to tease apart the necessity of Clu particles in the recovery rates of these proteins after a cycloheximide chase.

Consistent with our finding that cycloheximide feeding does not disrupt Clu particle stability (Figure 3a – 3a″), this result was also observed with acute treatment of follicles with cycloheximide (Video 1b) during live imaging. As we found that Clu particles could also reform in starved flies in the presence of cycloheximide (Figure 3b – 3b″), the next steps are to determine whether particle formation can be induced when follicles (from starved and fed flies) are first dissected in cycloheximide-containing media (little to no particles present) with the insulin added during imaging. These future experiments will provide more conclusive results about Clu particle dynamics in response to stalled translation as well as the question of whether Clu particles have an effect on translation globally. An exceptionally surprising result was that treatment with H_2O_2 following treatment with cycloheximide in culture still does not disrupt Clu particle stability (Video 1c). We do not yet know the mechanism by which cycloheximide treatment is stabilizing Clu particles. Therefore, this result warrants further investigation to elucidate the mechanism by which cycloheximide treatment is potentially stabilizing Clu particles.

Finally, thus far, we have used biochemical and imaging approaches to address the question of whether Clu particles are involved in translation of mitochondrial proteins. An important complementary genetic approach that we will also employ in the

future is ribosome profiling to determine if there are differences in actively translating mRNAs (42). Cell-type specific ribosome profiling, RiboTag, is possible in *Drosophila* germ cells and can be used to characterize differences in gene expression between wild-type fed and starved flies (particles vs no particles) and *clu* mutant flies (43).

MAIN FIGURES

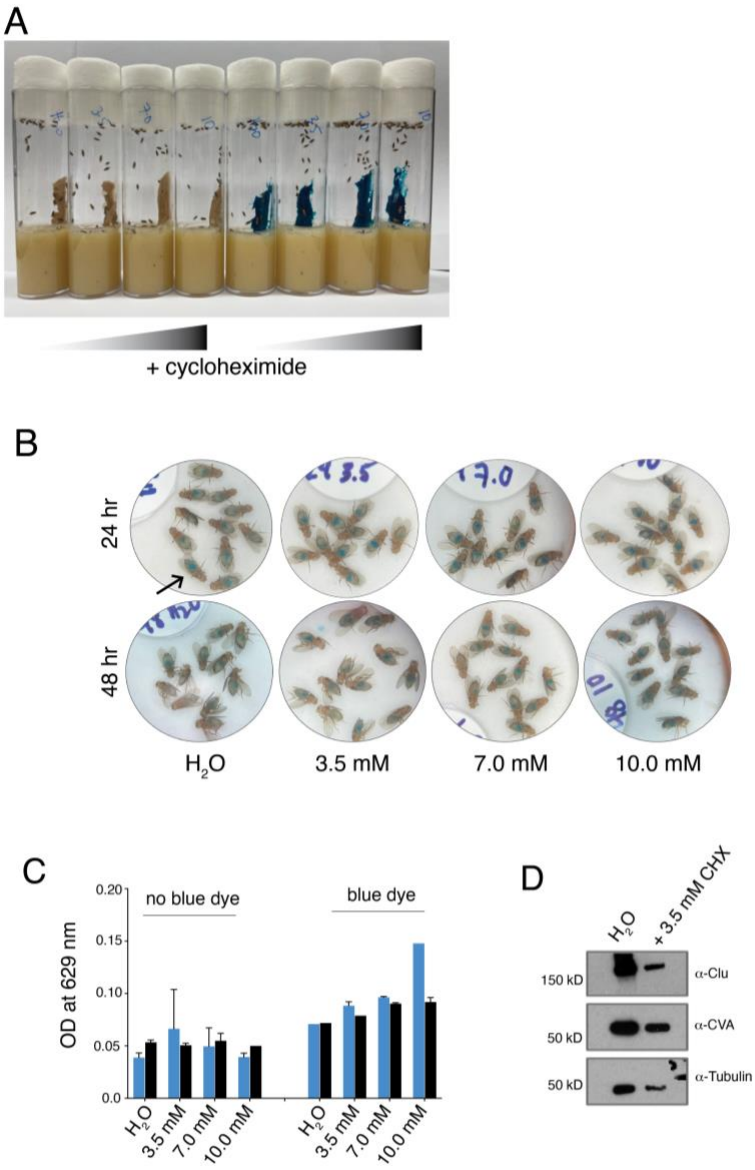

Figure 1. Cycloheximide feeding is feasible and effective.
(A) Vials of wild-type flies feeding on wet yeast paste spiked with either 0 mM, 3.5 mM, 7.0 mM, or 10 mM of cycloheximide were either not dyed (left 4 tubes) or dyed blue (right 4 tubes). (B) Blue food is visible in the guts (arrow) of female flies lying on their backs. (C) Quantification of the amount of cycloheximide-spiked blue food ingested in the control (no blue dye) vs dyed food (blue dye) groups. (D) Western blot analysis of proteins levels after feeding flies wet yeast paste spike with 3.5 mM cycloheximide for 1 day. (Sheard, unpublished)

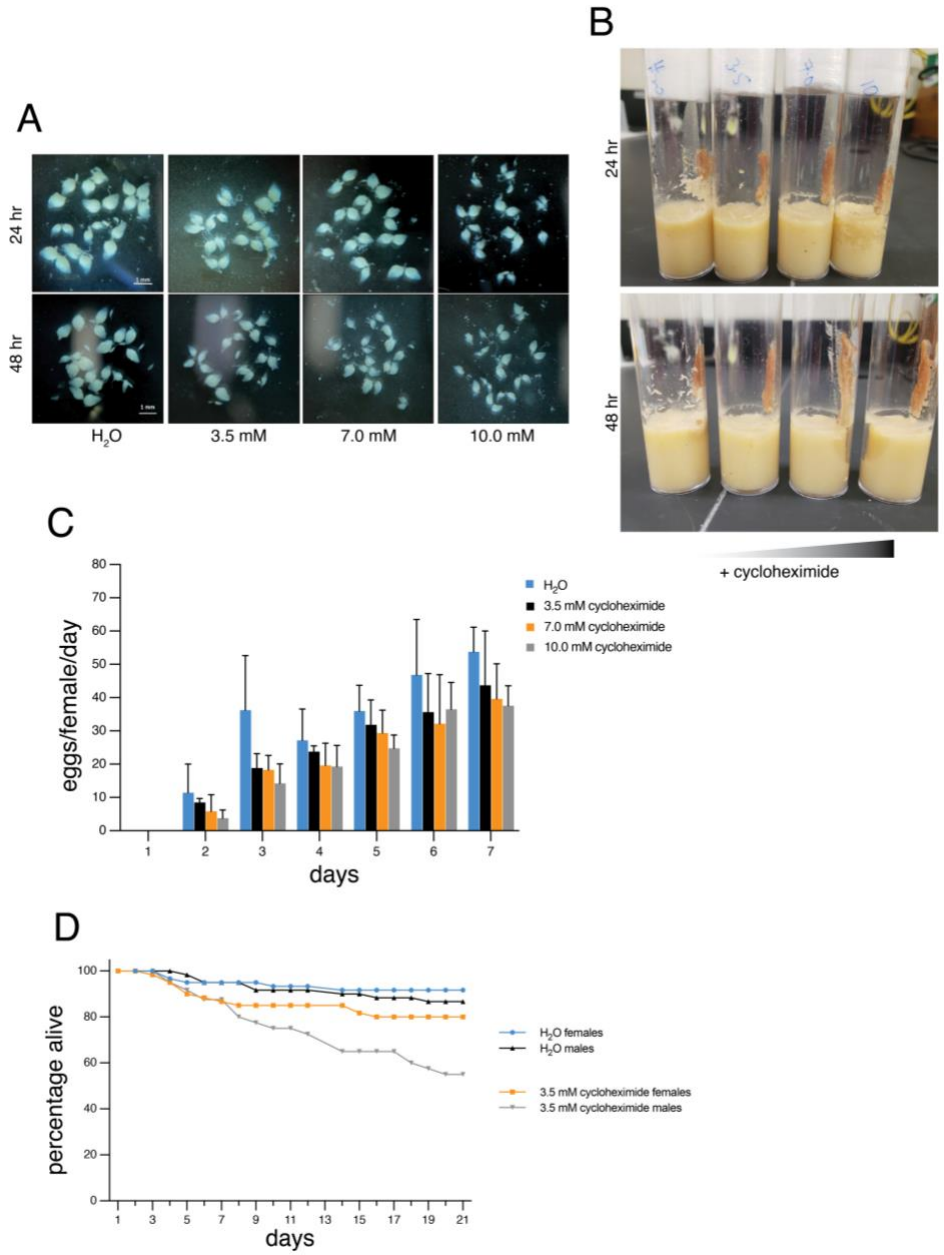

Figure 2. Cycloheximide feeding has developmental effects on *Drosophila* development and oogenesis.

(A) Ovaries dissected from wild-type flies fed wet yeast paste with increasing concentrations of cycloheximide for 1-2 days show a dose-dependent decrease in size. (B) Vials of larvae produced from flies fed wet yeast paste with either 0 mM, 3.5 mM, 7.0 mM, or 10 mM of cycloheximide for 1-2 days. The number of larvae visible decreases with increasing concentration. (C) Female wild-type flies fed wet yeast paste with increasing concentrations of cycloheximide show

a dose-dependent decrease in egg-laying. (D) Female survival is not sensitive and male survival is sensitive to 3.5 mM cycloheximide feeding over three weeks. (Sheard, unpublished)

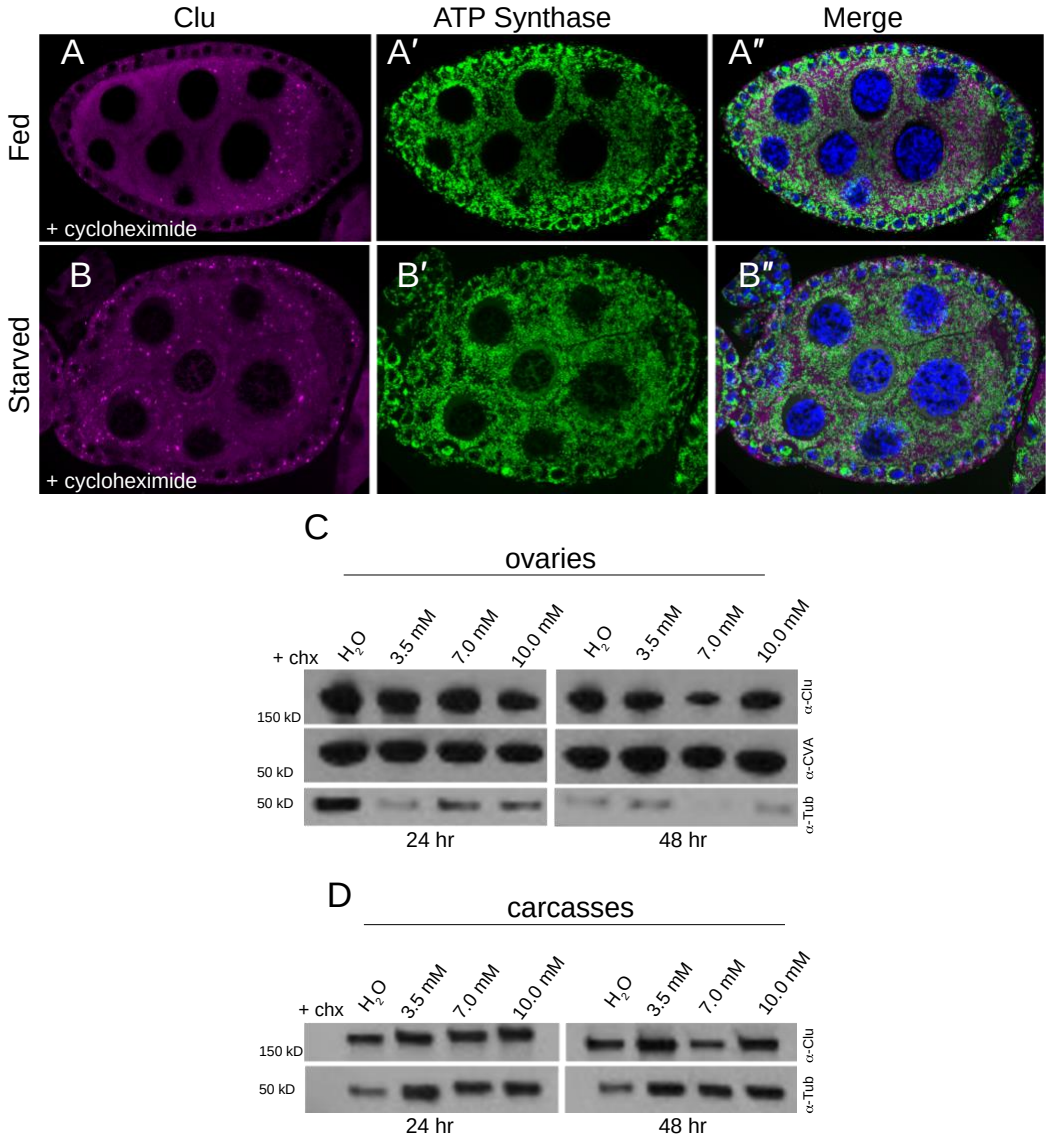

Figure 3. Cycloheximide feeding does not disrupt particle formation or stability. Follicle from w^{1118} female. (A) Feeding well-fed flies wet yeast paste spiked with 3.5 mM cycloheximide for 1 day does not disrupt Clu particles or mitochondria localization. (B) Flies which have been starved on water only for 5 hours are able to reform particles upon refeeding with wet yeast paste spiked with 3.5 mM cycloheximide for 1 day. (C and D) Western blot analysis of ovary (C) and carcass (D) extracts. Magenta = Clu (A, A″, B and B″), green = ATP synthase (A´ and B´), blue = DAPI (A″ and B″). (Sheard, unpublished)

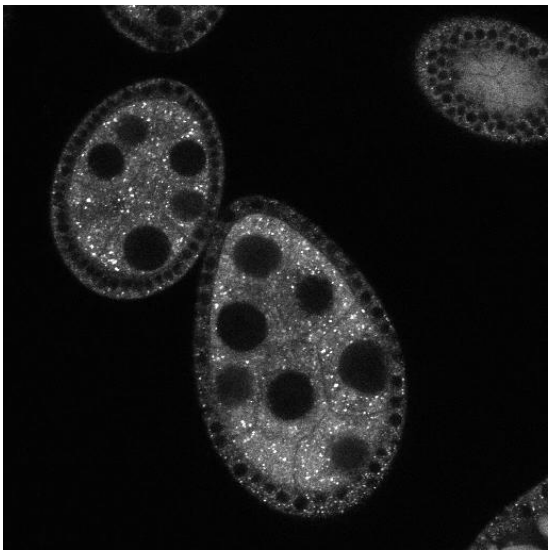

Video 1a. Follicles dissected from GFP-Clu flies dissected in insulin-containing media have robust and dynamic Clu particles.
Follicle from *clu*^{CA06604} (Clu-GFP) female. White = Clu::GFP. Imaged one frame per 5 seconds for 2 minutes. Video is 25 frames per second. (Sheard, unpublished)

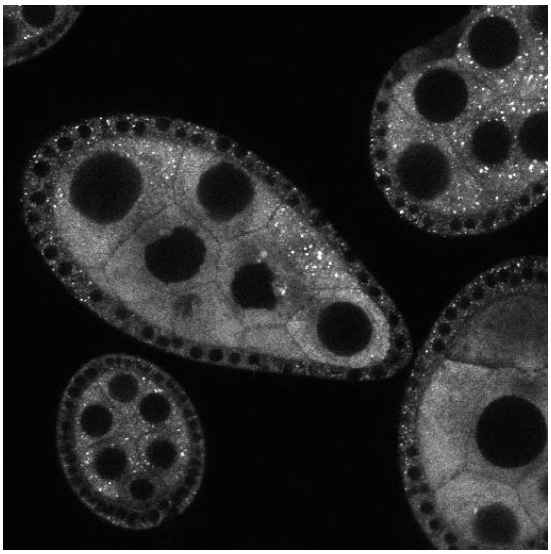

Video 1b. Treatment with cycloheximide does not cause Clu particles to disperse. Follicle from *clu*^{CA06604} (Clu-GFP) female. White = Clu::GFP. Imaged one frame per 5 seconds for 20 minutes. Video is 25 frames per second. (Sheard, unpublished)

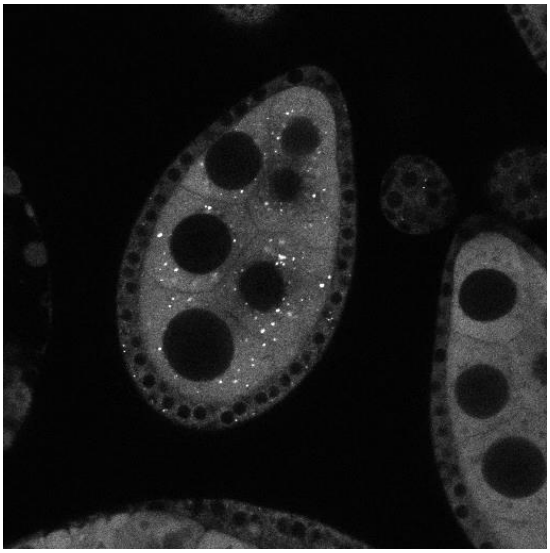

Video 1c. Treatment with H_2O_2 does not abolish cycloheximide stabilized particles. Follicle from *clu*^{CA06604} (Clu-GFP) female. White = Clu::GFP. Imaged one frame per 5 seconds for 20 minutes. Video is 25 frames per second. (Sheard, unpublished)

CHAPTER 5: DISCUSSION

Mitochondria contain their own DNA whose products are required for oxidative phosphorylation, and they also rely heavily on the import of approximately 1700 nuclear-encoded mitochondrial protein products necessary for mitochondrial function (36; 80). Mutations in mtDNA and nuclear-encoded products as well as dysregulation of nuclear-encoded products has been implicated in severe and multi-systemic mitochondrial diseases (10; 18; 37; 80). Mitochondrial diseases are difficult to diagnose and treat. Current treatments are primarily based in supportive therapy, not targeted, pharmacological therapy which treats specific pathological mechanisms (54; 88). This is partially attributable to the mechanisms which regulate nucleus-encoded mitochondrial proteins not being well-characterized. As such, there is a need for better understanding these molecular and cellular mechanisms to further assist in the treatment and therapy of mitochondrial diseases. One particular unknown is how these proteins are transported to, localized at, and translated prior to import into mitochondria.

Numerous studies have begun to shed light on a model for localized translation and co-translational import of mitochondrial proteins in mammals. This system is already well-established in yeast, where it has been shown that a significant portion of the mRNAs of nuclear-encoded mitochondrial proteins are localized to the mitochondria by attachment of cytosolic polysomes to the mitochondrial outer membrane (56; 74; 91). Furthermore, these cytosolic polysomes associate with the outer membrane through the nascent chain-associated complex (NAC), which tethers a ribosome-bound nascent polypeptide chain to the outer membrane (2; 35; 50). The NAC works in conjunction

with Puf3p, an mRNA-binding protein which is localized to the outer membrane and is responsible for localizing a subset of mRNAs which encode for mitochondrial proteins to the outer membrane (2; 33; 35; 74). This system is not as well-established in mammals. The RNA-binding proteins which regulate and assist with co-translational import in mammals are not yet fully defined. We have identified Clu, an RNA-binding protein which binds to mRNAs through its tetratricopeptide repeat (TPR) domain, ribosomal proteins, translation factors, and the mitochondrial transporters TOM20 and Porin, as a potentially important factor in this process (79; 82). Clu1p and CLUH, the yeast and human homologues of Clu, also bind to mRNAs, with CLUH in particular binding to a subset of nuclear-encoded mitochondrial proteins and their corresponding mRNAs through its TPR domain (30; 39; 79). In addition, these physical associations with CLUH are in close proximity to the mitochondrial outer membrane (39). The levels of mitochondrial proteins are also reduced in the absence of *clu* and *Cluh* (30; 82). For these reasons, Clu family members are strong candidates for function as an RNA-binding protein in the localization and translation of nuclear-encoded mitochondrial proteins. Here, we begin to address the identity of Clu as a ribonucleoprotein particle as well as how it functions in regulation and import of nuclear-encoded mitochondrial proteins.

Our previously published data characterized Clu as a ribonucleoprotein and demonstrated its effects on mitochondria. We had also observed that Clu formed cytoplasmic, mitochondria-associated particles, and that these particles were absent in *Drosophila* mutants with impaired mitochondrial function (21; 82). These findings, in combination with Clu's association with mRNA, led us to hypothesize that Clu particles

are a previously undescribed ribonucleoprotein particle which affects mitochondrial function. Prior to this work, we did not yet know the factors which affected Clu particle dynamics, or how these dynamics might be controlled.

The specific aims of this work were to characterize Clu particles as a new ribonucleoprotein granule which affects mitochondrial function by (1) determining Clu particle dynamics and behavior in stressed and unstressed conditions in order to determine what conditions control Clu particle formation, (2) identifying signaling pathways that control Clu particle formation, (3) standardizing using the presence of Clu particles and normal mitochondrial localization in germ cells as a control for healthy cells during live-imaging, and (4) determining how decreased translation affects Clu particle dynamics. This dynamic nature is observed in other ribonucleoprotein granules, and it follows that understanding the dynamics of Clu particles will provide insight into their function as a RNP granule and further contribute to knowledge of how Clu particles affect mitochondrial function.

CLU PARTICLE DYNAMICS

Ribonucleoprotein particles are cytoplasmic sites of spatial and temporal post-transcriptional mRNA regulation and spatial and temporal translational control, specifically involved in cell stress responses. The two most well-characterized types are stress granules and P-bodies. For example, P-bodies consist of mRNAs associated with translation repressors or mRNAs targeted for degradation and components of the mRNA decay machinery, the exonuclease Xrn-1, the protein Trailer hitch which aids in mRNA decay and turnover, and the decapping protein Dcp-1 which removes the 3’ cap of

mRNA during degradation (53). Our results demonstrate that Clu bliss particles are highly dynamic, novel cytoplasmic bodies whose dynamics are highly responsive to cell stressors. Live-imaging to visualize particle dynamics in real-time shows that Clu particles vary in size and are mobile in the cytoplasm. In addition, a subset of particles shows processive, microtubule-dependent movement. The average velocity of particles is 1.5μm/sec as measured by kymographic analysis, a finding which is consistent with the reported average velocity of mitochondria in neurons (3; 41; 52). The processive movement of Clu particles is also dependent upon an intact microtubule cytoskeleton as treatment with the microtubule destabilizer colcemide inhibited the movement of both Clu particles and mitochondria. Collectively, these results are significant as they are in agreement with what has already been shown of RNP granule dynamics. RNP granules respond to stress with changes in size, morphology, subcellular localization, and composition, and they rely on microtubules for formation and disassembly, cytoplasm transport, and spatial docking (77).

Based on the findings that Clu particles are dynamic and dependent on microtubule movement akin to other RNP granules, we next sought to determine whether Clu particles were a unique cytoplasmic body or were derived from or a part of another common organelle. Clu particles are always closely associated with mitochondria. However, Clu did not colocalize with markers for two other stress-responsive bodies - Atg8a, a marker for autolysosomes nor Trailer hitch, a marker for Processing bodies. It had also been previously reported that Clu associates with ER-exit sites in *Drosophila* larval muscle (103). In contrast, our results showed that Clu also did not colocalize with

components of the ER nor with cis- and trans-Golgi. These results signify that Clu particles are unique. Clu particles also behave distinctly from other stress-responsive bodies. Comparing the stress response of Clu particles to that of P-bodies shows that Clu particles disperse throughout the cytoplasm while P-bodies become larger and more numerous under cell stress. This is a distinctive dynamic of RNP granules which has not been previously observed. This result, in conjunction with not-colocalizing with other cytoplasmic bodies, are significant as they provide strong evidence that Clu particles are a novel, previously undescribed cytoplasmic particle.

Responses to a variety of cell stressors including heat shock, starvation, and hypoxia are a hallmark of RNP granules. Of note, the dynamic changes which occur in these granules under stress are reversible when the stress is removed (77). We have previously shown that Clu particles are absent in *clu* and *PINK1* and *Parkin* mutants, the mediators of mitophagy (21; 82). Mitochondrial stress from loss of *PINK1* and *parkin* causes particles to disperse without a corresponding decrease in Clu protein, signifying that the protein is not being degraded, only dispersed. Therefore, we evaluated the response of Clu particles to other cell stressors. The results indicate that Clu particles are also stress-responsive like other ribonucleoprotein granules. Particles in wild-type flies are sensitive to nutritional stress as they disperse after five hours of a water-only diet. Importantly, particles reappear within 3 hours of re-feeding. This result is in agreement with data from Burn et al. which shows that the formation of P-bodies as well as localization of proteins to P-bodies in response to starvation is rapidly reversible upon refeeding (13; 85). Though the reversible response of Clu particles to stress is consistent

with previous data for other RNP granules, it is not consistent with the response to nutritional stress reported for CLUH granules. Pla-Martin et al. reported that CLUH granules in livers from food-deprived mice and hepatocytes cultured in a low-glucose medium with no serum or amino acids formed bigger aggregates as compared to fed mice and hepatocytes cultured in glucose-rich media (69). Clu particles are also no longer visible in *Drosophila Superoxide Dismutase 2 (SOD2*) mutant flies which cannot clear reactive oxygen species from the cell and thus experience high levels of oxidative stress. Consistent with the *SOD2* mutant results, we also observed this effect using live-imaging to visualize the acute effects of inducing oxidative stress with the addition of hydrogen peroxide. Unlike the nutritional stress, oxidative stress is harsh and irreversibly damages the cells; therefore, the Clu particles cannot be recovered in this case. However, these results collectively show that Clu particles are also responsive to multiple different types of stress in general akin to other RNP granules.

Because of the nutrition response, we wanted to identify a potential signaling pathway responsible for the response. Probing the insulin signaling pathway using clonal analysis shows that overexpressing insulin signaling has no effect on Clu particle formation, but Clu particles are unable to form in mutant clones which do not have insulin signaling. This data corresponds to our observation that adding exogenous insulin to the imaging media during live-imaging studies can initiate particle reformation in follicles from starved flies. This data is significant as it provided us insight into at least one mechanism by which particle dynamics are controlled in response to nutritional stress. Furthermore, with regard to Clu's identity as an RNP granule, this data is also in

agreement with previously shown data in which endogenous insulin signaling mediates the reversible response of P-bodies to starvation and that adding exogenous insulin to culture media inhibits the formation of P-bodies (13).

Finally, for the first time, we categorically demonstrate how cell stress affects mitochondrial localization in germ cells and somatic follicle cells. We observed that mitochondria clumped and mislocalized in response to the same cell stressors as Clu particles. This result had previously been described in *clu*, *PINK1*, and *Parkin* mutant cells, which also notably do not contain Clu particles (21; 82). These results signify that mitochondrial mislocalization is downstream of general cell stress. Therefore, this is an important consideration in mitochondrial studies, and it is necessary to ensure that low-stress conditions and normal mitochondrial distribution are maintained.

In conclusion, we have shown in a step-wise fashion that Clu particles are dynamic, do not colocalize with other known cytoplasmic components, have a distinct response to multiple different cell stressors, and that insulin signaling is necessary and sufficient for their formation. In line with our hypothesis, these data suggest strong evidence that Clu particles are a novel ribonucleoprotein granule as well what signals control their dynamics. In addition, these results shed light on how Clu particle dynamics contribute to stress responses.

Limitations of the study

The main limitations into the study of Clu particle dynamics were the challenges we encountered with co-labeling Clu particles and mitochondria for live-imaging studies. Though we observed that Clu appears to be moving at a speed comparable to

mitochondria and that this movement is also microtubule-dependent, we do not yet know if Clu particles are moving in tandem with mitochondria. The addition of TMRE to the imaging media of cultured Clu-GFP ovarioles appeared to cause particles to disperse. Thus, we were not able to conclusively demonstrate if Clu particles move in tandem with mitochondria nor whether Clu particles are actively localized to locations with high mitochondrial density.

Another limitation of this study is the inability to perform structure-function studies of the different domains of Clu to determine which domains of Clu are important for particle dynamics. As all of the domains were shown to be necessary for proper protein functioning and only expressing full-length *Drosophila clu*, melanogaster specific (ms) domain deletion, or CLUH was sufficient to rescue *clu* null mutants, we cannot yet determine how Clu's domains impact its function (79). For example, we do not yet know which domain(s) nucleate a particle nor which domains are necessary for phase separation as both Clu particles and other RNP granules dynamically reshape themselves (93).

Future directions

There remain two very important questions to address with respect to particle dynamics. The first and most significant is the question of whether mRNAs in general or mRNAs of specific mitochondrial proteins are transported and localized to Clu particles. It has been shown that mRNAs of mitochondrial proteins are localized in close proximity to the mitochondrial membrane, and that all Clu family members bind mRNAs. It is also well-established that mRNAs are contained within other RNP granules. However, it is

currently unknown if mRNAs are enriched in Clu particles or bound to Clu monomers. Moving forward, we will address these questions by visualizing the real-time transport and localization of mRNAs using the MS2-MCP system. To determine if mRNAs are enriched in Clu particles using fixed-imaging, we will use fluorescence in situ hybridization in combination with antibody labeling for Clu. These experiments will elucidate if mRNAs are targeted to and sequestered in Clu particles.

The second question to address is the nature of the difference between the populations of Clu particles which are associated with mitochondria compared to those which are not and vice-versa. We have shown that even though particles are always closely associated with mitochondria, not all mitochondria are associated with particles. In the future, we will explore this question via live-imaging using transgenic flies which express both labeled Clu and mitochondria. We will Fluorescence Recovery After Photobleaching (FRAP) to determine if there are differences if the exchange rate of Clu particles which are associated with mitochondria compared to those which are not. We will also use these flies to assess how Clu particles move and localize in relation to mitochondria using live imaging.

CLU PARTICLE FUNCTION IN RELATION TO MITOCHONDRIA

Ribonucleoprotein particles also function in spatial and temporal translational control during cell stress responses. The previous aims have shown that Clu particles are a unique, mitochondria-associated particle, and that they are highly stress-sensitive. The last aim seeks to demonstrate the functional identity of Clu as an RNP granule. Based on the evidence that Clu physically interacts with mRNAs, ribosomal proteins, translation

factors, and mitochondrial transporters, Clu particles may affect mitochondrial function by translational regulation of mitochondrial proteins. As this is ongoing work which is not yet complete, the results we have gathered thus far cannot yet answer this part of our hypothesis - that Clu particles function in either in localized translation or co-translational import of nuclear-encoded mitochondrial proteins. However, our current results on the developmental effects of stalling translation in *Drosophila* as well as unexpected live-imaging results do provide a foundation for many questions related to the mechanisms by which stalling translation impacts particle formation and stability.

We used a cycloheximide-based approach to begin elucidating the effects of Clu particles on global translation as well as the translation of nuclear-encoded mitochondrial proteins. Our results showed that cycloheximide feeding is an effective method of drug delivery to the flies. However, it was immediately obvious in our initial studies performed with cycloheximide feeding in yeast paste that there were similar developmental defects as previously described. Though cycloheximide is a widely used drug in translation studies, to our knowledge, there has only been one study which systematically examined the effects of cycloheximide on the developmental stages of *Drosophila*. This study showed that cycloheximide feeding in 5% sucrose exhibited a toxic effect on all developmental stages with the embryos and larvae being most sensitive to treatment (57). Our initials results showed that ovaries from female flies fed wet yeast paste spiked with cycloheximide were consistently smaller compared to females fed normal wet yeast paste. Though the ovaries were smaller, we do yet know if the small size is due to reductions in follicle size or individual stages missing within the ovarioles.

We also showed that overall survival of female flies was more resistant to cycloheximide feeding than males. Even so, we did not observe a drastic decrease in survival in either males or females with 3.5 mM cycloheximide feeding. We did not expect that prolonged, stalled translation at any level would allow the flies to survive for long periods of time. This is also in contrast to Marcos et al.'s findings (57). This tolerance to low doses of cycloheximide feeding may be attributable to low bioavailability of the drug after ingestion. We have not yet determined if or how these developmental defects may impact our results in these studies. However, they are likely to have important implications for any future results as we will have to determine whether any observed results are truly due to changes in translation or an indirect effect of these developmental effects. Our results are also significant as they build upon the data already presented by Marcos et al. using a different feeding source.

If Clu particles do function in translation of mitochondrial proteins, we expect that the recovery rate of mitochondrial proteins in starved flies after a cycloheximide chase will be slower when compared to fed flies. To begin testing this hypothesis, we fed flies yeast paste spike with cycloheximide in order to examine the changes in protein levels via Western blot. Upon ovary dissection, we observed that the ovary sizes in females progressively decreased with increasing cycloheximide concentrations. We did not know whether the decrease in protein levels was due to the smaller ovary size or due to the decrease in protein production. Therefore, it was imperative that we spent time properly optimizing our samples based on weight as well as the antibody concentrations used. Though these results are not yet conclusive, we have strong existing evidence to

expect that our results will show that Clu particles will affect translation of mitochondrial proteins based on data from CLUH. Schatton et al. first established that CLUH exerts its function by regulating the stability and translation of mRNAs on mitochondrial proteins (75). Recently, Pla-Martin el al. built upon this data and showed that CLUH granules in particular regulate the translational fate of mRNAs of mitochondrial proteins in response to nutrient availability in primary hepatocytes using a ribopuromycylation assay (69). In addition, this regulation was found to be through mTORC1 signaling. This is a significant finding as we have showed that insulin signaling is both necessary and sufficient for Clu particle formation.

We also observed that cycloheximide feeding does not disrupt Clu particle formation or stability. Both fixed-imaging and live-imaging analysis showed that treatment with cycloheximide is not stressful for particles and does not cause them to disperse. This was a surprising result to us as this is the first time we have observed this dynamic. Furthermore, cycloheximide treatment stalls translation, but it does not disrupt the mRNA-ribosome-nascent polypeptide chain complex. Though we have previously shown that Clu bonds to mRNA, ribosomal proteins, and translation factors, the stabilization of Clu particles with cycloheximide treatment is the first evidence we have that Clu may be in a translationally active complex with its binding partners. We also found yet another unexpected result in that Clu particles could reform in starved flies in the presence of cycloheximide. Though we have not confirmed this result using live-imaging, this finding revealed another Clu particle dynamic which will require further investigation. One possible explanation for this finding is that though already formed Clu

particles are stabilized by cycloheximide treatment, nascent Clu particle formation is potentially upstream or independent of its association with translation complexes, and therefore is unaffected by cycloheximide treatment.

An exceptionally surprising finding was that treatment with H_2O_2 following treatment with cycloheximide in culture still does not disrupt Clu particle stability. We have previously shown that Clu particles are irreversibly sensitive to oxidative stress by employing a *SOD2* mutant with systemic oxidative stress and by adding H_2O_2 to the imaging media of particles to acutely induce oxidative stress. We do not yet know the mechanism by which Clu particles continue to be stabilized or if this relates to the stability of the translational machinery after cycloheximide treatment. Therefore, this result warrants further investigation to elucidate the mechanism by which cycloheximide treatment is potentially stabilizing Clu particles.

In conclusion, we have begun to investigate the functional effects of Clu particles on the translation of mitochondrial proteins as well as how decreasing active translation impacts Clu particle dynamics. Thus far, our current work demonstrates that Clu particle stability and formation is not impacted by stalling translation, suggesting that particle formation and stability may be independent of active translation. An alternative explanation for this finding can be found in recent work by Hémono et al. It was shown that CLUH only transiently interacts with mitochondrial proteins in close proximity to mitochondria using a time-course proximity labeling experiment in HCT116 cells (39). It was also shown the CLUH has a sustained interaction with mRNAs coding for the aforementioned proteins but did not have an effect on their translation efficiency. These

data suggest two possibilities: that binding of CLUH to mRNAs of mitochondrial proteins primarily functions to localize them in close proximity to the outer mitochondrial membrane, and that these mRNAs may be quickly translated and imported into mitochondria, thus they only transiently interact with CLUH (39). These speculations are consistent with a co-translational import model. Consequently, these data may show that Clu particle's main function in co-translational import is mRNA localization and stability (similar to Puf3p), and therefore their stability is not impacted by stalling translation.

Limitations of the study and future directions

The main limitation of this study thus far are the challenges which we have encountered with the developmental defects observed during the cycloheximide chase experiments. Future experiments will be performed to determine the source of the significant decreases seen in ovary size with cycloheximide feeding. This will provide us with more insight into how our results are being impacted as well as how to potentially overcome this challenge. We also need to validate that translation is stalled in the ovary by performing ribosome profiling.

Data from CLUH studies has consistently shown that CLUH is functionally responsible for the translation of nuclear-encoded mitochondrial proteins. Therefore, we expect that the continuation of the cycloheximide chase experiments after starvation of the flies will show similar results, and that these effects on translation will be dependent upon the presence and absence of particles.

Due to the results which we observed when treating cycloheximide-treated follicles with hydrogen peroxide during live imaging, we will further investigate the necessity for different components of the translational complex to further tease apart this unexplained dynamic. These future experiments include treating cycloheximide-treated follicles with both RNase and EDTA to visualize whether they are able to disrupt particle formation. RNase treatment will determine if Clu particles require mRNA binding to remain stable, and EDTA treatment will determine if Clu particles require an intact ribosomal assembly to remain stable.

REFERENCES

1. Ahmed AU, Beech PL, Lay ST, Gilson PR, Fisher PR. 2006. Import-associated translational inhibition: novel in vivo evidence for cotranslational protein import into Dictyostelium discoideum mitochondria. *Eukaryot Cell* 5:1314-27
2. Ahmed AU, Fisher PR. 2009. Chapter 2 Import Of Nuclear-Encoded Mitochondrial Proteins.49-68. Number of 49-68 pp.
3. Allen RD, Metuzals J, Tasaki I, Brady ST, Gilbert SP. 1982. Fast axonal transport in squid giant axon. *Science* 218:1127-9
4. Anderson P, Kedersha N. 2006. RNA granules. *J Cell Biol* 172:803-8
5. Anderson P, Kedersha N. 2009. RNA granules: post-transcriptional and epigenetic modulators of gene expression. *Nat Rev Mol Cell Biol* 10:430-6
6. Barbee SA, Estes PS, Cziko AM, Hillebrand J, Luedeman RA, et al. 2006. Staufen- and FMRP-containing neuronal RNPs are structurally and functionally related to somatic P bodies. *Neuron* 52:997-1009
7. Barth JM, Szabad J, Hafen E, Kohler K. 2011. Autophagy in Drosophila ovaries is induced by starvation and is required for oogenesis. *Cell Death Differ* 18:915-24
8. Baudin A, Ozier-Kalogeropoulos O, Denouel A, Lacroute F, Cullin C. 1993. A simple and efficient method for direct gene deletion in Saccharomyces cerevisiae. *Nucleic Acids Res* 21:3329-30
9. Brady J. 1965. A simple technique for making very fine, durable dissecting needles by sharpening tungsten wire electrolytically. *Bull World Health Organ* 32:143-4
10. Braun RJ, Westermann B. 2017. With the Help of MOM: Mitochondrial Contributions to Cellular Quality Control. *Trends Cell Biol* 27:441-52
11. Buchan RJaP, Roy. 2009. Eukaryotic Stress Granules: The Ins and Out of Translation. *Molecular Cell* 36
12. Buchanan BW, Lloyd ME, Engle SM, Rubenstein EM. 2016. Cycloheximide Chase Analysis of Protein Degradation in Saccharomyces cerevisiae. *J Vis Exp*
13. Burn KM, Shimada Y, Ayers K, Vemuganti S, Lu F, et al. 2015. Somatic insulin signaling regulates a germline starvation response in Drosophila egg chambers. *Dev Biol* 398:206-17
14. Buszczak M, Paterno S, Lighthouse D, Bachman J, Planck J, et al. 2007. The carnegie protein trap library: a versatile tool for Drosophila developmental studies. *Genetics* 175:1505-31
15. Celotto AM, Liu Z, Vandemark AP, Palladino MJ. 2012. A novel Drosophila SOD2 mutant demonstrates a role for mitochondrial ROS in neurodevelopment and disease. *Brain Behav* 2:424-34
16. Chacinska A, Koehler CM, Milenkovic D, Lithgow T, Pfanner N. 2009. Importing mitochondrial proteins: machineries and mechanisms. *Cell* 138:628-44
17. Chen C, Jack J, Garofalo RS. 1996. The Drosophila insulin receptor is required for normal growth. *Endocrinology* 137:846-56

18. Chinnery PF. 1993. Mitochondrial Disorders Overview. In *GeneReviews((R))*, ed. MP Adam, HH Ardinger, RA Pagon, SE Wallace, LJH Bean, et al. Seattle (WA). Number of.
19. Cox RT, Spradling AC. 2003. A Balbiani body and the fusome mediate mitochondrial inheritance during Drosophila oogenesis. *Development* 130:1579-90
20. Cox RT, Spradling AC. 2006. Milton controls the early acquisition of mitochondria by Drosophila oocytes. *Development* 133:3371-7
21. Cox RT, Spradling AC. 2009. *clueless*, a conserved Drosophila gene required for mitochondrial subcellular localization, interacts genetically with *parkin*. *Dis Model Mech* 2:490-9
22. de Nadal E, Ammerer G, Posas F. 2011. Controlling gene expression in response to stress. *Nat Rev Genet* 12:833-45
23. Decker CJ, Parker R. 2012. P-bodies and stress granules: possible roles in the control of translation and mRNA degradation. *Cold Spring Harb Perspect Biol* 4:a012286
24. Dimmer KS, Fritz S, Fuchs F, Messerschmitt M, Weinbach N, et al. 2002. Genetic basis of mitochondrial function and morphology in Saccharomyces cerevisiae. *Mol Biol Cell* 13:847-53
25. Drummond-Barbosa D, Spradling AC. 2001. Stem cells and their progeny respond to nutritional changes during Drosophila oogenesis. *Dev Biol* 231:265-78
26. El Zawily AM, Schwarzlander M, Finkemeier I, Johnston IG, Benamar A, et al. 2014. FRIENDLY regulates mitochondrial distribution, fusion, and quality control in Arabidopsis. *Plant Physiol* 166:808-28
27. Fazal FM, Han S, Parker KR, Kaewsapsak P, Xu J, et al. 2019. Atlas of Subcellular RNA Localization Revealed by APEX-Seq. *Cell* 178:473-90 e26
28. Fields SD, Conrad MN, Clarke M. 1998. The S. cerevisiae CLU1 and D. discoideum cluA genes are functional homologues that influence mitochondrial morphology and distribution. *J Cell Sci* 111 (Pt 12):1717-27
29. Fridovich I. 1995. Superoxide radical and superoxide dismutases. *Annu Rev Biochem* 64:97-112
30. Gao J, Schatton D, Martinelli P, Hansen H, Pla-Martin D, et al. 2014. CLUH regulates mitochondrial biogenesis by binding mRNAs of nuclear-encoded mitochondrial proteins. *J Cell Biol* 207:213-23
31. Gasch AP. 2007. Comparative genomics of the environmental stress response in ascomycete fungi. *Yeast* 24:961-76
32. Gehrke S, Wu Z, Klinkenberg M, Sun Y, Auburger G, et al. 2015. PINK1 and Parkin control localized translation of respiratory chain component mRNAs on mitochondria outer membrane. *Cell Metab* 21:95-108
33. Gerber AP, Herschlag D, Brown PO. 2004. Extensive association of functionally and cytotopically related mRNAs with Puf family RNA-binding proteins in yeast. *PLoS Biol* 2:E79
34. Giaever G, Chu AM, Ni L, Connelly C, Riles L, et al. 2002. Functional profiling of the Saccharomyces cerevisiae genome. *Nature* 418:387-91
35. Golani-Armon A, Arava Y. 2016. Localization of Nuclear-Encoded mRNAs to Mitochondria Outer Surface. *Biochemistry (Mosc)* 81:1038-43

36. Gorman GS, Chinnery PF, DiMauro S, Hirano M, Koga Y, et al. 2016. Mitochondrial diseases. *Nat Rev Dis Primers* 2:16080
37. Gorman GS, Schaefer AM, Ng Y, Gomez N, Blakely EL, et al. 2015. Prevalence of nuclear and mitochondrial DNA mutations related to adult mitochondrial disease. *Ann Neurol* 77:753-9
38. Guzikowski AR, Chen YS, Zid BM. 2019. Stress-induced mRNP granules: Form and function of processing bodies and stress granules. *Wiley Interdiscip Rev RNA* 10:e1524
39. Hémono M, Haller A, Chicher J, Duchêne A-M, Ngondo RP. 2021. CLUH interactome reveals an association to SPAG5 and a proximity to translation of mitochondrial protein.
40. Hirano M, Emmanuele V, Quinzii CM. 2018. Emerging therapies for mitochondrial diseases. *Essays Biochem* 62:467-81
41. Hollenbeck PJ. 1996. The pattern and mechanism of mitochondrial transport in axons. *Front Biosci* 1:d91-102
42. Hsu PY, Calviello L, Wu HL, Li FW, Rothfels CJ, et al. 2016. Super-resolution ribosome profiling reveals unannotated translation events in Arabidopsis. *Proc Natl Acad Sci U S A* 113:E7126-E35
43. Huang K, Chen W, Zhu F, Li PW, Kapahi P, Bai H. 2019. RiboTag translatomic profiling of Drosophila oenocytes under aging and induced oxidative stress. *BMC Genomics* 20:50
44. Hudson AM, Petrella LN, Tanaka AJ, Cooley L. 2008. Mononuclear muscle cells in Drosophila ovaries revealed by GFP protein traps. *Dev Biol* 314:329-40
45. Kato Y, Nakamura A. 2012. Roles of cytoplasmic RNP granules in intracellular RNA localization and translational control in the Drosophila oocyte. *Dev Growth Differ* 54:19-31
46. Kedersha N, Anderson P. 2002. Stress granules: sites of mRNA triage that regulate mRNA stability and translatability. *Biochem Soc Trans* 30:963-9
47. Kim I, Rodriguez-Enriquez S, Lemasters JJ. 2007. Selective degradation of mitochondria by mitophagy. *Arch Biochem Biophys* 462:245-53
48. LaFever L, Drummond-Barbosa D. 2005. Direct control of germline stem cell division and cyst growth by neural insulin in Drosophila. *Science* 309:1071-3
49. Lesnik C, Cohen Y, Atir-Lande A, Schuldiner M, Arava Y. 2014. OM14 is a mitochondrial receptor for cytosolic ribosomes that supports co-translational import into mitochondria. *Nat Commun* 5:5711
50. Lesnik C, Golani-Armon A, Arava Y. 2015. Localized translation near the mitochondrial outer membrane: An update. *RNA Biol* 12:801-9
51. Lezi E, Swerdlow RH. 2012. Mitochondria in neurodegeneration. *Adv Exp Med Biol* 942:269-86
52. Ligon LA, Steward O. 2000. Movement of mitochondria in the axons and dendrites of cultured hippocampal neurons. *J Comp Neurol* 427:340-50
53. Lin MD, Jiao X, Grima D, Newbury SF, Kiledjian M, Chou TB. 2008. Drosophila processing bodies in oogenesis. *Dev Biol* 322:276-88
54. Liufu T, Wang Z. 2020. Treatment for mitochondrial diseases. *Rev Neurosci*
55. Mager WH, Ferreira PM. 1993. Stress response of yeast. *Biochem J* 290 (Pt 1):1-13

56. Marc PM, Antoine; Devaux, Frédéric; Blugeon, Corinne; Corral-Debrinski, Marisol; Jacq, Claude. 2002. Genome-wide analysis of mRNAs targeted to yeast mitochondria
57. Marcos R, Lloberas J, Creus A, Xamena N, Cabré O. 1982. Effect of cycloheximide on different stages of Drosophila melanogaster. *Toxicology Letters* 13:105-12
58. Morris LX, Spradling AC. 2011. Long-term live imaging provides new insight into stem cell regulation and germline-soma coordination in the Drosophila ovary. *Development* 138:2207-15
59. Namkoong S, Ho A, Woo YM, Kwak H, Lee JH. 2018. Systematic Characterization of Stress-Induced RNA Granulation. *Mol Cell* 70:175-87 e8
60. Neupert W, Herrmann JM. 2007. Translocation of proteins into mitochondria. *Annu Rev Biochem* 76:723-49
61. Newbury SF, Muhlemann O, Stoecklin G. 2006. Turnover in the Alps: an mRNA perspective. Workshops on mechanisms and regulation of mRNA turnover. *EMBO Rep* 7:143-8
62. Nezis IP, Lamark T, Velentzas AD, Rusten TE, Bjorkoy G, et al. 2009. Cell death during Drosophila melanogaster early oogenesis is mediated through autophagy. *Autophagy* 5:298-302
63. Oldham S, Montagne J, Radimerski T, Thomas G, Hafen E. 2000. Genetic and biochemical characterization of dTOR, the Drosophila homolog of the target of rapamycin. *Genes Dev* 14:2689-94
64. Oldham S, Stocker H, Laffargue M, Wittwer F, Wymann M, Hafen E. 2002. The Drosophila insulin/IGF receptor controls growth and size by modulating PtdInsP(3) levels. *Development* 129:4103-9
65. Palmer CS, Anderson AJ, Stojanovski D. 2021. Mitochondrial protein import dysfunction: mitochondrial disease, neurodegenerative disease and cancer. *FEBS Lett* 595:1107-31
66. Parker DJ, Moran A, Mitra K. 2017. Studying Mitochondrial Structure and Function in Drosophila Ovaries. *J Vis Exp*
67. Parton RM, Valles AM, Dobbie IM, Davis I. 2010. Isolation of Drosophila egg chambers for imaging. *Cold Spring Harb Protoc* 2010:pdb prot5402
68. Paul A, Belton A, Nag S, Martin I, Grotewiel MS, Duttaroy A. 2007. Reduced mitochondrial SOD displays mortality characteristics reminiscent of natural aging. *Mech Ageing Dev* 128:706-16
69. Pla-Martin D, Schatton D, Wiederstein JL, Marx MC, Khiati S, et al. 2020. CLUH granules coordinate translation of mitochondrial proteins with mTORC1 signaling and mitophagy. *EMBO J* 39:e102731
70. Prasad M, Jang AC-C, Starz-Gaiano M, Melani M, Montell DJ. 2007. A protocol for culturing Drosophila melanogaster stage 9 egg chambers for live imaging. In *Nature Protocols*, pp. 2467-73: Nature Publishing Group
71. Ravera S, Podesta M, Sabatini F, Fresia C, Columbaro M, et al. 2018. Mesenchymal stem cells from preterm to term newborns undergo a significant switch from anaerobic glycolysis to the oxidative phosphorylation. *Cell Mol Life Sci* 75:889-903

72. Rebollo E, Llamazares S, Reina J, Gonzalez C. 2004. Contribution of noncentrosomal microtubules to spindle assembly in Drosophila spermatocytes. *PLoS Biol* 2:E8
73. Rugarli EI, Langer T. 2012. Mitochondrial quality control: a matter of life and death for neurons. *EMBO J* 31:1336-49
74. Saint-Georges Y, Garcia M, Delaveau T, Jourdren L, Le Crom S, et al. 2008. Yeast mitochondrial biogenesis: a role for the PUF RNA-binding protein Puf3p in mRNA localization. *PLoS One* 3:e2293
75. Schatton D, Pla-Martin D, Marx MC, Hansen H, Mourier A, et al. 2017. CLUH regulates mitochondrial metabolism by controlling translation and decay of target mRNAs. *J Cell Biol* 216:675-93
76. Schisa JA. 2012. New insights into the regulation of RNP granule assembly in oocytes. *Int Rev Cell Mol Biol* 295:233-89
77. Schisa JA. 2014. Effects of stress and aging on ribonucleoprotein assembly and function in the germ line. *Wiley Interdiscip Rev RNA* 5:231-46
78. Schneider-Poetsch T, Ju J, Eyler DE, Dang Y, Bhat S, et al. 2010. Inhibition of eukaryotic translation elongation by cycloheximide and lactimidomycin. *Nat Chem Biol* 6:209-17
79. Sen A, Cox RT. 2016. Clueless is a conserved ribonucleoprotein that binds the ribosome at the mitochondrial outer membrane. *Biol Open* 5:195-203
80. Sen A, Cox RT. 2017. Fly Models of Human Diseases: Drosophila as a Model for Understanding Human Mitochondrial Mutations and Disease. *Curr Top Dev Biol* 121:1-27
81. Sen A, Damm VT, Cox RT. 2013. Drosophila *clueless* is highly expressed in larval neuroblasts, affects mitochondrial localization and suppresses mitochondrial oxidative damage. *PLoS One* 8:e54283
82. Sen A, Kalvakuri S, Bodmer R, Cox RT. 2015. Clueless, a protein required for mitochondrial function, interacts with the PINK1-Parkin complex in *Drosophila*. *Dis Model Mech* 8:577-89
83. Sheard KM, Cox RT. 2021. Visualizing the Effects of Oxidative Damage on Drosophila Egg Chambers using Live Imaging. *J Vis Exp*
84. Sheard KM, Thibault-Sennett SA, Sen A, Shewmaker F, Cox RT. 2020. Clueless forms dynamic, insulin-responsive bliss particles sensitive to stress. *Dev Biol* 459:149-60
85. Shimada Y, Burn KM, Niwa R, Cooley L. 2011. Reversible response of protein localization and microtubule organization to nutrient stress during Drosophila early oogenesis. *Dev Biol* 355:250-62
86. Sieber MH, Thomsen MB, Spradling AC. 2016. Electron Transport Chain Remodeling by GSK3 during Oogenesis Connects Nutrient State to Reproduction. *Cell* 164:420-32
87. Singh A, Faccenda D, Campanella M. 2021. Pharmacological advances in mitochondrial therapy. *EBioMedicine* 65:103244
88. Slone J, Huang T. 2020. The special considerations of gene therapy for mitochondrial diseases. *NPJ Genom Med* 5:7
89. Snee MJ, Macdonald PM. 2009. Dynamic organization and plasticity of sponge bodies. *Dev Dyn* 238:918-30

90. Stojanovski DJ, Amelia J.; Streimann, Illo;, Hoogenraad NJaR, Michael T. 2003. Import of nuclear-encoded proteins into mitochondria. *Experimental Physiology*
91. Sylvestre JAM, A.; Jacq, C.; Dujardin, G.; and, Corral-Debrinski M. 2003. The Role of the 3' Untranslated Region in mRNA Sorting to the Vicinity of Mitochondria Is Conserved from Yeast to Human Cells. *Molecular Biology of the Cell* 14:3848–56
92. Tapon N, Ito N, Dickson BJ, Treisman JE, Hariharan IK. 2001. The Drosophila tuberous sclerosis complex gene homologs restrict cell growth and cell proliferation. *Cell* 105:345-55
93. Uversky VN. 2017. Intrinsically disordered proteins in overcrowded milieu: Membrane-less organelles, phase separation, and intrinsic disorder. *Curr Opin Struct Biol* 44:18-30
94. Valasek LS, Zeman J, Wagner S, Beznoskova P, Pavlikova Z, et al. 2017. Embraced by eIF3: structural and functional insights into the roles of eIF3 across the translation cycle. *Nucleic Acids Res* 45:10948-68
95. Vincow ES, Merrihew G, Thomas RE, Shulman NJ, Beyer RP, et al. 2013. The PINK1-Parkin pathway promotes both mitophagy and selective respiratory chain turnover in vivo. *Proc Natl Acad Sci U S A* 110:6400-5
96. Vincow ES, Thomas RE, Merrihew GE, Shulman NJ, Bammler TK, et al. 2019. Autophagy accounts for approximately one-third of mitochondrial protein turnover and is protein selective. *Autophagy* 15:1592-605
97. Vornlocher H-PH, Parisa; Ribeiro, Sofia; Hershey, John W.B. 1999. A 110-Kilodalton Subunit of Translation Initiation Factor eIF3 and an Associated 135-kilodalton Protein Are Encoded by the Saccharomyces cervisiae TIF32 and TIF31 Genes. *The Journal of Biological Chemistry* 274:1602-12
98. Wakim J, Goudenege D, Perrot R, Gueguen N, Desquiret-Dumas V, et al. 2017. CLUH couples mitochondrial distribution to the energetic and metabolic status. *J Cell Sci* 130:1940-51
99. Wang C, Schmich F, Srivatsa S, Weidner J, Beerenwinkel N, Spang A. 2018. Context-dependent deposition and regulation of mRNAs in P-bodies. *Elife* 7
100. Wang S, Hazelrigg T. 1994. Implications for bcd mRNA localization from spatial distribution of exu protein in Drosophila oogenesis. *Nature* 369:400-03
101. Wang Y, Branicky R, Noe A, Hekimi S. 2018. Superoxide dismutases: Dual roles in controlling ROS damage and regulating ROS signaling. *J Cell Biol* 217:1915-28
102. Wang ZH, Clark C, Geisbrecht ER. 2016. Drosophila clueless is involved in Parkin-dependent mitophagy by promoting VCP-mediated Marf degradation. *Hum Mol Genet* 25:1946-64
103. Wang ZH, Rabouille C, Geisbrecht ER. 2015. Loss of a Clueless-dGRASP complex results in ER stress and blocks Integrin exit from the perinuclear endoplasmic reticulum in Drosophila larval muscle. *Biol Open* 4:636-48
104. Weil TT, Parton RM, Davis I. 2012. Preparing individual Drosophila egg chambers for live imaging. *J Vis Exp*
105. Wilhelm JE, Buszczak M, Sayles S. 2005. Efficient protein trafficking requires trailer hitch, a component of a ribonucleoprotein complex localized to the ER in Drosophila. *Dev Cell* 9:675-85

106. Winterbourn CC. 1995. Toxicity of iron and hydrogen peroxide: the Fenton reaction. *Toxicol Lett* 82-83:969-74
107. Wong R, Piper MD, Wertheim B, Partridge L. 2009. Quantification of food intake in Drosophila. *PLoS One* 4:e6063